UNIVERSITÉ DE BOURGOGNE
École Doctorale Environnements – Santé
UFR Sciences Vie, Terre et Environnement
UMR 6282 CNRS/uB Biogéosciences

THÈSE

Pour obtenir le grade de
Docteur de l'Université de Bourgogne
en Sciences de la Terre
Spécialité Sciences du sol

par

JULIEN GUIGUE

Influence des facteurs biotiques et abiotiques sur la dynamique de la matière organique du sol à partir de la caractérisation biogéochimique des matières organiques solubles

Directeur de thèse : JEAN LÉVÊQUE
Co-encadrant : OLIVIER MATHIEU

Thèse soutenue publiquement le 8 décembre 2014

Membres du Jury

CLAIRE CHENU – Professeur, AgroParisTech	rapporteur
STÉPHANE MOUNIER – Maître de Conférence, Université de Toulon	examinateur
PHILIPPE AMIOTTE-SUCHET – Maître de Conférence, Université de Bourgogogne	invité
RICHARD BARDGETT – Professeur, University of Manchester	rapporteur
PHILIPPE SCHMITT-KOPPLIN – Professeur, Technische Universität München	examinateur

Remerciements

Je vais commencer par dire Merci…

Au ministère de l'enseignement supérieur et de la recherche. Douce France où l'on peut aller sur les bancs de l'Université sur le tard et sans vraiment savoir pour quelle raison… à part l'envie d'apprendre des choses nouvelles. C'est ce qui me manquait pendant ces quelques années à alterner l'usine, la cuisine, puis l'usine, puis la cuisine, puis l'usine m'a remplacé par un robot et j'ai remplacé l'usine par les amphithéâtres, les bibliothèques, et tout ce qui rythme la vie des étudiants.

Merci ensuite à celles et ceux qui m'ont donné l'envie de continuer. Et sur ce point, la personne que je remercie en premier est Jean Lévêque, mon directeur de thèse, il m'a ouvert sa porte à un moment où peu de gens l'auraient fait… Pour moi cette histoire a vraiment commencé quand cette porte s'est ouverte. Donc voilà le point de départ, c'est certainement une des étapes les plus importantes, et ça a continué sans interruption jusqu'à aujourd'hui. Merci Jean.

Merci aussi à Olivier Mathieu, qui s'est très vite retrouvé dans cette aventure. Ta participation a été essentielle. Je suis un affectif et si je suis resté faire cette thèse à Dijon, c'est avant tout pour continuer à bosser avec vous… Le microcode à l'époque, j'y connaissais rien !

Merci évidemment aux membres du jury Sylvie Dousset, Claire Chenu, Richard Bardgett, Philippe Amiotte-Suchet et Philippe Schmitt-Kopplin d'avoir accepté d'évaluer mon travail. Sur le papier ça fait une superbe équipe et je dois avouer que je ressens beucoup de fierté de devoir défendre ma thèse devant vous.

Je remercie également les gens avec qui j'ai pu collaborer au cours de cette thèse. Les portes qui s'ouvrent, c'est important.

Je remercie Yves Lucas, pour m'avoir proposer de venir travailler avec son équipe à l'Université de Toulon et pour m'y avoir accueilli chaleureusement. Je remercie également Stéphane Mounier, qui m'a assisté pour la fluorescence. Merci pour l'accueil et la bonne humeur.

Merci également à Pierre-Alain, Nicolas, Lionel et Sam, le gang de la rue de Sully. Vous m'avez aidé à sortir des infos des données microbio et ça, c'était pas gagné d'avance.

Et merci aussi à Philippe Schmitt-Kopplin, Marianna Lucio et Mourad Harir, qui m'ont accueilli au Helmholtz Zentrum de Munich. Là-bas aussi j'ai découvert, au niveau scientifique, un monde nouveau… et vaste. L'histoire continue…

Je continue en remerciant les gens du quotidien à Dijon, Mathieu Thévenot, en première ligne, car c'est le plus vaillant d'entre eux et en plus il fait une bonne mascotte ! Je ne développerai pas plus sur ton sex-appeal, tu risquerais encore de te sentir gêné. Au plaisir de faire chauffer ton joujou de laboratoire quand il sera prêt. Merci également à Marie-Jeanne Milloux, pour avoir attendu que je finisse cette thèse avant de vous libérer de vos obligations professionnelles. Je vous souhaite que du bonheur pour la suite. Merci aussi à Philippe Amiotte-Suchet, autre élément de l'équipe de géochimistes, j'ai été fier de faire partie de l'équipe avec vous tous.

Évidemment je me dois de citer le reste du club des amateurs de café : Thomas, Nicolas, Sébastien, Pierre-Yves… En fait j'ai eu la chance de tomber dans le meilleur couloir de l'Université, malgré que les dames se fassent rares.

Merci également à Dudu, pour nous avoir mis, avec Leo, Benjamin et Fabien, un des plus gros carton qui ait du exister sur les camps de terrain. On avait tout compris sur le terrain mais on a bien mérité ce carton. Ça nous a mis un bon coup de pied au c.. c'est juste ce qu'il nous fallait. Merci au passage à Benji pour avoir écrit ces quelques lignes qui ont valu ces cinq points…

Et Merci aussi au reste de l'équipe SEDS et aux membres du laboratoire Biogéosciences pour m'avoir accueilli parmi vous.

Protocole oblige, j'ai commencé par les anciens. Au tour des collègues doctorants !

Une mention spéciale pour Christophe, on est pote depuis le premier jour de fac et ça fait 10 ans… Le temps passe vite, t'es presque aussi vieux que moi… vas-y fonce mon gars!

Une autre mention spéciale pour Luca, ça fait moins longtemps qu'on se connaît mais on partage jours et nuits depuis des mois. J'apprécie, souvent mais pas tout le temps :o), ce style de tempérament explosif, tous mes potes sont presque aussi chiants que toi. Dans un lointain futur, quand je penserai à mes années de thèse, c'est évident que je penserai à toi. Un bon binôme, capable de ramasser un essaim d'abeilles sans protection quand les vrais apiculteurs détalaient !

La troisième mention spéciale pour Édouard, un temps rookie mais maintenant bel et bien en fin de vie de thésard. Je vais pas faire de blabla, c'est juste un plaisir de te croiser au quotidien. Ya Man !

Voilà, maintenant on va dégager tous les quatre mais je suis content d'être tombé sur vous.

Un grand Merci aussi à celles et ceux qui sont arrivés après : Élise, Jess, Axelle (un peu de présence féminine, si rare dans ce monde de géologue) Anthony (vive la bière !) et mon p'tit Titi l'aventurier. L'avenir est à vous.

Si j'ai tenu le coup pendant ces années, un peu éprouvantes quand même, c'est bien sûr aussi grâce aux personnes avec qui je ne travaille pas. Et tout d'abord grâce à ma chérie Hsin-yi. C'est évident que sans toi je n'aurais jamais fait tout ça. Je n'aurai même sûrement pas commencé.

Je remercie tout aussi fort ma Maman. Tu nous as donné tout ce que tu pouvais et je ne te remercierai jamais assez. Merci aussi à mon frère Guillaume, ce qu'on est on se le doit aussi l'un l'autre.

Un merci aussi pour le Daron, si je vois le monde sous cet angle, c'est sûrement un peu grâce à toi. Et merci bien sûr à toute la famille, je ne suis pas venu souvent ces derniers temps mais je pense à vous... Je m'attends encore à ce que le grand-père me demande quand est-ce que je trouverai un travail… encore étudiant à mon âge, c'est pas possible !

Et puis Merci à tout un tas de gens, qui font que j'avance tous les jours, qui donnent du goût à ma vie. La famille Bettoni, La Chapoline company (bientôt au complet), Les jardiniers de la commune indépendante des Lentillères (Tierra Y Libertad !), La famille Perrot (vivants, joyeux, chaleureux… vous avez été là quand il n'y avait plus grand monde… familialement vôtre !) et mon grand pote Denis ! et mon grand pote Léo ! et mon grand pote Benjamin ! et j'en oublie sûrement…

你愛我最

你幫了我最

謝謝你我的愛

我愛你

Sommaire

Introduction

Pour les sociétés des plus anciennes aux plus modernes, les sols sont une ressource primordiale. Le développement des sols, résultat de processus très lents à l'échelle des civilisations, et les équilibres fragiles qui les contrôlent, en font une richesse épuisable et leur dégradation met en péril la pérennité de nos modes de vie. Supports des activités agricoles, la production alimentaire apparaît incontestablement comme le service principal rendu par les sols. Depuis des milliers d'années, l'humanité a appris à tirer profit de l'exploitation des sols par l'agriculture, et la prospérité des peuples est étroitement liée à la fertilité des sols qui les nourrissent.

D'autres fonctions majeures sont également assurées par les sols. L'eau y est filtrée au cours de son transfert dans les différents horizons. Les sols permettent la fixation et la dégradation de polluants et ont donc un rôle protecteur sur la qualité de l'environnement.

Le contexte actuel de changement climatique, ainsi que les changements d'occupation des terres, sont susceptibles de modifier la dynamique de décomposition des matières organiques des sols (MOS). Les flux de CO_2 qui y sont associés pourraient entraîner des phénomènes de rétroactions positives qui amplifieraient les impacts du changement climatique.

En étant le support de la vie animale et végétale, les sols sont la base des écosystèmes terrestres et leur préservation est essentielle au maintien de la biodiversité. Ils sont, à leur échelle, des écosystèmes complexes, à l'interface entre l'atmosphère, l'hydrosphère, la lithosphère et la biosphère, et sont le lieu de réactions biotiques et abiotiques qui régulent les

cycles biogéochimiques, notamment ceux du carbone (C) et de l'azote. Cette dynamique a un lien direct avec la fertilité des sols, en permettant la production de nutriments et la disponibilité d'éléments minéraux, et est également à l'origine de la respiration des sols, avec la production de gaz à effet de serre comme le dioxyde de carbone, le protoxyde d'azote ou le méthane.

La quantité de C organique dans le mètre supérieur des sols est estimée à environ 1500 Gt, soit au moins autant que dans l'atmosphère (≈840 Gt C) et la végétation (450–650 Gt C) réunis (Batjes, 1996; Ciais et al., 2013; Scharlemann et al., 2014). Le flux annuel de CO_2 émis par la respiration hétérotrophe dans les sols est presque dix fois supérieur au flux de CO_2 émis par la combustion des énergies fossiles (Ciais et al., 2013), attestant de l'importance des stocks de C des sols pour la régulation des concentrations en CO_2 dans l'atmosphère.

La respiration des sols est le résultat de l'oxydation de la matière organique par les (micro)organismes. Des changements dans la dynamique de décomposition de la matière organique des sols pourraient impacter l'équilibre entre les différents réservoirs de C et induire une hausse des émissions de CO_2 par la respiration hétérotrophe. La matière organique des sols (MOS) provient essentiellement de l'apport de litières végétales et de leur transformation au cours de la décomposition par les (micro)organismes. Les MOS sont un mélange de milliers de molécules différentes, composées des éléments C, H, O, N et S, et ayant des temps de résidence très variables, allant de quelques minutes à plusieurs milliers d'années. La réactivité des MOS dépend de nombreux facteurs, comme les conditions climatiques (température et humidité), leur composition chimique et leur complexation avec les particules minérales du sol, l'activité de dégradation des (micro)organismes et les conditions physico-chimiques du milieu.

L'eau est un agent essentiel pour l'activité de décomposition des MOS par les (micro)organismes. Le compartiment de MOS présent dans l'eau du sol, communément appelé matière organique dissoute (MOD), est donc fortement impliqué dans la dynamique de décomposition des MOS, mais également dans les transferts de matière organique vers les horizons profonds du sol ou vers les systèmes hydrologiques. Les MOD, bien que correspondant à une faible proportion des MOS, présentent donc un intérêt majeur pour l'étude de la dynamique des MOS.

L'objectif de ce travail de thèse est d'identifier l'influence de paramètres biotiques (population microbienne, couvert végétal) et abiotiques (physico-chimie des sols) sur la quantité et la qualité des matières organiques extractibles à l'eau (WEOM, l'acronyme anglais de *water-extractable organic matter* est utilisé dans l'ensemble du manuscrit pour éviter les confusions). L'analyse de solutions de sol extraites en laboratoire est utilisée comme un moyen d'estimer les propriétés de la matière organique dissoute en conditions naturelles.

Ce manuscrit est divisé en cinq chapitres, regroupant les principaux résultats acquis au cours de cette thèse.

Le premier chapitre est une brève synthèse bibliographique des connaissances en lien avec la thématique de la thèse, dans le but de présenter les grandes idées liées à la thématique de cette thèse.

Le deuxième chapitre porte sur une comparaison de méthodes d'extraction des matières organiques dissoutes en laboratoire.

Dans le troisième chapitre, l'effet de la diversité bactérienne sur la décomposition de la matière organique a été étudié en utilisant une approche par marquage isotopique ^{13}C.

Les travaux des deux chapitres suivants sont basés sur l'analyse des 120 échantillons de sol prélevés en Bourgogne dans le cadre du projet RMQS (Réseau de Mesures de la Qualité des Sols).

Le quatrième chapitre présente les liens entre les propriétés physico-chimiques des sols, les paramètres microbiens et les caractéristiques des matières organiques dissoutes.

Enfin le cinquième chapitre met en relation la composition moléculaire des matières organiques dissoutes avec la diversité des environnements pédologiques à l'échelle régionale.

Chapitre 1

Étude bibliographique et problématique

La matière organique des sols (MOS) a été étudiée par des générations de chercheurs, d'abord pour son effet sur la fertilité des sols et par curiosité pour ces substances qui colorent l'eau du sol. Plus récemment, les conséquences sur les concentrations en gaz à effet de serre que peut avoir l'évolution des stocks de carbone organique des sols ont contribué à l'essor de la thématique.

Ce travail de thèse porte sur le rôle des matières organiques extractibles à l'eau (WEOM), souvent étudiées pour estimer les propriétés des matières organiques dissoutes (MOD) dans la solution du sol en conditions naturelles. Ce premier chapitre a pour but de présenter brièvement les notions générales issues des recherches effectuées en lien avec le sujet, dans le but d'introduire la thématique générale de la thèse.

Après avoir exposé les notions importantes sur la MOS, le rôle des communautés microbiennes dans la dynamique de la MOS est présenté. La partie suivante de ce chapitre aborde les questions méthodologiques liées à l'échantillonnage des MOD et rappelle les concepts principaux sur la dynamique des MOD dans les sols. Les principales méthodes de caractérisation utilisées pour l'étude de la MO en science du sol sont présentées dans une quatrième partie puis la problématique et les principaux objectifs de la thèse sont annoncés.

1 La matière organique du sol

1.1 Définitions et généralités

Dans ce manuscrit, les MOS sont considérées comme la totalité des composés organiques à l'exception des tissus animaux et végétaux facilement isolables et de la biomasse vivante du sol. Cette fraction représente souvent une proportion faible de la masse totale, comprise entre des concentrations en carbone organique (C_{org}) inférieures à 1% et jusqu'à environ 15%. Des valeurs en C_{org} supérieures sont mesurées pour des sols plus spécifiques comme les Histosols (IUSS Working Group WRB, 2006).

Malgré cette proportion relativement faible, la fraction organique des sols a une grande influence sur les propriétés physiques, biologiques et chimiques des sols (Baldock & Nelson, 2000). Sa complexation avec la fraction minérale améliore la stabilité structurale des sols et la rétention de l'eau. Les molécules qui la composent sont une source d'énergie pour les (micro)organismes, alors que certaines substances peuvent être toxiques pour ces mêmes (micro)organismes. Enfin la MOS, principalement les molécules contenant les éléments N, S et P, est un réservoir de micronutriments pour les plantes.

La source quasi-exclusive de MO dans les sols provient de l'apport par les litières végétales. Leur décomposition correspond à la transformation de molécules complexes (polysaccharides, polymères aliphatiques, lignines, lipides et protéines, notamment) par les (micro)organismes. Cette étape mène à la libération de composés simples, le plus souvent solubles, et à la minéralisation, avec notamment la production de CO_2. La fraction organique transformée et préservée dans le sol entre dans la catégorie des substances humiques (Sutton & Sposito, 2005).

Le temps de résidence des MOS varie en fonction des différents constituants, à des échelles de temps allant de quelques jours (Chen et al., 2009) à plusieurs milliers d'années (Kögel-Knabner et al., 2008). La persistance des MOS a longtemps été interprétée comme le résultat de la structure des molécules, qui les rendrait plus ou moins récalcitrantes (Sollins et al., 1996). Cependant, souvent considérées comme difficilement dégradables du fait de leur grandes tailles et parce qu'elles contiennent des liaisons non-hydrolysables, les lignines ne sont pourtant pas davantage conservées dans les sols

(Kiem & Kögel-Knabner, 2003; Heim & Schmidt, 2007). A l'inverse, les carbohydrates sont un substrat censé être facile à dégrader pour les microorganismes, mais plusieurs études montrent que cette classe de composés a des temps de résidence comparables aux autres (Gleixner et al., 2002; Derrien et al., 2006).

Ce concept basé sur la récalcitrance des molécules est aujourd'hui complété par la prise en compte de l'inaccessibilité des composés organiques pour les microorganismes, du fait de leur isolement dans des espaces poraux déconnectés, des interactions de ces composés avec la fraction minérale, ou encore d'une interdépendance de ces composés pouvant inhiber ou favoriser leur décomposition (Marschner et al., 2008; Kleber, 2010; Schmidt et al., 2011).

1.2 Association avec la phase minérale

L'association des molécules organiques avec la fraction minérale du sol, principalement les argiles et les oxydes de Fe et d'Al, est un processus majeur pour la préservation de la MO dans les sols. Ces associations, probablement formées par des liaisons chimiques fortes, rendent les composés organiques moins susceptibles d'être dégradés (Kalbitz et al., 2005; Kaiser & Guggenberger, 2007). La proportion relative de MO liée à la fraction minérale augmente avec la profondeur, avec une plus grande implication des phyllosilicates, alors que les oxydes de Fe ont un rôle plus important dans les horizons supérieurs (Kögel-Knabner et al., 2008).

Les champignons semblent être un agent de l'association des MO avec la fraction grossière des sols, du fait d'une abondance plus élevée d'enzymes provenant de l'activité fongique dans la fraction sableuse (Marhan et al., 2007). Au contraire, les bactéries sont dominantes dans la fraction fine des sols, et la signature microbienne des polysaccharides dans cette fraction suggère leur implication pour la stabilisation des MO dans les particules les plus fines (Kiem & Kögel-Knabner, 2003; Kögel-Knabner et al., 2008).

Une étude récente par imagerie NanoSIMS a montré que seulement une proportion mineure (<19%) des surfaces minérales étaient impliquées dans les associations avec la MO (Vogel et al., 2014). Les surfaces d'associations préférentielles sont situées sur des amas de particules rugueux alors que les particules individualisées, plus lisses, ne sont quasiment pas associées aux molécules organiques. Le suivi de l'incorporation d'une litière enrichie en ^{13}C et en ^{15}N a également permis à ces auteurs de démontrer que cette MO fraîche réagissait

immédiatement avec les particules du sol et que les liaisons se faisaient principalement avec les complexes organo-minéraux déjà existants.

Si les associations organo-minérales sont souvent considérées comme une phase stabilisée de MO, la décomposition de cette fraction organique reste possible, surtout pour les composés ayant des liaisons chimiques faibles avec les phases minérales, comme les ponts calciques ou les forces de van der Walls. Au contraire, les molécules plus fortement liées au oxydes de Fe sont moins facilement désorbées et leur préservation dans le sol est plus durable (Mikutta et al., 2007).

1.3 Décomposition

Une des clés de l'équilibre des stocks de MOS dans les sols dépend des processus de stabilisation (associations organo-minérales, condensation) et de la minéralisation par les microorganismes de molécules plus labiles. Plusieurs facteurs contrôlent la minéralisation de la MOS.

La température est supposée avoir un effet négatif sur les stocks de MOS, en entrainant une augmentation de l'activité des microorganismes et par conséquent la décomposition de la MOS (Field et al., 2007). Cependant, l'augmentation de la température peut également entraîner une augmentation de la production primaire et donc des entrées de MO dans les sols, ce qui contrecarrerait la hausse de la minéralisation de la MOS. Grâce à des mesures en ^{14}C dans le CO_2 minéralisé, Hopkins et al. (2012) ont observé que si la minéralisation de la MOS augmentait avec la hausse de température, la contribution principale à cette hausse venait de la MO incorporée au sol depuis 7 à 13 ans.

Dans une autre étude, Plante et al. (2010) ont montré que la hausse de température entrainait une augmentation de la minéralisation des MO particulaires, mais que la dégradation des composés hydrolysables, considérés comme représentatifs des MO stables, n'était pas modifiée. Cependant, l'effet de la température est surtout étudié dans des expériences d'incubations, qui ne permettent pas de reproduire les effets conjugués à une hausse des températures dans le milieu naturel, tels que la modification du régime des précipitations ou l'évolution des communautés microbiennes, par exemple.

Une autre étude a montré que la modification du régime hydrique des sols, avec des cycles d'inondation et de sécheresse, menait à l'augmentation des quantités de MOD produites et

que des températures plus élevées favorisaient la minéralisation de la MOD (Chow et al., 2006). Ces résultats mettent en avant l'importance de l'interaction des facteurs environnementaux sur la minéralisation des MOS.

Les différences de couvert végétal semblent avoir un effet plus mesuré sur la minéralisation. Une hiérarchisation des différents facteurs influençant la respiration du sol montre que la température, l'humidité du sol et les propriétés chimiques des MOS ont un effet plus important que le type de végétation sur la minéralisation des MOS (Raich & Tufekcioglu, 2000).

2 Activité microbienne

2.1 Abondance des microorganismes à différentes échelles

Les régulateurs principaux de la décomposition des MOS sont les microorganismes. Ainsi, les différences dans l'abondance microbienne et dans la composition des communautés sont d'une grande importance pour la compréhension du fonctionnement des sols.

A l'échelle de la France, l'abondance des microorganismes est principalement contrôlée par le pH, le taux de matière organique et la texture des sols (Dequiedt et al., 2011). Les sols développés sur substratum carbonatés, et qui contiennent souvent une plus grande proportion de particules fines, hébergent une plus grande quantité de microorganismes. Le type de couvert végétal a également un effet sur l'abondance des microorganismes et des niveaux d'abondance plus faibles sont observés dans les sols servant à la monoculture. Ces paramètres sont également structurant à l'échelle de la parcelle (Johnson et al., 2003; Lejon et al., 2005, 2007).

A une échelle encore plus fine, qui reflète davantage les processus de dégradation, la distribution des microorganismes est gouvernée par la structure du sol et la porosité, ainsi que par les teneurs en MO (Ruamps et al., 2011). L'accessibilité au substrat organique en fonction de l'agencement des particules est déterminante pour le développement des microorganismes. Une étude utilisant le traçage isotopique ^{13}C a montré une activité de décomposition par les microorganismes plus importante dans les pores du sol les plus larges, où la MO est plus accessible, et des structures des communautés différentes ont été observées dans les pores de tailles différentes (Ruamps et al., 2011).

2.2 Action de décomposition

L'hétérogénéité chimique des MOS peut être mise en relation avec la grande diversité taxonomique des communautés microbiennes. La MOS est la principale source d'énergie pour les microorganismes, à l'origine de la respiration hétérotrophe. Plusieurs études ont montré l'implication de groupes d'espèces distincts (par exemple K-stratégistes vs r-stratégistes ou champignons vs bactéries) dans la décomposition des différents types de MOS. La distinction majeure porte sur l'origine du substrat et met en opposition les composés dérivés des plantes aux composés dérivés de la MOS.

L'utilisation de matière organique fraîche enrichie en ^{13}C permet de suivre l'assimilation de ce C par les microorganismes en mesurant l'enrichissement isotopique dans les biomarqueurs, comme les PLFA (*phospholipid fatty acids*). Les bactéries Gram-négatives ont une préférence pour le C récent issu des tissus végétaux alors que le C issu de la décomposition des MOS est davantage assimilé par les bactéries Gram-positives (Kramer & Gleixner, 2006), avec jusqu'à 40% de la MOS utilisée comme substrat par les microorganismes.

Williams et al. (2006) ont également constaté que seule une partie de la communauté était capable d'assimiler les résidus végétaux. Ces espèces semblent capables de s'adapter à différents types de substrat labile, alors que les espèces spécialisées dans la décomposition des matières organiques plus complexes semblent s'adapter moins facilement au changement de composition du substrat (Waldrop & Firestone, 2004). En s'intéressant uniquement aux décomposeurs des MO fraîches, Paterson et al. (2008) ont pu montrer que des groupes bactériens différents prenaient en charge la décomposition de la fraction soluble et de la fraction insoluble des MO fraîches.

2.3 Diversité

Les communautés bactériennes sont composées de différents groupes microbiens, qui sont spécialisés dans des fonctions particulières, comme les fonctions énoncées dans le paragraphe précédent ou par exemple la dénitrification ou la sulfato-réduction. Le concept de la redondance fonctionnelle des communautés, basé sur la grande diversité taxonomique d'une communauté et sur le fait que les espèces microbiennes sont capables d'assurer plusieurs fonctions, est souvent cité pour s'affranchir de la prise en compte de la diversité microbienne.

Wertz et al. (2007), en créant artificiellement un gradient extrême de diversité (estimée à 99% d'espèces absentes pour la plus faible diversité) n'ont observé aucun effet de cette érosion de diversité, ni sur la minéralisation du C, ni sur la nitrification ou la dénitrification. Au contraire, en utilisant un gradient de diversité similaire et une approche par traçage ^{13}C, Baumann et al. (2012) ont observé une baisse de la décomposition des sucres issus de la matière organique fraîche avec la baisse de diversité bactérienne. La diversité bactérienne est également importante pour maintenir la stabilité des communautés et permettre leur résilience en cas de perturbations, comme une pollution ou un changement des conditions environnementales (Girvan et al., 2005).

3 La matière organique dissoute

3.1 Notions générales sur la matière organique dissoute

La matière organique dissoute (MOD) est un compartiment labile de C dans les sols (Marschner & Kalbitz, 2003). Sa biodisponibilité comme ressource trophique a été démontrée dans plusieurs études (Kalbitz et al., 2003; Andreasson et al., 2009) avec la minéralisation d'une fraction considérable de la MOD en seulement quelques semaines.

La MOD est un mélange de molécules complexes avec des origines diverses. La matière organique fraîche contribue aux flux de MOD. Plusieurs études utilisent la fraction hydrosoluble de la MO fraîche et suivent son évolution dans le sol (Fröberg et al., 2003; Qualls, 2005; Paterson et al., 2008). Cette MOD produite au niveau de la litière est ensuite susceptible d'être fixée sur la fraction solide des horizons supérieurs lors de sa migration vers la profondeur (Müller et al., 2009).

L'autre source principale de MOD est la MOS, via des phénomènes de désorption depuis les complexes organo-minéraux (Mikutta et al., 2007), ou la libération de composés solubles au cours de la dégradation de la MOS par les microorganismes (Hagedorn et al., 2004). Le pH et la force ionique de la phase aqueuse détermine la solubilité des matières organiques (Kalbitz et al., 2000b), tandis que la sorption et la désorption de la MOD sont également contrôlées par la force des liaisons avec les oxydes de Fe et d'Al, et les argiles (Kaiser et al., 2001; Mikutta et al., 2007).

La libération par les plantes d'exsudats racinaires est également une source importante de MOD avec la mise en solution de carbohydrates et de composés aliphatiques (Rosenfeld et al., 2014). Cette dernière étude a montré que du C assimilé par la plante depuis seulement quelques heures était transféré dans le sol sous forme de MOD.

Enfin la biomasse microbienne peut également contribuer aux flux de MOD, notamment avec la libération de métabolites liée à leur activité ou encore la lyse des cellules au moment de la mort des microorganismes.

Kaiser & Kalbitz (2012) ont récemment proposé un modèle de la dynamique de la MOD dans les sols. Dans ce modèle, la décomposition de la litière et des substances humiques dans les horizons de surface est la principale source de MOD. En comparant les transferts de MOD vers les horizons profonds avec la migration d'une phase mobile dans une colonne chromatographique, ils mettent en avant l'importance des phénomènes successifs de sorption et de désorption, et de la transformation par les microorganismes, sur l'évolution de la quantité de MOD et de sa composition au cours de son transfert.

3.2 Méthodes de prélèvements

De nombreuses méthodes d'échantillonnage de la MOD existent, et ont montré des résultats différents et parfois contradictoires pour l'étude des espèces chimiques hydrosolubles dans les sols. Plusieurs équipements permettent de collecter directement la solution du sol *in situ*. Les échantillons obtenus à l'aide de ces méthodes permettent d'étudier la fraction des matières organiques considérée comme la MOD présente en situation naturelle. Les extractions à l'eau en laboratoire (WEOM), réalisées avec de l'eau ou des solutions faiblement salines, sont souvent utilisées. Choisies principalement pour des raisons pratiques, elles sont considérées comme un moyen d'approximer les caractéristiques de la MOD.

Les méthodes de prélèvement au terrain utilisent des systèmes de collection de l'eau du sol par capillarité (bougies poreuses, cannes lysimétriques) en utilisant une différence de pression, ou par gravité (plaques lysimétriques). Ces méthodes, censées permettre d'obtenir des échantillons représentatifs de la MOD présente *in situ*, ont cependant plusieurs inconvénients. Les méthodes par gravité ne permettent pas de récolter la fraction d'eau liée à la matrice du sol, qui correspond pourtant à la fraction où la réactivité de la MOD est favorisée du fait de l'interaction entre les phases liquides et solides du sol. Les méthodes de prélèvement par

capillarité ont montré des biais dus aux interactions entre les composés de la solution du sol et les céramiques poreuses, et l'équilibrage de ces appareils avec la solution du sol est une étape cruciale. De plus ces méthodes nécessitent beaucoup de temps pour collecter des échantillons.

Une approche intéressante est d'utiliser des forces de tensions différentes pour une comparaison de la MOD présente dans l'eau libre à celle présente dans l'eau liée (Andreasson et al., 2009). Un gradient dans le potentiel de biodégradabilité des MOD a été constaté par ces auteurs, avec une biodégradabilité croissante depuis les molécules organiques présentes dans l'eau libre, à celles présentes dans l'eau liée puis dans le WEOM.

Les méthodes d'extraction en laboratoire permettent d'isoler la matière organique extractible à l'eau (WEOM). Les quantités de WEOM sont souvent élevées en comparaison avec la quantité de MOD naturellement présente dans la solution du sol, et plusieurs études ont montré une aromaticité ($SUVA_{254}$) plus élevée du WEOM par rapport à la MOD (Rennert et al., 2007; Perdrial et al., 2012).

Ces résultats montrent une tendance à l'évolution de la composition et de la réactivité de la MOD en fonction du mode de prélèvement, et il est donc important de ne pas négliger la méthode d'échantillonnage dans l'interprétation des caractéristiques de la MOD. De plus les différences observées entre les méthodes de prélèvement *in situ* et les extractions en laboratoire (Hagedorn et al., 2004) justifient l'utilisation de termes différents pour leur dénomination. Dans la suite de ce chapitre introductif, et pour une facilité de lecture, l'utilisation générale du terme MOD fait référence à des études utilisant les différentes méthodes d'échantillonnage.

3.3 Réactivité et rôle dans le fonctionnement des sols

La MOD est systématiquement présentée comme un compartiment de MO très réactif, soumis aux influences conjuguées du climat, de l'activité microbienne et des propriétés physico-chimiques des sols. Comme annoncé précédemment, la production de MOD et sa minéralisation sont influencées par la température et par le régime hydrique des sols, ce qui démontre le rôle important de ce compartiment de MO dans le contexte actuel de changement climatique (Chow et al., 2006).

La mise en solution des MOS est décrite comme une étape de déstabilisation des MOS, et la composition des ces MOS solubilisées a montré une influence majeure de l'historique du sol. Le traçage isotopique naturel, dû à un remplacement de végétation C3 par du maïs (C4)

est un outil très adapté à l'étude du turn-over des MOS. Par exemple, Ellerbrock & Kaiser (2005) ont montré que plus de quarante ans après l'implantation de la culture du maïs, la MOD contenait autant de composés issus de la nouvelle culture que de l'ancienne. Ainsi le C plus vieux, est progressivement solubilisé et remplacé par du C issu de la décomposition du matériel végétal récent.

La MOD est considérée par certains auteurs comme un cortège de molécules continuellement transformées par l'activité microbienne et échangées entre la solution du sol et la matrice minérale solide au cours de sa migration vers la profondeur (Kaiser & Kalbitz, 2012; Malik & Gleixner, 2013) pour finalement contribuer à la stabilisation de la MO (Kalbitz & Kaiser, 2008).

3.4 Interaction avec les facteurs environnementaux

Plusieurs facteurs environnementaux ont une influence sur la dynamique de la MOD dans les sols. Les effets du climat, notamment de la température et du régime hydrique, ont été évoqués dans les sections précédentes.

Le type de sol est également un facteur important. La roche mère sur laquelle se développe le sol influence le pH et la proportion de surface de fixation (argiles, oxydes de Fe et Al). L'effet du pH induit des effets contradictoires. Si un pH plus élevé favorise la solubilisation des matières organiques, la baisse du pH entraîne la dissolution des complexes organo-métalliques, libérant les molécules organiques dans la solution du sol (Kalbitz et al., 2000b). Le pH a également un effet indirect sur les flux de MOD, via son impact sur les communautés microbiennes.

Le type de couvert végétal est également important pour la dynamique de la MOD. Du fait de teneurs en MOS souvent plus importantes, les concentrations de MOD dans les sols de forêt sont généralement plus élevées. Cependant l'exportation sous forme dissoute depuis les sols vers les systèmes hydrologiques est plus conséquente dans les écosystèmes de prairie (Kindler et al., 2011). Les sols de cultures sont le plus souvent caractérisés par des concentrations et des flux inférieurs.

La qualité de la MOD est également liée au type de sol et de couvert végétal. En analysant des échantillons d'eau de rivière, Mosher et al. (2010) ont observé des différences qualitatives de la MOD en fonction du pH, lui-même influencé par le type des

roches mères présentes dans le bassin versant. Une plus grande contribution de composés hydrocarbonés condensés a été observée pour les milieux à pH élevé alors que les lignines et tannins sont plus caractéristiques des milieux à pH bas (Roth et al., 2013). Dans une autre étude, Roth et al. (2014) ont également mis en évidence les différences de la composition de la MOD en fonction du type de couvert végétal. Des molécules organiques plus riches en oxygène et une plus grande contribution des lignines et des tannins a été observée pour la MOD prélevée dans des écosystèmes forestiers. Ces travaux ont également montré que le type d'environnement forestier (feuillus, conifères ou mixtes) se traduisait par des différences dans la composition chimique de la MOD, comme observé par Amiotte-Suchet et al. (2007).

4 Les principales techniques de caractérisation de la matière organique des sols

Un enjeu majeur pour les recherches sur les MO est sa caractérisation chimique. La MOS résulte de la transformation par de nombreux mécanismes différents des diverses molécules apportées par la litière. Il en résulte une diversité chimique extrêmement grande et à ce jour il n'existe pas de technique unique capable de décrypter l'ensemble des caractéristiques de la MOS au niveau moléculaire.

Une approche qui fut largement appliquée consiste à séparer des pools de MO en fonction de leur différence de solubilité en milieu acide ou alcalin. Ainsi les notions d'acides humiques, d'acides fulviques et d'humine ont été à la base d'un très grand nombre d'études sur la MOS. La limite majeure de cette approche est que si l'étude de ces compartiments de C a démontré leurs différences chimiques et physiques, la mise en relation entre ces fractions et leurs fonctions respectives dans les sols est toujours débattue.

Le fractionnement granulométrique du sol est également pratiqué depuis longtemps et a permis de montrer que la stabilisation des MO correspondait à un transfert vers la fraction fine (Angers et al., 1997). Les techniques isotopiques, en utilisant des traceurs naturels (végétation C3/C4) ou le marquage artificiel (le plus souvent ^{13}C et ^{15}N), permettent de suivre l'incorporation dans les différents compartiments du sol des MO ajoutées et de calculer les temps de résidence des différentes fractions (Balesdent et al., 1987; Jolivet et al., 2003; Schmitt et al., 2012; Dippold & Kuzyakov, 2013). Leur utilisation, couplée à des techniques

de chromatographie en phase gazeuse, permet la détermination des enrichissements isotopiques au niveau moléculaire (Kracht & Gleixner, 2000).

Le développement de méthodes permettant d'obtenir une information structurale des molécules organiques, comme la résonance magnétique nucléaire (RMN) ou la spectroscopie infrarouge (FTIR) ont permis d'obtenir des informations précieuses sur la qualité et l'origine des MOS, en fournissant une vue d'ensemble des structures moléculaires présentes dans un échantillon (Kögel-Knabner, 1997, 2002; Ellerbrock & Kaiser, 2005; Artz et al., 2008).

Développée récemment, la technique par imagerie NanoSIMS permet de visualiser la matière organique en ciblant différents isotopes. Son utilisation couplée au traçage isotopique permet l'observation des sites d'incorporation et de complexation de la MO (Vogel et al., 2014).

Les MOD peuvent également être caractérisées par les méthodes citées précédemment, mais bénéficient aussi de techniques applicables sur des échantillons liquides sans être dénaturées. De nombreuses techniques de fractionnement sont employées afin de surmonter les difficultés liées à la complexité moléculaire des échantillons.

Les séparations par taille moléculaire (chromatographie d'exclusion stérique, ultrafiltration) ou en fonction des propriétés chimiques (résines, chromatographie liquide) permettent une bonne discrimination des catégories moléculaires et une comparaison de nombreuses méthodes est présentée par Peuravuori et al. (2005). Ces techniques de séparation sont souvent couplées aux autres méthodes de caractérisation citées dans ce paragraphe.

Les techniques par spectroscopie dans l'ultraviolet et le visible, comme les mesures d'absorbance ou de fluorescence, sont également très utilisées. Elles permettent d'estimer l'aromaticité moyenne d'une solution, ou de quantifier la présence de groupes de molécules fluorescentes, ou fluorophores, et sont relativement bien documentées (Weishaar et al., 2003; Bowen et al., 2009; Fellman et al., 2009).

Enfin les techniques par spectrométrie de masse (Py-MS, qTOF-MS, FTICR-MS) permettent de déterminer le poids moléculaire d'un grand nombre de molécules en une seule analyse, avec une résolution permettant l'attribution de formules moléculaires irréfutables pour les techniques les plus puissantes (Kujawinski et al., 2002; Kunenkov et al., 2009b).

5 Problématique et objectifs de la thèse

Les MOD sont un compartiment réactif des sols et une meilleure évaluation des flux et de leur composition chimique permettrait d'améliorer considérablement les modèles de la dynamique du cycle du C dans les écosystèmes terrestres, et particulièrement les processus de stockage et de déstockage de C par les sols. Si des estimations des facteurs contrôlant les quantités de MOD lessivées depuis les sols ont été proposées (Kindler et al., 2011; Camino-Serrano et al., 2014), la détermination des facteurs liés à la composition de la MOD des sols reste peu élucidée.

Les objectifs de cette thèse sont d'évaluer l'importance des facteurs biotiques et abiotiques sur les caractéristiques de la MOD. Pour y parvenir, plusieurs approches expérimentales ont été développées. La totalité des expériences est basée sur des méthodes d'extraction à l'eau en laboratoire (WEOM)

La première étape, présentée dans le chapitre 2, avait pour objectif de déterminer les différences sur les propriétés du WEOM induites par trois méthodes d'extraction. Nous avons ensuite tenté de répondre aux trois grandes questions suivantes :

Existe-t-il un lien entre l'activité microbienne et la dynamique des matières organiques ?

L'influence des populations microbiennes sur la dynamique et les propriétés du WEOM a été étudiée dans le chapitre 3 en s'intéressant à l'impact de la diversité microbienne sur la dégradation de la MO. Dans le chapitre 4, une étude réalisée sur une large gamme de sols aux propriétés physico-chimiques variées a ensuite été réalisée afin de déterminer le lien entre le WEOM et la structure des communautés bactériennes.

Quelles sont les caractéristiques des sols qui contrôlent les propriétés du WEOM ?

Le chapitre 4 a également permis de rechercher les propriétés chimiques des sols agissant comme des facteurs de contrôle sur les propriétés du WEOM.

Quels sont les facteurs de contrôle de la composition moléculaire du WEOM ?

Dans le chapitre 5, une caractérisation moléculaire à haute résolution de la composition chimique du WEOM a été réalisée sur ces mêmes échantillons et une méthode d'estimation différente a été utilisée afin d'identifier les facteurs contrôlant la signature chimique du WEOM dans les sols.

Chapitre 2

Comparaison de protocoles d'extraction de la matière organique des sols extractible à l'eau

A comparison of extraction procedures for water-extractable organic matter in soils

J. Guigue[a], O. Mathieu[a], J. Lévêque[a], S. Mounier[b], R. Laffont[a], P.A. Maron[c]

N. Navarro[a,d], C. Chateau[e], P. Amiotte-suchet[a] and Y. Lucas[b]

[a] UMR 6282 Biogéosciences uB/CNRS, Université de Bourgogne, Dijon, France

[b] Laboratoire PROTEE-CAPTE, Université du Sud Toulon Var, La Garde, France

[c] UMR 1347 Agroécologie uB/INRA/AgroSup Dijon, Université de Bourgogne, Dijon, France

[d] Laboratoire PALEVO, Ecole Pratique des Hautes Etudes, Dijon, France

[e] UFR SVTE, Université de Bourgogne, Dijon, France

Published in *European Journal of Soil Science*

Résumé

Les caractéristiques de la matière organique dissoute des sols sont souvent étudiées au moyen d'extractions en laboratoire. De nombreux protocoles peuvent être utilisés pour extraire les matières organiques du sol (WEOM). Dans cette étude, nous avons utilisé cinq sols séchés à l'air pour comparer trois méthodes d'extraction des matières organiques extractibles à l'eau : (i) extraction haute pression et haute température (PH-WEOC), (ii) extraction par agitation (WEOC) et (iii) lixiviation de colonnes de sols (LEOC).

Nous avons quantifié la quantité de carbone organique extraite ; la qualité du WEOM a été caractérisée par absorbance UV, biodégradabilité potentielle (incubation pendant 48 jours), et par analyse factorielle parallèle (PARAFAC) de matrices d'excitation et d'émission de fluorescence (FEEMs).

La biodégradabilité du carbone organique dissout (DOC) a été décrite par deux pools de carbone organique. Les proportions des pools labiles et stables de DOC diffèrent peu entre les méthodes WEOC et LEOC , alors que les extraits obtenus par la méthode PH-WEOC contiennent plus de DOC stable. Les constantes de minéralisation des pools labiles et stables de DOC sont similaires pour les trois méthodes.

Les FEEMs ont été décomposées en trois composants de fluorescence : deux fluorophores de type humique et un fluorophore de type tryptophane. L'effet de la méthode d'extraction est peu discriminant et les protocoles les plus similaires sont PH-WEOC et LEOC, alors que la méthode WEOC produit des extraits appauvris en fluorophores de type humique.

Cette étude démontre que la qualité du WEOM est d'abord déterminée par les caractéristiques du sol et que les méthodes d'extraction ont un effet moins important, mais tout de même significatif, sur la qualité du WEOM. De plus, nous avons observé une interaction considérable entre les procédures d'extraction et les différents sols, montrant que les différences induites par la méthode d'extraction varient en fonction des caractéristiques du sol.

Abstract

The characteristics of dissolved organic matter (DOM) in soils are often determined through laboratory experiments. Many different protocols can be used to extract organic matter from soil. In this study, we used five air-dried soils to compare three extraction methods for water-extractable organic matter (WEOM) as follows: (i) pressurised hot-water extractable organic carbon (PH-WEOC); a percolation at high pressure and temperature, (ii) water extractable organic carbon (WEOC); a one-hour end-over shaking and (iii) leaching extractable organic carbon (LEOC); a leaching of soil columns at ambient conditions.

We quantified the extraction yield of organic carbon; the quality of WEOM was characterized by UV absorbance, potential biodegradability (48-day incubation), and parallel factor analysis (PARAFAC) modelling of fluorescence excitation emission matrices (FEEMs).

Biodegradation of dissolved organic carbon (DOC) was described by two pools of organic C. The proportions of labile and stable DOC pools differed only slightly between the WEOC and LEOC methods, while PH-WEOC contains more stable DOC. The mineralization rate constants of both labile and stable DOC pools were similar for the three methods.

The FEEMs were decomposed into three components: two humic-like fluorophores and a tryptophan-like fluorophore. The effect of extraction method was poorly discriminant and the most similar procedures were PH-WEOC and LEOC while WEOC extracts were depleted in humic-like fluorophores.

This study demonstrates that WEOM quality is primarily determined by soil characteristics and that the extraction method has a smaller, but still significant, impact on WEOM quality. Furthermore, we observed considerable interaction between extraction procedure and soil type, showing that method-induced differences in WEOM quality vary with soil characteristics.

1 Introduction

Mineralization and humification are major processes controlling the evolution of soil organic matter (SOM) in soil horizons and are closely related to dissolved organic matter (DOM) degradation and/or production. As DOM is the most active and mobile form of SOM (Zech et al., 1997; Corvasce et al., 2006), the comprehension of its dynamics is crucial in order to evaluate better the implication of soils in the terrestrial carbon (C) cycle. The concentration of DOM in the soil solution is regulated by the balance between production, degradation, stabilisation and leaching (Kalbitz et al., 2000b). The production of DOM is mainly controlled by biological processes, such as the decomposition of SOM, the release of root exudates and the lysis of microorganisms (Kalbitz et al., 2000b). The DOM represents a source of energy and nutrients for soil ecosystems and is the direct precursor of microbial growth and activity. It is thus the main driver for the decomposition processes of organic matter in soil (Boyer & Groffman, 1996; Marschner & Kalbitz, 2003).

Concentrations and fluxes of DOM in soils are often determined in laboratory experiments by characterizing water-extractable organic matter (WEOM). Many extraction protocols have been used to extract organic matter from soil (Wagai & Sollins, 2002; Kalbitz et al., 2003; McDowell et al., 2006), which complicates inter-study comparison. Such protocols diverge in terms of pressure, temperature (up to 200° C), extraction duration (from a few minutes to several hours), type and proportion of extractant, and type of extraction (including leaching, end-over shaking, or soil suspension). This variety of protocols could therefore lead to differences in the results obtained for extraction yield and WEOM quality (Schwesig et al., 1999; Wagai & Sollins, 2002; Landgraf et al., 2006). The implications of these potential differences have rarely been studied, and were limited to a single soil type in any given study (Schwesig et al., 1999; Zaccone et al., 2009; Nkhili et al., 2012).

In this study, we compare three different extraction procedures (high pressure and temperature, shaking and leaching) by quantifying and characterizing the WEOM from five different soils, all collected in France. The main objective was to determine the effect of each method on WEOM quality by measuring its potential biodegradability, absorbance and fluorescence properties.

2 Materials and methods

2.1 Sampling design

The three extraction procedures were compared, with samples from the A-horizon of five different soil types (IUSS Working Group WRB, 2006) developed on different parent materials, with various vegetation types, all from France. The sampling areas were all located within clearly identified soil units. The soils were selected with particular attention to texture and organic C content, to ensure that various types of organo-mineral associations would be studied. At each site, a five-kilogram composite of the A-horizon was collected from a soil pit with well-defined horizons. All soils were air-dried, sieved through a 2-mm mesh, and homogenized before further experiments.

Nine samples were randomly taken from each of the five soil composites. We then allocated, for each of the five soils, three of these nine samples to one of the three extraction methods (see below), thus giving a balanced design (5 soils x 3 replicates x 3 methods) with 45 observations. For the biodegradation experiment and the fluorescence analysis, all measurements were performed on each of the 45 extracts.

2.2 Soils

Soil 1: DA is a Dystric Andosol collected from "Le Puy de la Vache" in the Auvergne region (N 45°40'37''; E 2°57'53''), on the eastern slope of a Holocene scoria cone, at an elevation of 1032 m above sea level. It is an organic-rich soil, characterized by a small bulk density and the presence of allophanes. Vegetation is transitional woodland, mainly composed of conifers and ferns.

Soil 2: EP is an Entic Podzol collected from the top of "Le Massif de la Serre" in the Franche-Comté region (N 47°11'29''; E 5°33'50''), at an elevation of 378 m above sea level. The bedrock is Buntsandstein siliceous sandstone (Lower Triassic). This soil is well drained, and a thick, acidic mor-type organic horizon is present. Vegetation is a broad-leaved forest composed of oak, hornbeam and beech.

Table 1 Organic C and N contents, texture and pH of soils analysed for the comparison of extraction procedures. Values are means of three replicates and standard errors are given in parentheses.

Soil	Classification WRB 2006	C	N	C/N	$CaCO_3$	Sand	Silt	Clay	pH
		/ mg g^{-1}			/ mg g^{-1}	/ %			
DA	Dystric Andosol	135.9 (1.6)	8.60 (0.23)	15.8 (0.3)	-	31.5 (0.2)	47.3 (0.3)	21.2 (0.1)	5.49 (0.05)
EP	Entic Podzol	65.9 (0.4)	2.91 (0.01)	22.7 (0.2)	-	70.2 (0.4)	18.8 (0.1)	11.0 (0.1)	4.11 (0.02)
DC	Dystric Cambisol	29.7 (0.3)	2.88 (0.01)	10.3 (0.1)	-	58.5 (0.3)	21.6 (0.1)	19.9 (0.1)	5.29 (0.05)
GL	Gleyic Luvisol	9.6 (0.1)	1.00 (0.02)	9.4 (0.1)	-	22.3 (0.1)	64.6 (0.3)	13.1 (0.1)	5.98 (0.05)
EC	Eutric Cambisol	24.9 (0.2)	2.82 (0.03)	8.8 (0.1)	193 (3)	9.0 (0.1)	57.7 (0.3)	33.3 (0.2)	7.58 (0.05)

Soil 3: DC is a Dystric Cambisol collected in the Burgundy region (N 47°06'16"; E 4°25'55"). The site is located 390 m above sea level, near the top of a slightly sloping topographic depression. Vegetation is a mainly gramineous pasture, and bedrock consists of Upper Triassic siliceous sandstone.

Soil 4: EC is a Eutric Cambisol collected in the Burgundy region (N 47°23'12"; E 4°39'19"). The site is located 361 m above sea level, at the bottom of a valley, on calcareous alluvial deposits surrounded by Jurassic carbonate rocks. Vegetation is a mainly gramineous pasture.

Soil 5: GL is a Gleyic Luvisol collected from an agricultural area in the Burgundy region (N 47°07'23"; E 5°05'08"). The site is located 196 m above sea level, in the Bressan Graben and the parent material is recent loam deposits (Plio-Pleistocene). The soil has a massive structure and was bare when sampled.

Organic C and N contents were measured by dry combustion (Vario MICRO cube, Elementar, Hanau, Germany) after inorganic C removal from carbonate-containing samples by addition of an excess of 2 M HCl. Soil pH was determined in soil suspension (soil:water ratio of 1:4). Soil texture was determined using the Robinson pipette method and total carbonate content was quantified by the volumetric method using a Bernard calcimeter according to the standard French procedures (AFNOR, 1983; AFNOR, 1995). All measurements were performed in triplicate and characteristics for each soil are reported in Table 1.

2.3 Extraction procedures

Extraction Method 1: Pressurised hot-water extractable organic carbon (PH-WEOC) was extracted using a solvent extractor (ASE200, Dionex Corporation, Sunnyvale, USA). A 10-g soil sample was thoroughly mixed with 10 g of acid-washed sand, to enhance the drainage capacity of the soil. This mixture was placed in an extraction cell with a capacity of 22 ml and glass beads were added to completely fill the cell. Extraction consisted of five steps: (i) the cell was filled with water; (ii) pressure and temperature were stabilized at 100° C and 10 MPa, respectively, over a five-minute period; (iii) the extractable organic matter was dissolved at 100° C and 10 MPa during the static phase, which lasted for 10 minutes; (iv) the cell was flushed with 13 ml of ultrapure water; and (v) the cell was purged with an inert gas

(N_2) for two minutes. All conditions were based on the study of Schwesig et al. (1999) who have shown that WEOM was not altered at these settings. Before further analyses, all extracted solutions were filtered through 0.45 µm pore-size cellulose acetate filters.

Extraction Method 2: Water extractable organic carbon (WEOC) was obtained by shaking a 50-g soil sample with 200 ml ultrapure water at 120 revolutions per minute for 60 minutes at room temperature. Extraction solutions were then centrifuged for 15 minutes at 4600 g and filtered through 0.45 µm pore-size cellulose acetate filters. Unlike the two other methods, the WEOC extraction method led to the breakdown of soil aggregates.

Extraction Method 3: Leaching extractable organic carbon (LEOC) extractions were carried out on 100-g soil samples placed in glass columns (inner Ø = 54 mm). Glass beads were placed on the top to allow a homogeneous distribution of water over the section. Acid-washed sand was placed at the bottom of the column to prevent clogging and loss of soil particles. Columns were moistened overnight to avoid the creation of preferential flow paths. Each column was leached at room temperature with 400 ml ultrapure water at a flow rate of 1.5 ml per minute. The percolated solutions containing LEOC were collected and filtered through 0.45-µm pore-size cellulose acetate filters.

For each of the five soils, the three extraction methods were repeated three times on different samples, thus giving 45 observations (5 soils x 3 replicates x 3 methods). During subsequent steps, all measurements were performed on each of the 45 extracts.

2.4 Preliminary measurements

The extraction volume was determined gravimetrically and the pH was measured with a microelectrode N 5800 A (Schott Instruments, Mainz, Germany). The ultraviolet (UV) absorbance at 254 nm was measured with a Jenway 6715 (Essex, England). The specific UV absorbance at 254 nm ($SUVA_{254}$) of the samples was calculated as follows:

$$SUVA_{254} = UV_{254} \times (b \times C)$$

where UV_{254} is ultraviolet absorption at 254 nm; b is the optical path length in metres; and C is the DOC concentration of the samples in mg l^{-1}.

Organic C content in the extracted solutions was quantified in 5-ml sub-samples with a total organic carbon analyser (TOC 5000A, Shimadzu, Kyoto, Japan), after the addition of 20 µl 2 M HCl to remove inorganic C. The extraction ratio (ER), expressing the yield of the extraction procedure, was calculated as the ratio of extracted C to soil total organic C.

2.5 Determination of dissolved organic carbon biodegradability

The biodegradability of DOC was assessed by incubating the extracted solutions in the dark at 21° C for 48 days, with regular shaking. After a 0.22 µm membrane-filtration (cellulose nitrate) to remove microorganisms, solutions were diluted to a final concentration of 20 mg C l^{-1} or less, to avoid excessive microorganism growth. Sixty ml of each DOC solution was transferred to 145-ml incubation flasks. We then added one ml of a nutrient solution (ionic strength = 0.12 M), prepared with $(NH_4)_2SO_4$ and KH_2PO_4 to ensure C/N/P/S/K molar ratios of ≤5:1:1:1:1 (Bowen et al., 2009). To obtain a broad microbial diversity (Kalbitz et al., 2003), an inoculum was prepared from a mixture of the five soils and added to each sample, just before the flasks were sealed and incubated. A glucose solution (20 mg C l^{-1}) and an ultrapure water solution, each with the addition of the nutrient solution and the inoculum, were used as controls.

The CO_2 concentration was measured in the headspace of the flasks on days 1, 3, 5, 7, 14, 28 and 48, using gas chromatography and thermal conductivity detection (7890A, Agilent, Santa Clara, USA). The molar amount of CO_2 in the gas phase was calculated using the ideal gas law equation, and the calculation of CO_2 in the liquid phase was based on Henry's law. The sum of these two pools was considered as the total amount of CO_2 produced by microbial degradation. Mean values measured for the controls (ultrapure water) were deducted from values for the DOC-containing flasks.

To analyse the kinetics of DOC mineralization in the incubation experiment, following Kalbitz et al. (2003), a double exponential model with two distinct DOC pools was fitted to the calculated amount of produced CO_2 by means of the Quasi-Newton least-squares optimization method, using the maxLik package (Toomet & Henningsen, 2012) in R software (R Core Team, 2012).

The double exponential mineralization curve was in the form:

$$\text{Mineralized DOC} = (100 - a)(1 - \exp^{-k1t}) + a(1 - \exp^{-k2t})$$

where mineralized DOC is the CO_2 produced in percent of initial DOC; t is time in days; $(100 - a)$ is the percentage of DOC that is rapidly mineralized (labile pool); a is the percentage of DOC that is slowly mineralized (stable pool); $k1$ is the mineralization rate constant of the labile pool of DOC; $k2$ is the mineralization rate constant of the stable pool of DOC (both in day^{-1}).

2.6 Fluorescence analysis and PARAFAC modelling

For 3D-Fluorescence spectroscopy measurements, water-extracted solutions were diluted with ultrapure water in order to reach UV_{254} of 0.1. The fluorescence excitation emission matrices (FEEMs) were obtained with a Hitachi F-4500 (San Jose, USA) with the following settings: speed scan, 2400 nm per minute; excitation and emission bandwidth, 5 nm; excitation and emission step, 5 nm; response, 0.1 s; excitation interval, 250–500 nm; and emission interval, 250–600 nm. The FEEMs were corrected for inner-filter effects following the controlled dilution approach (Luciani et al., 2009). The 45 FEEMs were numerically corrected for Rayleigh and Raman scattering peaks before parallel factor analysis (PARAFAC) treatment.

The PARAFAC treatment of FEEMs is well referenced (Coble, 1996; Stedmon & Bro, 2008) and will not be detailed in this paper. Briefly, the 45 FEEMs were computed to identify the fluorescent components present in samples and their relative contribution to total fluorescence (Luciani et al., 2008) using the alternating least square algorithm of the 'N-way toolbox for MATLAB' (Andersson & Bro, 2000). The most appropriate number of components was assessed by using the core-consistency diagnostic (CORCONDIA) score. A three-component model, explaining 98.9% of FEEM variability and giving a CORCONDIA score of 81.7%, was selected as the appropriate PARAFAC model.

2.7 Statistical data analysis

Two-way ANOVAs were computed to estimate the effect of soil, of extraction method and of their interaction, on extraction ratio (ER), pH, $SUVA_{254}$, biodegradation characteristics and contribution scores of PARAFAC components. When necessary,

we applied log transformations to satisfy the requirements of residual normality and variance homogeneity.

Our interest lies in the pairwise differences between the three extraction methods, as none was considered as the reference method. These simple pairwise comparisons of the three methods were therefore assessed using the least significant difference test (LSD, $P \leq 0.05$), once their main effect had been found significant in the ANOVAs. The nine WEOM samples obtained from the EC soil were excluded from the ANOVAs for biodegradation parameters and PARAFAC components, since preliminary tests showed that the EC results biased the ANOVAs for these variables. The values obtained for the EC soil for these parameters are nevertheless presented and discussed in the following sections.

A principal component analysis (PCA) was performed on the correlation matrix of the DOC quality characteristics. The plot of the PCA individual scores on the first two components shows graphically the reproducibility of the methods. This reproducibility was numerically assessed with respect to the sum of the variances of the extraction triplicates on all principal components. All computations used JMP 9.0 (SAS Institute) statistical software.

3 Results and discussion

3.1 Extraction ratio, pH and $SUVA_{254}$

We observed great variability in extraction ratios (ERs), ranging from 2.1 ± 0.2 (mean ± standard error of the mean) to 35.6 ± 0.5 mg C g^{-1} soil C, depending on soils and extraction procedures (Fig. 1). For all methods, the ERs measured were of the same order of magnitude as in other studies using comparable extraction procedures (Schwesig et al., 1999; Gregorich et al., 2003; Akagi et al., 2007). The two-way ANOVA revealed a significant effect of both extraction procedure and soil on ER (Table 2). For all three methods, the largest ERs were found for soils GL and EP, and the smallest were found for EC and DA. The PH-WEOC method had the largest extraction yields, with ERs larger by a factor of 2 to 12 than the two other methods (Fig. 1). A positive correlation between WEOM content and CO_2 fluxes was reported in Zhao et al. (2008). These authors measured about four times more C mineralized as CO_2 after 35 days than C in WEOM at the initial stage, suggesting

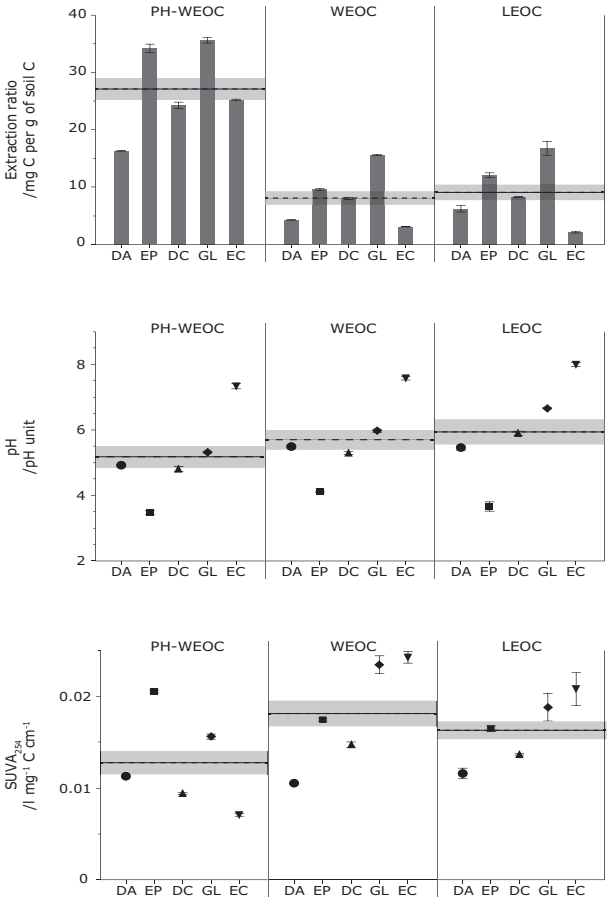

Figure 1 Extraction ratio (ER) in mg C extracted per gram of soil organic carbon (SOC), pH and specific UV absorbance at 254 nm ($SUVA_{254}$) in L mg^{-1} C cm^{-1}. Error bars represent the standard error of the mean of the three replicates. For each method, the dashed line and grey band represent the mean and the standard error of the mean.

Table 2 Summary table for the two-way ANOVAs of extraction ratio (ER), pH and $SUVA_{254}$. We excluded three observations for ER and two observations for $SUVA_{254}$, in order to fit correctly the ANOVA model on our data.

Source of variation	Degrees of freedom	Sum of squares	Mean square	*F*	*P*
Log(ER)					
Method	2	16.056	8.02788	7929.5	<0.05
Soil	4	8.598	2.14957	2123.2	<0.05
Method : Soil	8	2.556	0.31952	315.6	<0.05
Residuals	27	0.027	0.00101		
Total	41	26.508			
pH					
Method	2	4.574	2.2871	191.0	<0.05
Soil	4	70.983	17.7457	1482.1	<0.05
Method : Soil	8	1.871	0.2338	19.5	<0.05
Residuals	30	0.359	0.0120		
Total	44	77.787			
Log($SUVA_{254}$)					
Method	2	1.126	0.5631	377.9	<0.05
Soil	4	1.793	0.4482	300.9	<0.05
Method : Soil	8	2.316	0.2895	194.3	<0.05
Residuals	28	0.042	0.0015		
Total	42	5.271			

that a large proportion of potentially biodegradable C was not extracted at the initial stage. In our study, therefore, the increase in ER with the PH-WEOC method could corresponds to the extraction of a potentially reactive organic pool. The smaller ERs for the WEOC and LEOC methods were in similar ranges, and values were consistent for all soils (Fig. 1). The effect of interaction between extraction procedure and soil was also significant, meaning that the impact of the extraction procedure varied from one soil to another (Table 2). This interaction is clearly apparent for soil EC, which had the smallest ERs with the WEOC and LEOC methods and an intermediate ER with PH-WEOC (Fig. 1). The ER depends both on the extraction procedure and on the soil characteristics (such as texture, organic matter content and quality and/or type of aggregation). This result confirms the relevance of using several different soils to compare extraction procedures.

The pH measurements showed that parent material was the major influence on the chemistry of the extracted solutions, with smaller values for DA, EP and DC, which are all soils developed on siliceous rocks, while the highest pH values were measured for EC, a soil developed on calcareous rocks (Fig. 1). We also observed different pH values for the extracts from the three methods. The PH-WEOC extracts were more acidic, with pH values between 0.5 and 1.3 pH units lower than the other two methods. These lower pH values are attributed to the greater organic C concentrations in the extracted solutions, as observed in the study by Nkhili et al. (2012). The statistical analysis confirmed the major effect of soil on pH and the less pronounced, but considerable, effect of extraction method (Table 2).

The values of specific UV absorbance at 254 nm ($SUVA_{254}$) for extracted solutions ranged from 0.007 to 0.024 l mg C^{-1} cm^{-1} (Fig. 1) and the ANOVA revealed the significant effects of soil, of method and of their interaction on $SUVA_{254}$ (Table 2). We measured smaller $SUVA_{254}$ values for DA and DC soil extracts, while there were larger values in extracts from EP and GL soils, indicating greater aromatic C contents (Chin et al., 1994; Weishaar et al., 2003). The PH-WEOC extracts were less aromatic, suggesting that the increase in ER with PH-WEOC corresponds to the solubilization of less aromatic organic compounds, such as carbohydrates or organic acids. The smaller $SUVA_{254}$ values could also result from the alteration of aromatic organic molecules during extraction, as suggested by Nkhili et al. (2012) for hot-water extraction performed at 60° C. However, Schwesig et al. (1999) established with NMR measurements that, up to 150° C, WEOM was not altered with the PH-WEOC method. The biodegradation of labile organic compounds,

such as carbohydrates and amino acids, may have occurred during the LEOC and WEOC extractions (Rousk & Jones, 2010), which take more time and were conducted at ambient conditions. This process would not occur during PH-WEOC extraction because the extraction conditions of temperature and pressure must inhibit biodegradation. The preservation of labile compounds might thus explain the smaller $SUVA_{254}$ values measured in PH-WEOC extracts.

The $SUVA_{254}$ values for PH-WEOC extracts were smaller for DC and GL, but larger for EP, while the aromaticity of DA remained unchanged (Fig. 1). The EC soil gave contrasting results, with the largest $SUVA_{254}$ values for WEOC and LEOC and the smallest for PH-WEOC. These differences in the effect of method in relation to soil highlight the significant interaction between the extraction method and the soil, suggesting that generalizations about method-induced effects are not without risk.

3.2 Biodegradation experiment

The CO_2 produced from the glucose solution after the 48-day incubation confirmed that microorganism activity was adequate, with 85.7 ± 2.3% of the initial glucose C mineralized. For soil extract samples, the proportion of mineralized C ranged from 45% to 100% of the initial DOC stock and no lag phases were detected. It must be noted that the standard errors for biodegradation parameters were large, confirming the limited reproducibility of such experiments, as observed in other studies (Kalbitz et al., 2003; Kiikkilä et al., 2005). This type of experiment is based on the colonization of a sterile medium by microorganisms, and slight differences at the initial stage of incubation may result in divergence in microbial community composition and establishment. For this reason, the double exponential model was fitted to each replicate.

The good fit of the model (all fitted curves had R^2 >0.96) confirms that DOC mineralization was adequately described when considering two pools of organic C: a readily decomposable labile pool, and a stable pool that was more resistant to mineralization. The labile pool accounted for 15.5 to 41.2% of total DOC in our samples with mineralization rate constants ranging from 0.17 to 1.07 day^{-1}. For the stable pool, which accounted for 58.8 to 84.5% of total DOC, the mineralisation rate constants ranged from 0.007 to 0.048 day^{-1} (Fig. 2). The EC extracts are unusual and will be discussed after the main trends.

As the values obtained for the EC extracts were so atypical, they masked the main trends in the data, and were therefore removed from the ANOVA for stable DOC (*a*) and mineralization rate constants (*k1* and *k2*).

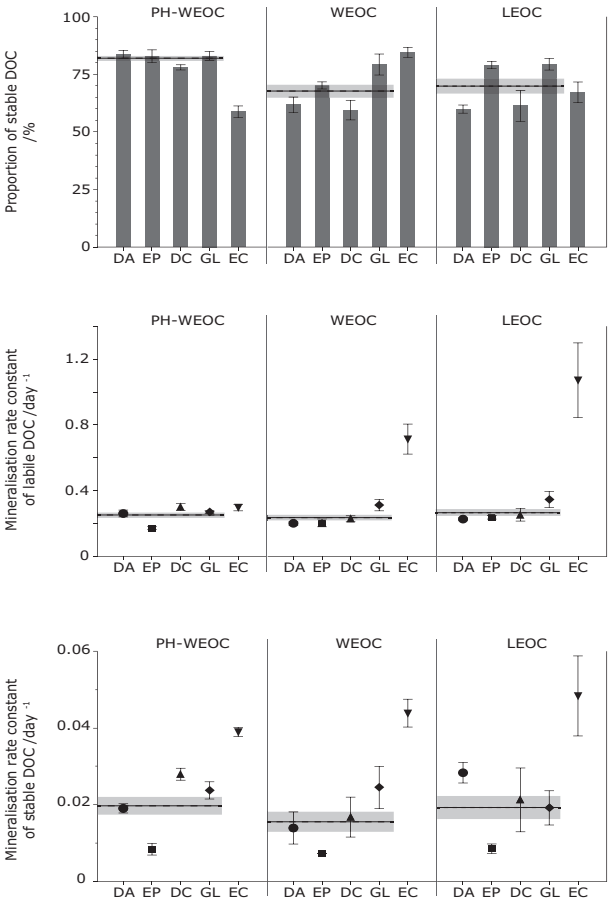

Figure 2 Percentage of stable DOC pool (*a*) and mineralisation rate constants of labile (*k1*) and stable (*k2*) pools both in day^{-1}. Error bars represent the standard error of the mean of the three replicates. For each method, the dashed line and grey band represent the mean and the standard error of the mean. The values for the EC soil were not included in the calculation of means and standard errors.

Table 3 Summary table for the two-way ANOVAs of the biodegradation characteristics. *a* is the percentage of stable DOC, *k1* is the mineralization rate constant of labile DOC and *k2* is the mineralization rate constant of stable DOC. The nine observations corresponding to the EC soil were excluded from the dataset because preliminary tests revealed that these samples biased the ANOVA models.

Source of variation	Degrees of freedom	Sum of squares	Mean square	*F*	*P*
a					
Method	2	1403.9	701.9	22.53	<0.05
Soil	3	1274.9	425.0	13.64	<0.05
Method : Soil	6	552.3	92.1	2.95	<0.05
Residuals	24	747.9	31.2		
Total	35	3978.9			
k1					
Method	2	0.0053	0.0026	1.45	0.25
Soil	3	0.0545	0.0181	9.96	<0.05
Method : Soil	6	0.0237	0.0040	2.17	0.08
Residuals	24	0.0438	0.0018		
Total	35	0.1272			
k2					
Method	2	0.00012	0.000062	1.36	0.27
Soil	3	0.00126	0.000420	9.17	<0.05
Method : Soil	6	0.00044	0.000073	1.59	0.19
Residuals	24	0.00110	0.000046		
Total	35	0.00292			

The two-way ANOVA indicated significant effects of method, of soil and of their interaction on the size of the stable pool (Table 3). The stable pool was large for solutions obtained from soils EP and GL while DC gave solutions with smaller proportions of stable DOC (Fig. 2). The proportions of stable DOC were consistent for samples obtained by either the LEOC or the WEOC method. For all these samples, we found a good correlation between the aromaticity ($SUVA_{254}$) and the size of the stable pool (r = 0.66; n = 30). Relationships between poor biodegradability and high aromaticity of WEOM have already been reported in other studies (Kalbitz et al., 2003; McDowell et al., 2006; Zhao et al., 2008). The PH-WEOC extracts were more enriched in stable DOC than extracts from the two other methods. This result is contradictory, as these extracts were previously characterized by small $SUVA_{254}$ values. Therefore the additional amounts of DOC extracted with this method preferentially originated from a more recalcitrant C pool that would release organic compounds with less aromaticity. The EC extracts produced very different results, with a smaller proportion of stable DOC in the PH-WEOC extracts, but much more in the WEOC extracts (Fig. 2), consistent with the $SUVA_{254}$ values.

The mineralization rate constants of the labile (*k1*) and stable (*k2*) pools give additional indications about DOC pool biodegradability. We detected no effect of the extraction procedure on *k1* (Table 3). For soils DA, EP, DC and GL, values of *k1* ranged from 0.17 to 0.35 day^{-1} (Fig. 2), and decreased in the following order: GL>DC>DA>EP. For soil EC, *k1* ranged from 0.30 to 1.07 day^{-1} and greatly different values were obtained for each method.

The mineralization rate constants of the stable pool (*k2*) ranged from 0.007 to 0.048 day^{-1} (Fig. 2). For the three methods, stable DOC from soil EP had the smallest *k2*, while the largest values were obtained for soil EC. The values obtained for DA, DC and GL were close, and were all intermediate. No significant differences in *k2* were induced by the extraction procedure, nor by interaction (Table 3), revealing similar potential for biodegradation of the stable pool of DOC, whatever the method used.

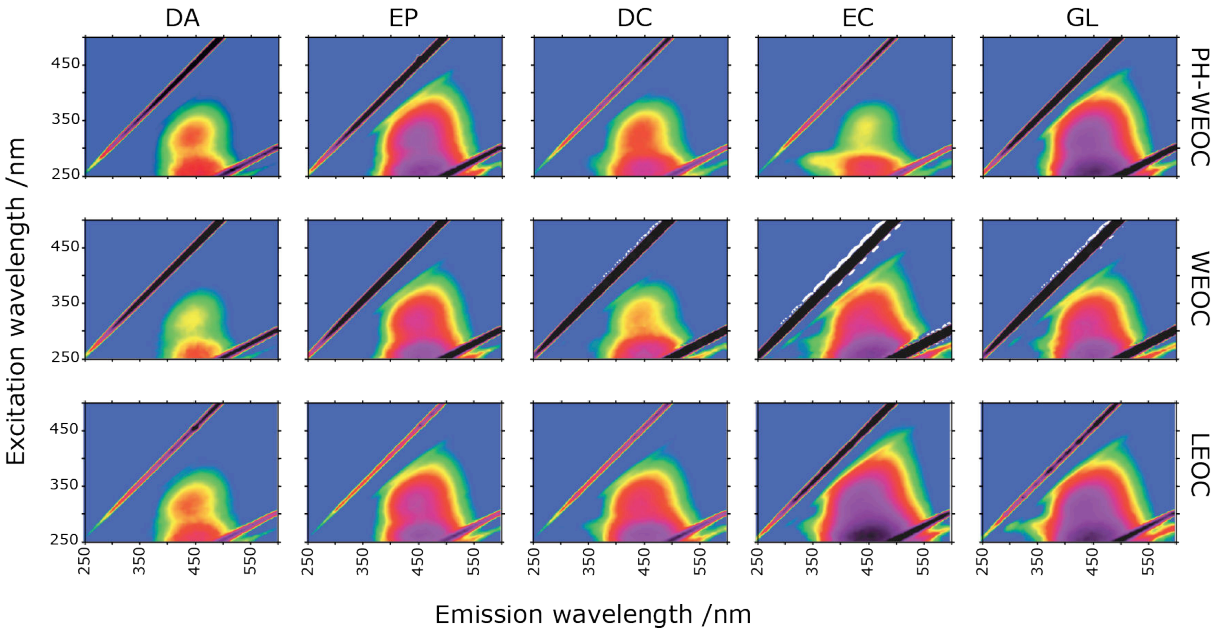

Figure 3 Fluorescence excitation-emission matrices of one replicate for each of the DOM samples extracted using PH-WEOC, WEOC and LEOC extraction procedures for the five soils. Fluorescence intensity is an arbitrary unit and all matrices were normalised relative to their respective carbon concentrations.

The *k2* parameter was strongly correlated with the pH of the solution extracted (r = 0.76; n = 45), suggesting that pH controls the biodegradation of this large pool of DOC. This correlation may indicate why EC, which is the most alkaline soil in our study, was characterized by the larger mineralization rate constant. The WEOM extracted from soils with higher pH values may contain more easily biodegradable molecules, but the biodegradation dynamics of DOC could also be enhanced by higher pH in the incubated solution. Indeed, pH is known to strongly control microorganism diversity and activity in soils, with higher pH favouring the degradation of organic matter (Ranjard et al., 2010). It is not possible here to distinguish the respective influence of each of these two different causes. The influence of pH appears to be of major importance for monitoring DOC biodegradation and we therefore recommend standardizing pH in further experiments, to assess the potential degradability of DOC from different sources in more stringently rigorous conditions.

3.3 Fluorescence analysis

Visual analysis of the fluorescence excitation emission matrices (FEEMs) showed considerable method-induced differences in fluorescence characteristics for the EC soil, while for each of the other soils the FEEMs obtained with the three methods were similar (Fig. 3). However, for all of the methods, the FEEMs revealed apparent differences between the soils. All 45 samples had primary fluorescence regions around 250 nm/450 nm (λ excitation / λ emission) and 325 nm/450 nm. Another fluorescence region at approximately 275 nm/350 nm was observed, especially for EC.

This descriptive approach is a first step in explaining FEEMs. The PARAFAC modelling of FEEMs and their decomposition into individual component contributions is an adequate complementary approach, because it allows differences in fluorescence components for each sample to be quantified. The representations in FEEMs of the three normalized PARAFAC components are presented in Figure 4. In order to compare samples, contribution scores of these three components were normalized to C concentration (Fig. 4).

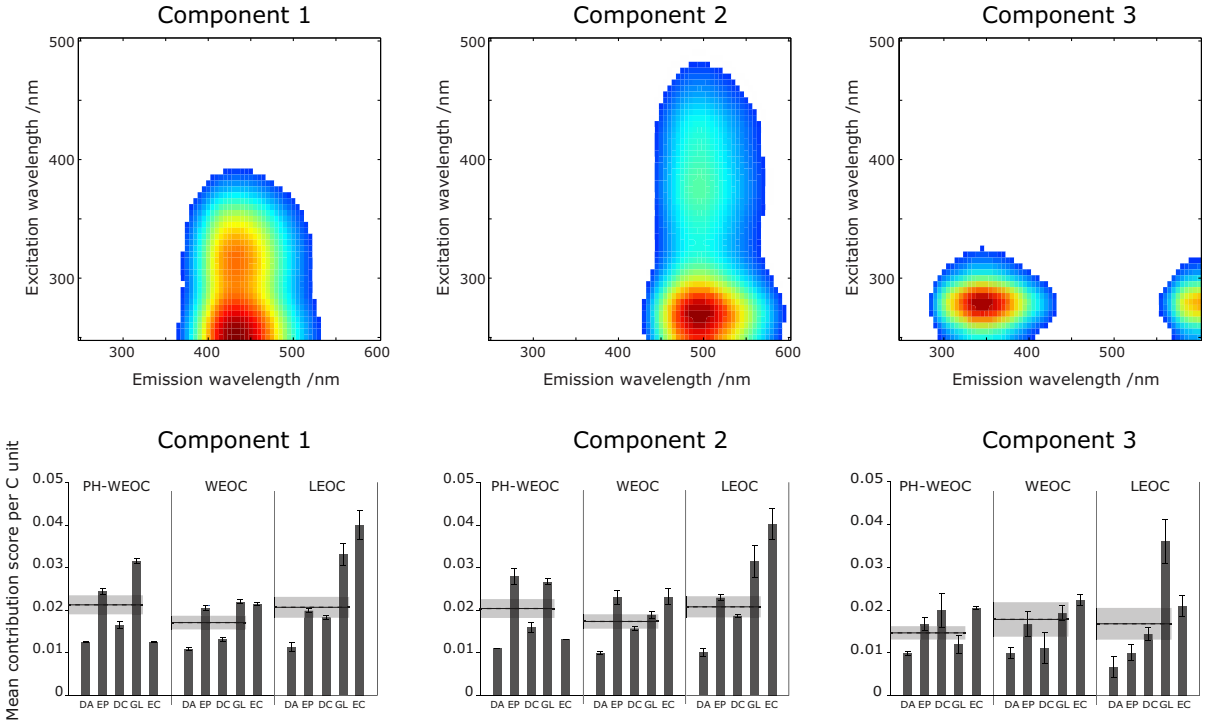

Figure 4 Fluorescence excitation-emission matrix (FEEM) representations of the three normalised PARAFAC components (top row). Mean contribution scores of the three PARAFAC components (normalised per C unit) for the solutions extracted from the five soils using the three methods (bottom row). Component 1 is a humic-like fluorophore. Component 2 is a humic-like fluorophore with longer excitation and emission wavelengths, characteristic of a higher content in aromatic and high molecular weight humic materials. Component 3 is a tryptophan-like fluorophore. More details of the three components are given in the text. Error bars represent the standard error of the mean of the three replicates. For each method, the dashed line and grey band represent the mean and the standard error of the mean. The values for the EC soil were not included in the calculation of means and standard errors.

Table 4 Summary table for the two-way ANOVAs of contribution scores of PARAFAC components. The nine observations corresponding to the EC soil were excluded from the dataset because preliminary tests revealed that these samples biased the ANOVA models.

Source of variation	Degrees of freedom	Sum of squares	Mean square	*F*	*P*
Log(Cp1)					
Method	2	0.284	0.142	19.46	<0.05
Soil	3	4.147	1.382	189.43	<0.05
Method : Soil	6	0.279	0.047	6.38	<0.05
Residuals	24	0.175	0.007		
Total	35	4.885			
Log(Cp2)					
Method	2	0.172	0.086	7.13	<0.05
Soil	3	4.802	1.601	132.48	<0.05
Method : Soil	6	0.349	0.058	4.81	<0.05
Residuals	24	0.290	0.012		
Total	35	5.613			
Log(Cp3)					
Method	2	0.088	0.044	0.25	0.78
Soil	3	3.820	1.273	7.26	<0.05
Method : Soil	6	4.457	0.743	4.23	<0.05
Residuals	24	4.212	0.175		
Total	35	12.576			

Components 1 (Cp1) and 2 (Cp2) comprised two unresolved peaks with two excitation spectral peaks and a single emission peak. The first peak of Cp1 had a wavelength domain of about 330 nm/410–460 nm. The second peak is more intense and had a wavelength domain of about 260 nm/390–480 nm. These two fluorescence regions were respectively attributed to type C and type A humic-like compounds (Coble, 1996; Stedmon & Markager, 2005). The Cp2 covered longer wavelengths for excitation and emission (Fig. 4) and had a domain of about 360–400 nm/470–510 nm for its first peak, and one of about 270 nm/450–550 nm for the more intense, second peak. The shift in longer wavelengths is characteristic of terrestrial humic-like compounds (Stedmon & Markager, 2005) and may result from a larger content of aromatic and large molecular weight humic materials, with a large degree of conjugation (Barančíková et al., 1997). In comparison with Cp1, Cp2 is interpreted as a consequence of a more advanced maturation of organic molecules. These two humic-like fluorophores were well correlated (r = 0.95; n = 45) and will therefore be discussed together. This correlation shows that these two humic-like components are composed of molecules that are mobilized and extracted together. These two components were attributed to the results of lignin breakdown (Cory & McKnight, 2005) and have been identified in DOM from forest and agricultural streams, wastewater and seawater environments.

In our samples, the results for EC extracts were not included in the ANOVAs because, once again, they biased the results, masking the main trends present in the data. We found a major effect of soil and much less pronounced effects of method and interaction on abundance in Cp1 and Cp2 (Table 4). The EP and GL extracts contain more of these humic-like fluorophores, while smaller abundances were found in DA and DC (Fig. 4). These results are consistent with the soil differences observed for aromaticity and biodegradability of extracted DOC. The LSD tests revealed that the contribution scores for Cp1 and Cp2 were not statistically different for the PH-WEOC and LEOC extracts, while the WEOC method is characterised by a smaller contribution of these two components. This result revealed greater similarities in the DOM extracted by the PH-WEOC and LEOC methods, while DOM was depleted in humic-like components in the WEOC extracts.

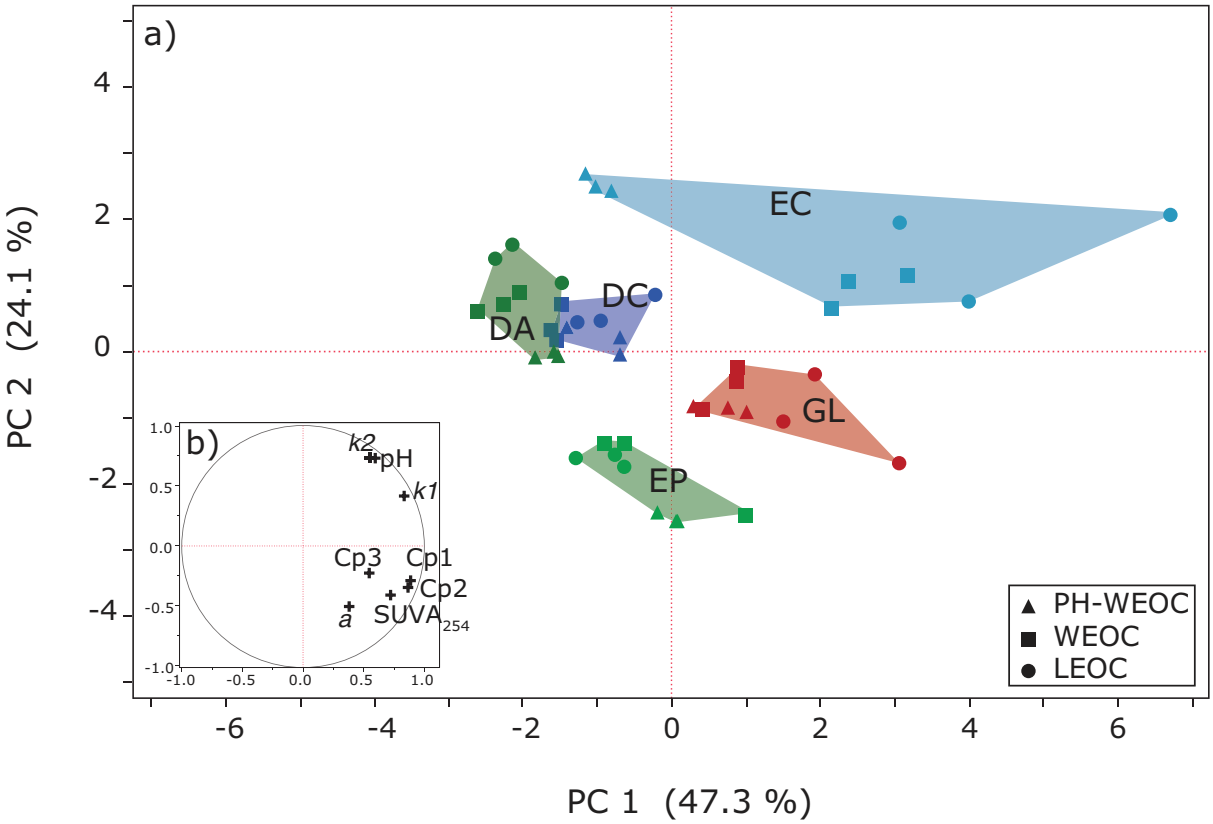

Figure 5 Biplot of the Principal Component Analysis (PCA) of the 45 DOM solutions (corresponding to the three extraction procedures, applied to the three replicates for each of the five soils) along the first (PC 1) and second (PC 2) principal components. Eight variables were investigated in the PCA (*a*: the proportion of stable DOC; *k1*: the mineralisation rate constant for the labile DOC; *k2*: the mineralisation rate constant for the stable DOC; pH; $SUVA_{254}$; and the three PARAFAC components (Cp 1, Cp 2 and Cp 3). The variable loadings are represented in the PCA space by crosses. The coloured domains correspond to the convex hulls for soils and have no statistical significance.

Component 3 (Cp3) is composed of two peaks with two distinct spectral emission peaks. The wavelength domain of about 275 nm /330–360 nm is attributed to peak T, a tryptophan-like fluorophore (Coble et al., 1998; Stedmon & Markager, 2005), reported to be a good indicator for the size and activity of the microbial community (Cammack et al., 2004; Hudson et al., 2008), and to be correlated with dissolved organic N and P concentrations (Fellman et al., 2009). The other peak with a maximum emission around 600 nm is, to our knowledge, not reported in the literature, and is therefore considered as the result of noisy signals in this short excitation wavelength region (Fig. 4).

For Cp3, we found a significant effect induced by the soil but not by the extraction procedure (Table 4). However, the interaction is significant, and a global view of the data clearly highlights that the three extraction methods produced contrasting results when applied to the different soils (Fig. 4). Therefore, this pronounced interaction makes it difficult to interpret and/or compare results concerning this tryptophan-like fluorophore in extracts obtained by any of the three methods.

To sum up the information obtained from fluorescence measurements, there are considerable differences in the fluorescence properties of the solutions extracted from the five soils (Fig. 3 and 4). In contrast, the effect of extraction method was less discriminant and the two most similar methods were PH-WEOC and LEOC, while WEOC was characterized by smaller proportions of humic-like fluorophores, Cp1 and Cp2. The influence of extraction is more apparent for Cp3, and we detected considerable interaction between the three methods and the soils.

3.4 Global quality of extracted DOM

The first two dimensions of the PCA space obtained from DOM qualitative characteristics are presented in Figure 5. The first principal component (PC 1), accounting for 47.3% of the variation, is mainly driven by the PARAFAC components, the $SUVA_{254}$ and *k1* (Fig. 5b). For the second principal component (PC 2), explaining 24.1% of the variation, pH and *k2* contributed the most to the ordination on this second axis (Fig. 5b). The PCA corroborates the discrimination between soils, as the five groups are clearly disconnected in the score plot of the PCA (Fig. 5a). This pattern indicates that the soil type determines the major differences observed for WEOM quality and adequately summarizes the results reported here.

The WEOM from EP and GL was enriched in humic-like and aromatic compounds and in stable DOC (*a*) whereas that from DA and DC was less aromatic, contained fewer humic-like fluorophores and had a smaller proportion of stable DOC. The PCA also demonstrates the limited impact of the extraction procedure on overall DOM quality. For soils DA, DC, EP and GL, the PCA reveals no clear patterns corresponding to a method-induced effect, whether for PH-WEOC, WEOC or LEOC, as all samples for a given soil are tightly clustered in the PCA space. The PCA therefore indicates only slight changes in the quality of the DOM obtained by the three extraction methods. The impact of method on DOM quality is much more evident for EC, with a clear separation along PC 1 for extracts obtained by each of the three extraction procedures. The alkaline pH and the presence of calcium carbonate in this soil could be a reason for its particular behaviour. The effect of calcium on WEOM was well described by (Balaria, 2011). Finally, PH-WEOC replicate sample locations were closer in the PCA space than those obtained with the WEOC and LEOC extraction methods. The comparisons of the pooled variance between extraction procedures reveal similar reproducibility for the WEOC and LEOC extraction methods, while the reproducibility of the extraction was significantly better for samples extracted using the PH-WEOC method.

Conclusion

This study provides evidence that WEOM quantity and quality depend primarily on soil characteristics. We found that different extraction methods also lead to differences in the quantity and quality of WEOM. However, these differences are not overly pronounced and none of the three methods led to great differences in the chemical properties of the WEOM extracted, except for EC, an alkaline grassland soil.

The WEOC and LEOC methods give very similar results for the extraction yields (ER) and for the biodegradation characteristics. The main differences observed in WEOM obtained by these two methods were the fluorescence properties, as smaller abundances of humic-like fluorophores were found in the WEOC extracts.

In comparison with WEOC and LEOC, the extraction yields were considerably increased and reproducibility was enhanced with the PH-WEOC method. The PH-WEOC extracts were less aromatic and contained a larger proportion of stable DOC. These results showed

that the increase in the extraction yields with this method corresponded to the preferential solubilisation of organic compounds with low aromaticity, and which were resistant to biodegradation. The fluorescence properties of the WEOM obtained with the PH-WEOC method were very close to those observed with the LEOC method. As the PH-WEOC method did not extract WEOM with greatly different characteristics, it can therefore be used in WEOM studies.

Finally, this work confirms that caution should be exercised when comparing results obtained using different extraction methods. As results for the alkaline loamy soil sample (EC) showed, the use of different extraction methods may considerably modify the quality of the organic material extracted. Therefore further studies seem essential to develop standardized methods for the extraction of WEOM from soils. The ecological role of WEOM in soils is of primary importance and better knowledge of this role is required in order to propose a standardized extraction method.

Acknowledgements

This work was supported by the French National Research Agency (ANR Systerra, DIMIMOS project). We thank Marie-Jeanne Milloux, Ida Fleure Ibinga, Jennifer Mignon, Fidimpali Thiombiano and Brice Marlet for their assistance in the laboratory and Etienne Brulebois for his help in data analysis. We also wish to thank the Editor in Chief Stephen Jarvis, the associate editor, the statistical panel and the anonymous reviewers for the handling of our manuscript, their constructive criticism and their valuable suggestions.

Chapitre 3

Effet de la diversité bactérienne sur la dégradation des matières organiques. Approche par traçage isotopique ^{13}C

The effect of bacterial diversity on soil organic matter decomposition. An approach using a ^{13}C-labelling technique

Contributions

L'expérience présentée dans ce chapitre a été réalisée en 2009, dans le cadre de la tâche 1 du projet **ANR DIMIMOS** (Lien entre la diversité microbienne et le turn-over des matières organiques dans les sols agricoles).

Ce travail, coordonné par **Pierre-Alain Maron** et **Jean Lévêque**, a été initié grâce à la contribution d'**Aurore Kaisermann**, au cours de son stage de Master 2 en 2009, qui a conduit l'expérience d'incubation ainsi que les mesures des concentrations en CO_2 et de son enrichissement isotopique, et le suivi de l'abondance, de la diversité, et de la structure des communautés bactériennes.

L'année suivante, **Maud Naulier**, également au cours de son stage de Master 2, a procédé aux extractions de matière organique soluble et aux mesures de concentration et d'enrichissement isotopique sur le sol et la fraction soluble.

Amadou Sarr a également été impliqué dans ces travaux, notamment pour la gestion logistique des échantillons et de la base de données.

Ma contribution personnelle à ce travail a donc débuté après que l'expérience ait été réalisée et porte sur la vérification et la correction des calculs sur les données transmises, ainsi que la répétition des extractions de matière organique soluble, avec la contribution de **Marie Denis**, et des mesures de concentration et d'enrichissement isotopique sur le sol et la fraction soluble.

Résumé

Les matières organiques du sol représentent le pool de carbone (C) principal des écosystèmes terrestres, avec des quantités de C à peu près deux fois plus grandes que pour le CO_2 atmosphérique. Dans les agrosystèmes, les amendements organiques sont une pratique commune pour maintenir les stocks de C organique dans les sols. Cependant, des études récentes ont révélé que ces pratiques peuvent induire le phénomène de *priming effect*, qui correspond à une augmentation du transfert de C vers l'atmosphère, due à la surminéralisation du carbone organique endogène du sol. Une meilleure compréhension des cycles biogéochimiques associés à la dynamique des matières organiques du sol permettrait donc de prendre les décisions les plus appropriées en terme d'amendement organique. Puisque les microorganismes du sol sont des acteurs majeurs de la transformation de la matière organique, leur diversité influence probablement cette dynamique. Dans ce contexte, il serait intéressant de caractériser plus précisément les relations entre la diversité microbienne et la dynamique de dégradation des matières organiques du sol.

Trois niveaux de diversité bactérienne (D1>D2>D3) ont été obtenus par des dilutions en série d'une solution de sol. Des microcosmes de sol stérilisé par rayonnement γ ont été inoculés avec les trois niveaux de diversité pour étudier les conséquences de l'érosion de diversité. Des résidus de blé enrichis en ^{13}C (à plus de 95%) ont été incorporés dans les microcosmes. La décomposition de ce résidu marqué et de la matière organique endogène a été estimée au cours d'une expérience d'incubation de 60 jours. L'enrichissement en ^{13}C a été mesuré dans le CO_2 produit par l'activité microbienne, dans les matières organiques extraites à l'eau (PH-WEOC) et dans la matière organique du sol (MOS).

L'apport de matière organique fraîche enrichie en ^{13}C est à l'origine de changements de la qualité et des quantités de PH-WEOC dans les microcosmes amendés, et révèle l'influence de la diversité bactérienne sur le pool de matière organique labile. Nous avons observé que l'évolution de l'enrichissement en ^{13}C dans le PH-WEOC était synchrone avec le mécanisme de *priming effect*. Cette découverte met en évidence la connexion étroite entre ce pool labile de C et la biodégradation du C dans les sols. Les résultats montrent également que l'intensité de la respiration du sol, et le *priming effect*, sont fortement impactés par le niveau de diversité bactérienne, avec les flux de CO_2 mesurés les plus élevés pour la communauté bactérienne la plus diversifiée. Ces résultats illustrent l'importance de considérer la diversité bactérienne

comme une variable prédictive pour le stockage/déstockage du C dans les sols. La technique de marquage isotopique ^{13}C est considérée comme une technique fiable pour suivre à la fois l'incorporation de matière organique fraîche dans les pools labiles et stables, ainsi que pour différencier les sources de C minéralisées. Enfin, cette étude montre la pertinence de la technique de marquage isotopique ^{13}C pour la quantification du *priming effect*.

Abstract

Soil organic matter (SOM) represents the main pool of carbon within terrestrial ecosystems, estimated at roughly twice that in atmospheric CO_2. In agrosystems, organic amendments are common to maintain soil C stocks. However, recent studies have revealed that these practices can lead to a priming effect, corresponding to enhanced release of CO_2 into the atmosphere, due to over-mineralisation of soil organic carbon. Therefore, appropriate decisions regarding organic input management require better understanding of the biogeochemical cycles related to SOM dynamics. As soil microorganisms are major actors in SOM turnover, their diversity is likely to influence SOM dynamics. In this context, the relationship between microbial diversity and SOM decomposition should be characterised more precisely.

Three levels of soil bacterial diversity (D1>D2>D3) were obtained by serial dilutions of a soil suspension. γ-ray sterilised soil microcosms were subsequently inoculated with the three levels of microbial diversity to investigate the consequences of the erosion of bacterial diversity. Wheat residues labelled at more than 95% with ^{13}C were incorporated into microcosms. Decomposition of these labelled residues and of endogenous organic matter was assessed during a 60 day-incubation experiment. The enrichment in ^{13}C was measured in the CO_2 produced by the microbial activity, in the pressurised hot-water extractable organic carbon (PH-WEOC) and in the SOM.

The input of ^{13}C-labelled FOM resulted in changes in the quality and amount of PH-WEOC in the amended microcosms, and reveals the influence of bacterial diversity on the labile organic matter pool. We observed that the evolution of ^{13}C enrichment in the PH-WEOC pool was synchronous with the priming effect mechanism. This finding highlights the close connection between this labile pool of C and the biodegradation of C in soils leading to mineralisation. Results also showed that the intensity of soil respiration as well as of the priming-effect induced by the addition of plant residues was strongly linked to bacterial diversity, with the highest CO_2 production measured when bacterial diversity was greatest. These results illustrate the importance of considering bacterial diversity as a predictive variable for organic carbon storage/release in soils. The ^{13}C-labelling technique is considered as a suitable technique for monitoring both the incorporation of FOM into labile and stable pools of soil organic matter, and the amount of carbon mineralised from

FOM ($^{13}CO_2$) and SOM ($^{12}CO_2$). Lastly, this study clearly shows that the ^{13}C-labelling technique is highly relevant for priming effect quantification.

1 Introduction

La dynamique des matières organiques du sol est une composante majeure du cycle du carbone (C) dans les écosystèmes terrestres. Les sols contiennent à peu près autant de C organique (C_{org}) dans le mètre supérieur (≈1500 Gt C) que l'atmosphère (≈840 Gt C) et la végétation (450–650 Gt C) réunis (Batjes, 1996; Ciais et al., 2013; Scharlemann et al., 2014). L'équilibre des stocks de C_{org} du sol est susceptible d'être impacté par des changements d'occupation du sol, par les pratiques culturales ou par de nombreuses perturbations de l'environnement (Murty et al., 2002; Sainju et al., 2005; Treat & Frolking, 2013). Une augmentation du stockage de C_{org} dans le sol pourrait permettre de compenser la hausse des concentrations en CO_2 atmosphériques et le réchauffement climatique qui en résulte.

Dans les sols, la matière organique (MO) est utilisée comme source d'énergie par les microorganismes. Une partie de cette MO est minéralisée alors qu'une autre partie subit une transformation permettant la préservation d'une partie des composés organiques ainsi formés (Lutzow et al., 2006). La structure complexe des communautés bactériennes ainsi que la grande diversité de composés organiques font que le rôle joué par les communautés bactériennes dans la dynamique des matières organiques n'est pas encore bien expliqué. La diversité des communautés bactériennes est parfois considérée comme ayant peu d'impact sur la dynamique de dégradation de la MO et sur la fonctionnalité de l'écosystème du sol du fait de la redondance fonctionnelle (Nannipieri et al., 2003; Wertz et al., 2006). Cette supposition est basée sur le fait que des milliers d'espèces bactériennes différentes peuvent constituer une communauté et que ces espèces sont capables d'assurer des fonctions relativement variées. Ainsi, ces auteurs considèrent qu'une perte de diversité ne résulterait pas en une modification des fonctions assurées par la communauté, d'autres espèces assurant le rôle qui était celui des espèces ayant disparu.

Le maintien des stocks de C_{org} dans le sol dépend de l'entrée régulière de C_{org} dans le système, pour contrebalancer les pertes dues à la minéralisation de la MO. Cependant, des études montrent que l'apport de MO fraîche a parfois pour effet une baisse des teneurs en C_{org} dans les sols (Fontaine et al., 2004; Guenet et al., 2012). Ces auteurs ont expliqué que l'ajout de MO fraîche pouvait stimuler la croissance des communautés bactériennes et menait à une minéralisation accrue des différents stocks de la MO du sol. Ce phénomène, appelé *priming effect* (PE) peut mener à des conséquences inattendues des pratiques culturales,

causant un déstockage du C_{org} des sols vers l'atmosphère. Si ce phénomène a été démontré dans de nombreuses études (e.g. Dalenberg & Jager, 1981; Hamer & Marschner, 2005; Pascault et al., 2013), la compréhension de la dynamique du PE après l'apport de MO fraîche reste une problématique d'actualité et l'effet d'une baisse de la diversité bactérienne a été très peu étudié (Juarez et al., 2013).

La matière organique dissoute (MOD) représente généralement moins de 2% du stock total de MO dans un sol, mais son implication dans la dynamique des matières organiques du sol illustre son importance. Des augmentations des flux de MOD exportée lors de changements d'occupation du sol et une relation étroite entre les concentrations en MOD et les flux de CO_2 ont notamment été rapportés (Kalbitz et al., 2000a; Zhao et al., 2008). Les études sur la MOD sont souvent menées en analysant la matière organique extractible à l'eau (WEOM). Des auteurs ont ainsi fait le lien entre les caractéristiques de la WEOM obtenue par une extraction à l'eau chaude et la biomasse microbienne des sols, et ont suggéré que ce pool représente le pool de MO labile dans les sols (Sparling et al., 1998). Le WEOM, qui est caractérisé comme réactif et sensible au changement de la dynamique de la MO, présente donc un intérêt pour l'étude de la minéralisation du C_{org} et du phénomène de PE.

Les différences de composition isotopique entre les différents compartiments de C_{org} dans les sols sont utilisées depuis de nombreuses années afin de quantifier les stocks et d'estimer leur évolution. Cette approche a été souvent utilisée dans des contextes de changement de végétation, en profitant des signatures isotopiques naturellement distinctes entre les plantes C3 et C4 (Balesdent et al., 1987; Desjardins et al., 1994; Flessa et al., 2008). L'enrichissement artificiel de végétaux, notamment en ^{13}C et ^{15}N, permet de créer des différences plus grandes dans la composition isotopique d'un matériel enrichi (pouvant approcher une abondance en ^{13}C de 100%) par rapport à l'enrichissement naturel de la MO (environ 1% de ^{13}C). Cette approche permet de tracer le devenir du matériel enrichi au cours de sa transformation dans le sol (Yevdokimov et al., 2006; Schmitt et al., 2012).

L'objectif de cette étude était de déterminer l'effet de la diversité bactérienne sur la dynamique de décomposition de la MO. L'expérience a également été conçue afin de pouvoir estimer si un amendement organique provoque un stockage ou un déstockage de C via le phénomène de PE. L'amendement organique a été apporté sous la forme d'un résidu de blé enrichi en ^{13}C. Un gradient de diversité bactérienne a été créé artificiellement et inoculé dans

des microcosmes de sols préalablement stérilisés. La dynamique du C a été suivie pendant deux mois d'incubation, avec des mesures régulières du C total et du ^{13}C dans le sol, dans les extractions de WEOM et dans l'atmosphère des fioles (CO_2 minéralisé). L'évolution de la taille et de la composition isotopique des différents réservoirs de C nous a permis d'estimer les contributions relatives de la MO du sol et de l'amendement dans la dynamique de dégradation de la MO.

2 Matériels et méthodes

2.1 Caractéristiques du sol

Le sol utilisé pour la préparation des microcosmes est un Dystric Cambisol (IUSS Working Group WRB, 2006). Les 10 cm supérieurs ont été prélevés, en septembre 2008, sur le site de l'observatoire régional de l'environnement de Lusignan dans l'ouest de la France (46°25'13"N; 0°07'29"E). Il a ensuite été tamisé (<4 mm), puis stérilisé par rayonnement γ (35kGy).

Le sol prélevé contient 15% de sable, 67% de limons et 18% d'argiles. Le pH (sol:eau 1:5) est de 6,6 et les teneurs en C_{org} et en azote par gramme de sol sec sont respectivement de 13,2 mg g^{-1} et 1,5 mg g^{-1}. La stérilité du sol après le traitement par rayonnement γ a été confirmée par étalement de solution de sol (5 g de sol broyés avec 15 ml d'eau stérile) sur gel TSA 1/10ème (Trypsine Soy broth Agar).

2.2 Réalisation du gradient de diversité microbienne et inoculation

Trois niveaux de diversité microbienne différents ont été créés à partir d'une solution de sol obtenue en broyant 100 g de sol mélangés à 300 ml d'eau ultrapure stérile pendant 1 min 30. Cette solution de sol a ainsi constitué le premier niveau de diversité (D1), et des dilutions en cascade de cette solution ont permis d'obtenir les niveaux de diversités inférieurs D2 (facteur de dilution = 10^3) et D3 (facteur de dilution = 10^5). Les facteurs de dilutions sont basés sur les travaux de Griffiths et al. (2001) et tiennent compte de la densité microbienne préalablement déterminée par PCR quantitative. Les solutions ont ensuite été ré-inoculées par ajout de 11,5 ml dans des fioles de 150 ml contenant 40 g de sol stérile, permettant d'obtenir une humidité à 60% de la capacité au champ.

2.3 Design expérimental et expérience d'incubation

Dans cette expérience, la modalité « amendé » correspond aux échantillons dans lesquels le résidu de blé enrichi en ^{13}C a été apporté alors que les échantillons « contrôles » n'ont reçu aucun amendement. Un total de 99 fioles fermées hermétiquement a été pré-incubé pendant six semaines à 20° C et dans l'obscurité. Ces microcosmes correspondent à trois réplicats indépendants pour chaque modalité, pour chaque niveau de diversité et pour des prélèvements aux temps d'incubation 0 (fin de la pré-incubation), 3, 7, 14, 29 et 60 jours. Les fioles correspondantes au temps initial (T0) devant recevoir l'amendement sont manquantes pour les trois niveaux de diversité, ce qui nous prive des observations pour le début de l'expérience dans les échantillons « amendé ». L'objectif de cette pré-incubation était de permettre le développement et la stabilisation des communautés microbiennes. Après cette période de six semaines, 200 mg de résidus de blé hautement enrichis en ^{13}C (96% d'atomes de ^{13}C, blé cultivé en phytotron au CEA de Cadarache) ont été ajoutés dans les microcosmes de la modalité « amendé ». La totalité des microcosmes a ensuite été remis en incubation pendant 60 jours à 20° C et dans l'obscurité. Quatre fioles contenant uniquement le sol stérile, et n'ayant pas reçu d'amendement, ont également été incubées afin de détecter une éventuelle contamination pendant l'expérience.

2.4 Mesures effectuées au cours de l'incubation

Trois microcosmes de chacune des deux modalités ont été sacrifiés à chaque temps de prélèvements (T0, T3, T7, T14, T29 et T60). La concentration en C_{org} a été déterminée par combustion sèche (Vario MICRO cube, Elementar). Des extractions des matières organiques solubles ont été réalisées en appliquant, dans des conditions strictement identiques, la méthode à haute pression et haute température (PH-WEOC) décrite dans Guigue et al. (2014). La concentration en carbone organique dissous dans les extraits a été mesurée par oxydation thermique (TOC5000A, Shimadzu) sur des aliquotes acidifiées (pH 2). Les extraits ont ensuite été lyophilisés et conservés au sec et à l'obscurité.

L'atmosphère des fioles incubées a été prélevée (aux temps d'incubation T0, T3, T7, T10, T14, T21, T28, T44 et T60) afin de déterminer la concentration de CO_2 produit par la respiration microbienne par chromatographie en phase gazeuse (GC Agilent 7890A) équipée de colonnes *PoraPlotQ* et *Molecular sieves* et d'un détecteur par conductivité

thermique (TCD). L'enrichissement isotopique du C ($\delta^{13}C$) a été mesuré par spectrométrie de masse de rapport isotopique (IsoPrime, Elementar) couplé à un analyseur élémentaire pour les échantillons de sol (C_{org}) et les lyophilisats (PH-WEOC), et à une interface par chromatographie (Trace Gas, Micromass) pour les échantillons de gaz (CO_2).

2.5 Equation de mélange isotopique pour le calcul du *priming effect*

La concentration de CO_2 issue du PE est déterminée d'après l'équation 1. La concentration de CO_2 produit par la minéralisation du résidu de blé enrichi en ^{13}C ($[CO_2]_R$) ne peut pas être mesurée directement. Elle est déterminée grâce à l'équation de mélange isotopique (équation 2), basée sur l'hypothèse que le fractionnement isotopique entre le sol « contrôle » et le CO_2 produit par sa minéralisation est négligeable.

(Eq. 1) $$[CO_2]_{PE} = [CO_2]_A - [CO_2]_R - [CO_2]_C$$

avec $[CO_2]_{PE}$: concentration en CO_2 produit par le *priming effect* ; $[CO_2]_A$: concentration en CO_2 mesurée dans les microcosmes « amendé » ; $[CO_2]_R$: concentration en CO_2 produit par la minéralisation du résidu de blé et $[CO_2]_C$: concentration en CO_2 mesurée dans les microcosmes « contrôle ». Toutes les concentrations sont exprimées en mg de CO_2 par g de sol.

(Eq. 2) $$[CO_2]_R = \frac{[CO_2]_A \times (^{13}C\text{-}CO_{2\,A} - {}^{13}C_S)}{^{13}C\text{-}CO_{2\,R} - {}^{13}C_S}$$

avec $[CO_2]_R$: concentration en CO_2 produit par la minéralisation du résidu de blé ; $^{13}C\text{-}CO_{2R}$: enrichissement isotopique du CO_2 produit par la minéralisation du résidu de blé ; $[CO_2]_A$: concentration en CO_2 mesurée dans les microcosmes « amendé » ; $^{13}C\text{-}CO_{2A}$: enrichissement isotopique du CO_2 mesurée dans les microcosmes « amendé » ; $^{13}C_S$:enrichissement isotopique du sol. Toutes les concentrations sont exprimées en mg de CO_2 par g de sol. Les enrichissements isotopiques sont exprimés en pourcentage de ^{13}C.

2.6 Analyse de la densité bactérienne et de la structure génétique des communautés

L'ADN a été extrait des sols incubés en suivant la procédure d'extraction et de purification optimisée par Ranjard et al. (2003). Les extraits d'ADN ont ensuite été quantifiés par migration électrophorétique sur gel d'agarose (1%), en présence de « smart ladder » comme marqueur de poids moléculaires. Les ADN sont ensuite révélés dans un bain de Bromure

d'Ethidium et photographiés grâce au système InfinityCapt (Vilber Lourmat). La densité bactérienne est ensuite déterminée par qPCR (quantitative Polymerase Chain Reaction) et par le suivi du nombre de copies d'ADN 16S amplifiées, déterminé par mesure de fluorescence. La diversité bactérienne est déterminée par pyroséquençage de l'ADNr 16S.

Le génotypage des communautés bactériennes permettant l'étude de la structure des communautés a été effectué à T0. Cette mesure est basée sur le polymorphisme de taille de l'espace intergénique entre les gènes codant pour l'ARN 16S et l'ARN 23S. L'espace intergénique varie pour la majorité des espèces de procaryotes, offrant un critère de discrimination. Dans cette étude l'empreinte génétique a été déterminée par la méthode B-ARISA (Bacterial-Automated Ribosomal Intergenic Spacer Analysis), détaillée dans d'autres travaux (Lejon et al., 2007; Dequiedt et al., 2009; Chemidlin Prévost-Bouré et al., 2010).

2.7 Analyses statistiques

L'analyses en composantes principales (ACP) sur les matrices de covariances, générées à partir des 100 bandes les plus dominantes issues des profils de B-ARISA a été réalisée afin de résumer l'information sur les structures génétiques des communautés bactériennes à T0, en utilisant les programmes prepRISA (Ranjard et al., 2001) et ade4TkGUI (Dray et al., 2013) avec le logiciel R (R Core Team, 2012). Pour les mesures du C_{org} et du ^{13}C effectuées sur le sol et le PH-WEOC, ainsi que pour les flux de CO_2 et le PE, les différences entre les trois niveaux de diversité au cours du temps sont basées sur la lecture graphique et l'individualisation des points (moyennes de trois réplicats) et de leur barres d'erreur (erreur standard de la moyenne). Ces différences sont pour l'ensemble confirmées par des tests non-paramétriques de Steel-Dwass ($p<0,05$) appliqués séparément pour chaque temps d'incubation sur chaque variable. La grande quantité de résultats produits par ces nombreux tests rend leur présentation fastidieuse et n'ajoute pas d'informations à celles déjà présente sur les graphiques.

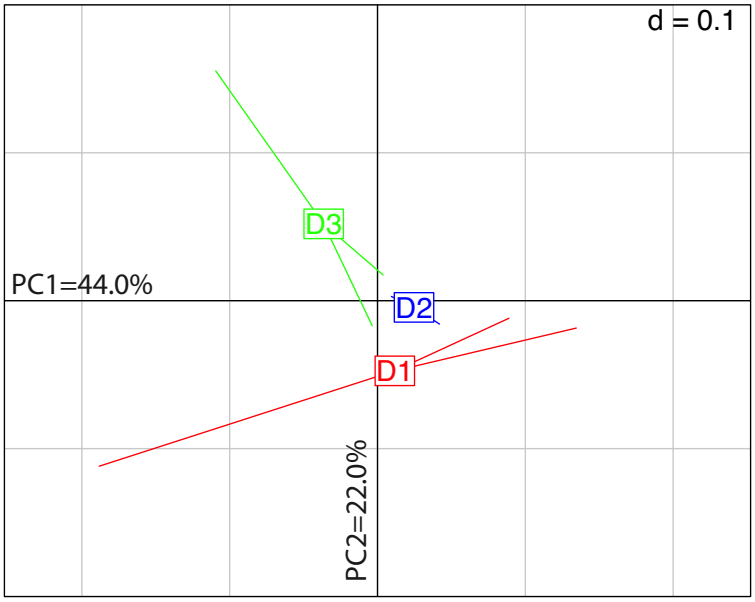

Figure 1 Représentation de la structure génétique des communautés bactériennes D1, D2 et D3 à T0. Le score moyen des trois réplicats de chaque niveau de diversité est projeté dans le plan de l'ACP, construit sur les deux premières composantes principales et regroupant 66% de la variance totale du jeu de données obtenues par B-ARISA.

3 Résultats

La grande quantité de résultats obtenue au cours de cette expérience nous a amené à sélectionner ceux qui seront présentés dans la suite de ce chapitre. L'étude de l'impact de l'érosion de diversité microbienne sur la dynamique de dégradation des différents pools de matière organique (MO) au cours de l'incubation sera basée sur l'évolution des concentrations en carbone organique (C_{org}) et de son enrichissement isotopique dans le sol et dans le compartiment soluble (PH-WEOC) mesurée sur les échantillons « amendé ». La minéralisation des pools de MO provoquée par la dégradation microbienne dans les échantillons « contrôle » et « amendé » a été retenue pour évaluer les effets de l'amendement organique et de la diversité microbienne. Les mesures de la composition isotopique du CO_2 dans ces échantillons ont ensuite permis d'estimer les flux de CO_2 générés par le phénomène de *priming effect* (PE).

3.1 Caractéristiques des communautés bactériennes après la période de pré-incubation

Les mesures par PCR quantitative ont confirmé que la densité bactérienne était à des niveaux similaires (1 x 10^6 copies de 16S par ng d'ADN) dans tous les microcosmes après la phase de pré-incubation, puis au cours des 60 jours d'incubation. Le bon déroulement de cette étape avait déjà été observé dans une étude précédente (Maron et al., 2004). Ce résultat garantit que la pré-incubation a permis le bon déroulement de la colonisation du sol stérile par les bactéries du sol, ainsi que leur stabilisation, et qu'aucune dérive des microcosmes en terme de densité n'a eu lieu pendant l'expérience. Dans le même temps, l'évaluation de la diversité bactérienne à T0 a montré que le gradient de diversité avait été créé avec succès (indices de Shannon : D1=4,6 ; D2=4,3 et D3=3,5).

Ainsi, l'influence des communautés bactériennes sur les autres variables sera uniquement attribuable au gradient de diversité créé. Ce gradient de diversité génère des différences dans la structure génétique des communautés bactériennes entre les trois niveaux de diversité. Les mesures par B-ARISA à T0 et leur analyse au moyen de l'ACP (Fig. 1) montrent l'individualisation des trois niveaux de diversité dans le plan de l'ACP, confirmant que les structures des communautés D1, D2 et D3 sont différentes après la période de pré-incubation.

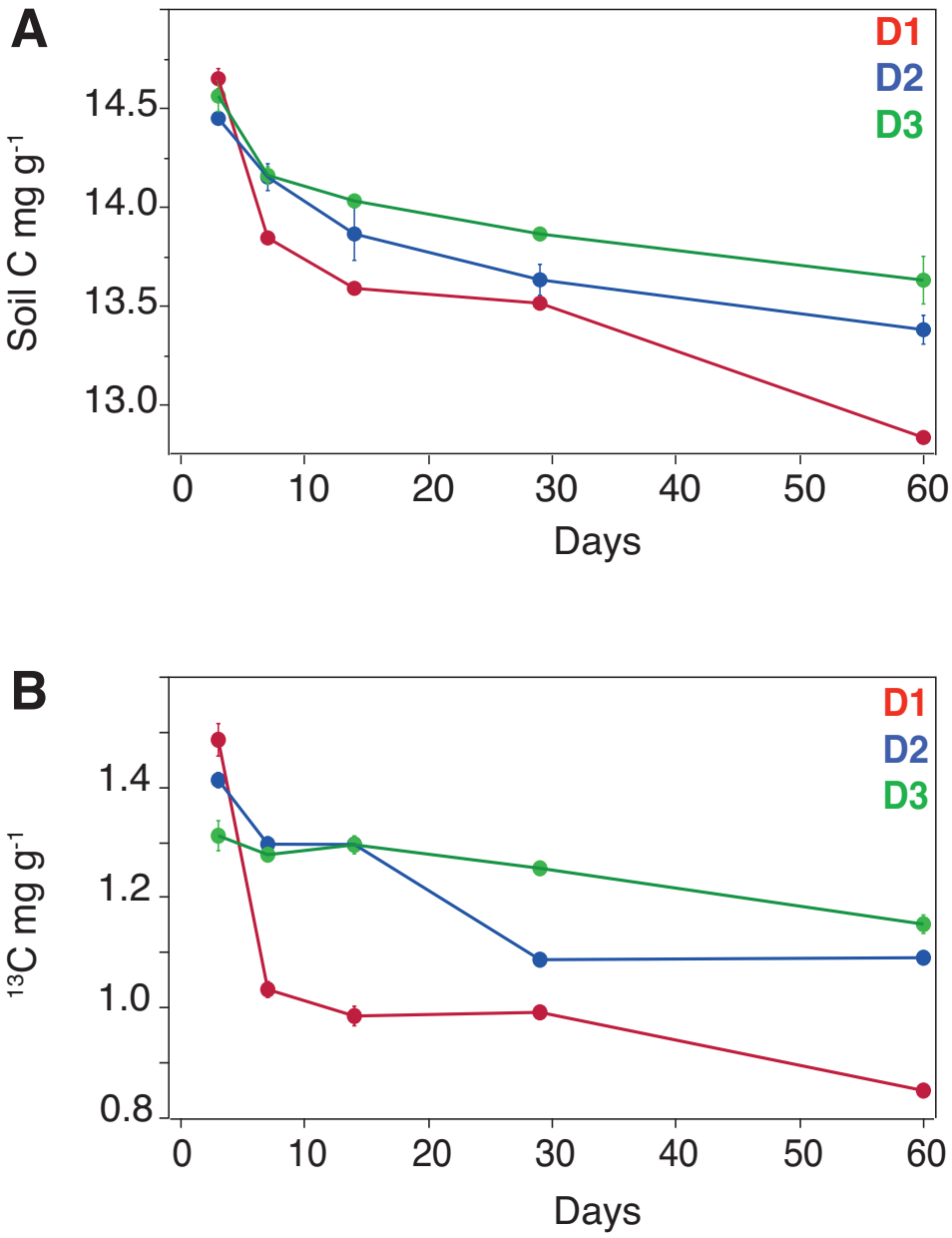

Figure 2 (A) Evolution de la concentration en carbone organique dans le sol (mg g^{-1}) au cours de l'incubation pour les trois niveaux de diversité microbienne dans les échantillons « amendé ». (B) Evolution de la concentration en ^{13}C dans le sol (mg g-1) au cours de l'incubation pour les trois niveaux de diversité microbienne dans les échantillons « amendé ». Chaque point est une moyenne de trois réplicats et les barres d'erreur représentent l'erreur standard.

Ces résultats sont en accord avec Griffiths et al. (2001) qui avaient utilisé la même approche expérimentale et avaient montré que la dilution-inoculation permettait de créer des niveaux de diversité différents.

3.2 Evolution des pools de matière organique dans le sol

Les concentrations en C_{org} des sols amendés montrent une diminution de 1 à 2 mg g^{-1} de sol au cours de l'incubation (Fig. 2). Cette diminution est plus marquée pendant la première phase de l'expérience et, à partir de T14, une deuxième phase caractérisée par une baisse plus modérée au cours du temps se met en place. L'allure des courbes de décroissance des concentrations en C_{org} montre ainsi deux phases de décomposition aux cinétiques différentes. Cette observation est interprétée comme le résultat de la minéralisation rapide de composés labiles apportés avec l'amendement lors de la première phase, et de la minéralisation d'un pool de C_{org} plus récalcitrant et suivant une cinétique plus lente, qui est observée au cours de la deuxième phase mais qui a probablement débuté dès le début de l'incubation.

Les courbes des concentrations en C_{org} correspondant aux trois niveaux différents de diversité bactérienne montrent que le gradient de diversité a un impact considérable sur l'évolution des concentrations en C_{org} au cours de l'incubation. En effet, pour les microcosmes inoculés avec la diversité bactérienne la plus élevée (D1), les concentrations en C_{org} diminuent plus rapidement, dès le début de l'incubation. La baisse des concentrations en C_{org} la plus faible est observée pour les échantillons correspondant à la diversité bactérienne la plus basse (D3), et la diversité D2 montre des valeurs intermédiaires. Ces premières observations mettent déjà en avant le rôle de la diversité microbienne sur la décomposition des matières organiques et révèlent une perte partielle des fonctions de dégradation de la MO par les communautés bactériennes lorsque la diversité diminue.

Dans les microcosmes « amendé », environ 97% du ^{13}C provient du résidu apporté à T0, les 3% restant correspondent à l'abondance naturelle en ^{13}C dans la matière organique endogène du sol. Le suivi des transferts de ^{13}C au cours de l'expérience donne donc des indications sur l'évolution du C_{org} apporté avec le résidu. Comme pour le C_{org} total, les concentrations en ^{13}C dans le sol baissent également au cours de l'incubation (Fig. 2) et montrent que le résidu de blé marqué est consommé au cours de l'expérience.

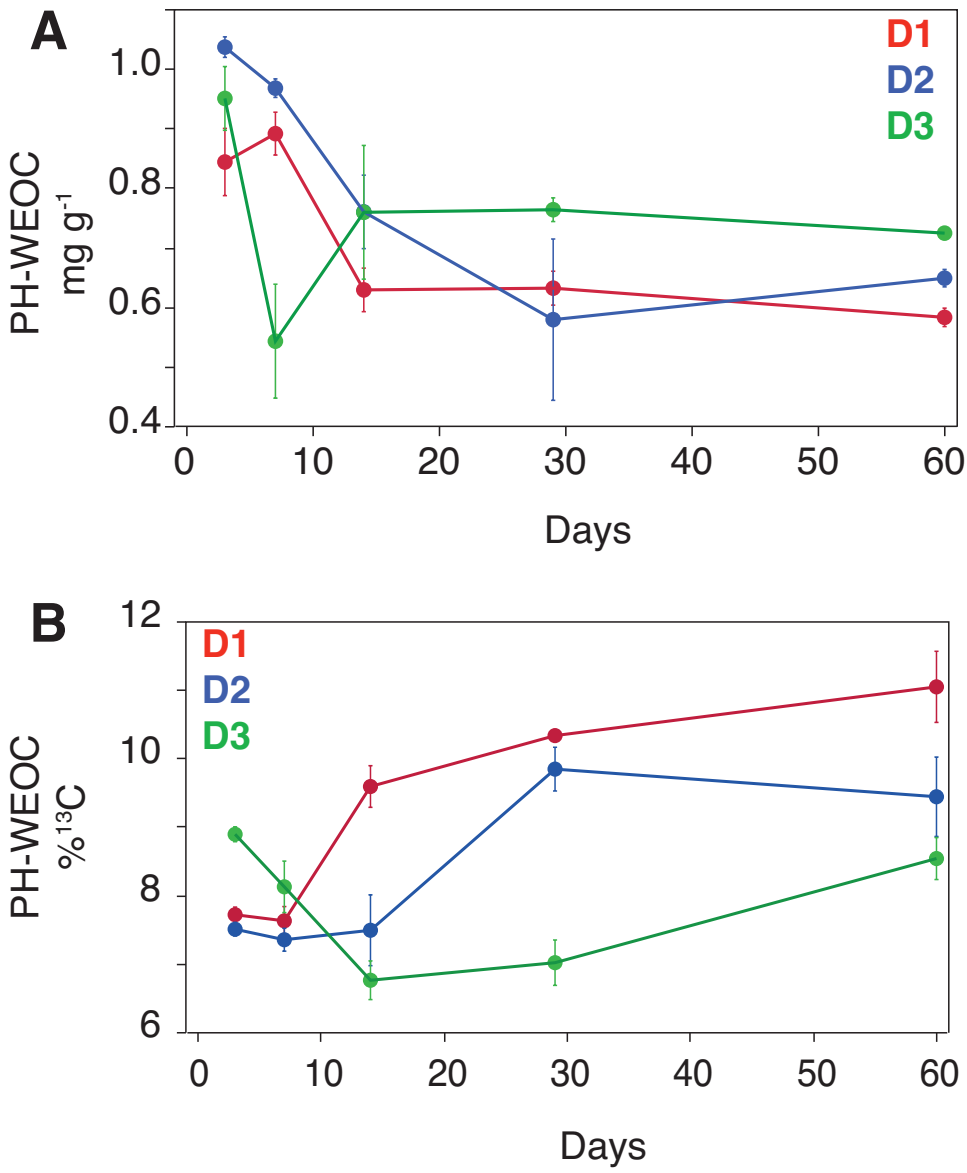

Figure 3 (A) Evolution de la quantité de ^{13}C extraite du sol (mg g^{-1}) au cours de l'incubation pour les trois niveaux de diversité microbienne dans les échantillons « amendé ». (B) Evolution du pourcentage de ^{13}C dans le PH-WEOC au cours de l'incubation pour les trois niveaux de diversité microbienne dans les échantillons « amendé ». Chaque point est une moyenne de trois réplicats et les barres d'erreur représentent l'erreur standard.

Il est intéressant de constater que le gradient de diversité bactérienne a également un effet sur la décomposition de cette MO apportée au système. Les mesures montrent que comme pour le carbone total du sol, le ^{13}C est davantage consommé lorsque la diversité bactérienne est plus élevée et qu'il y a une relation étroite entre l'érosion de diversité et la baisse en ^{13}C dans le sol. Dans le même temps, des analyses en RMN ^{13}C ont montré que les carbohydrates provenant du résidu marqué était moins décomposés lorsque la diversité était plus basse (Baumann et al., 2012). Ces résultats sont en accord avec l'évolution de la composition isotopique dans le sol.

Ces premières observations amènent à considérer le concept d'après lequel la diversité taxonomique des microorganismes n'a pas d'influence sur le fonctionnement des communautés du fait de la grande diversité fonctionnelle et de la grande adaptabilité des microorganismes. Alors que certains travaux supportent cette théorie (Nannipieri et al., 2003; Wertz et al., 2006, 2007), d'autres la contredisent (Carney & Matson, 2005; Plassart et al., 2008). Nos premiers résultats nous mènent à des interprétations en accord avec ces derniers qui montrent que des modifications de la diversité bactérienne amènent à des changements de la fonctionnalité des communautés. La décomposition moins marquée des différents réservoirs de C_{org} du sol en lien avec la baisse de diversité suggère que la capacité de ces communautés microbiennes à décomposer la MO est maintenue mais que la dynamique subit un ralentissement, comme observé par Juarez et al. (2013).

3.3 Indices de la dégradation des pools de matière organique par l'analyse de la dynamique du PH-WEOC et de sa composition isotopique ^{13}C

Dans les microcosmes « amendé », l'étude du PH-WEOC montre qu'il y a entre 0,5 et 1,0 mg de C_{org} extractible par gramme de sol dans l'ensemble des échantillons « amendé » au cours de l'incubation (Fig. 3). Pour les trois niveaux de diversité microbienne, une plus grande quantité de PH-WEOC est mesurée au début de l'expérience. Ces quantités diminuent jusqu'à des valeurs comprises entre 0,6 et 0,8 mg g^{-1} et apparaissent relativement stables entre T14 et T60. L'effet de la diversité bactérienne sur les quantités de PH-WEOC est constaté, avec notamment une stabilisation plus précoce (T14) à des quantités basses de PH-WEOC lorsque la diversité est plus élevée que pour la diversité intermédiaire (T28). Pour la diversité la plus basse (D3), les valeurs se stabilisent à T14 mais restent plus élevées que pour les autres niveaux de diversité.

Les résultats observés pour D3 à T7 apparaissent comme anormalement bas, en comparaison de la dynamique générale observée pour les trois dilutions, ce qui suggère que la baisse de diversité a entraîné une baisse de la production de C_{org} soluble dans ces échantillons. Ce phénomène ne dure pas au cours de l'expérience et la résilience des communautés bactériennes et de leurs fonctionnalités semblent se mettre en place entre T7 et T14.

La composition isotopique du PH-WEOC montre des variations importantes au cours des deux mois d'incubation avec des pourcentages en ^{13}C compris entre 7 et 11% (Fig. 3). Ces valeurs montrent qu'environ 10% du C_{org} contenu dans le PH-WEOC provient de la solubilisation de composés organiques issus de la dégradation du résidu marqué. Il y a un effet majeur de la diversité bactérienne sur la composition isotopique du PH-WEOC. Pour les diversité D1 et D2 les valeurs les plus basses sont observées à T3 puis augmentent respectivement à T7 et T14. Les abondances en ^{13}C continuent d'augmenter légèrement pour la diversité D1 alors qu'elles restent stables pour D2. Pour D3, la tendance est différente avec un pourcentage de ^{13}C dans le PH-WEOC plus élevé au début de la période d'incubation. L'abondance en ^{13}C diminue progressivement jusqu'à T14, puis la tendance s'inverse et une augmentation du pourcentage en ^{13}C est observée jusqu'à la fin de l'expérience.

De nombreux processus peuvent être à l'origine des variations de la composition isotopique du PH-WEOC. La baisse de l'abondance en ^{13}C concorde avec un transfert des atomes de ^{13}C vers un autre compartiment de C des microcosmes. Ce processus peut correspondre à la minéralisation par les communautés bactériennes des composés organiques issus de la dégradation du résidu, ainsi qu'à leur immobilisation par adsorption sur le complexe argilo-humique ou par co-précipitation avec une fraction minérale (Kaiser et al., 2001). Elle peut aussi s'expliquer par une entrée de ^{12}C plus importante dans le PH-WEOC, qui serait le résultat de la solubilisation de composés organiques au cours de la dégradation et de la transformation de la MO autochtone du sol par l'activité microbienne. Á l'inverse, l'augmentation de l'abondance en ^{13}C dans le PH-WEOC peut être influencée par une entrée de ^{13}C avec le transfert en solution de produit de la dégradation du résidu, ou par une perte de ^{12}C dans le PH-WEOC contrôlée soit par la minéralisation des composés solubles hérités de la MO du sol, soit par leur fixation sur la fraction solide du sol. Tous ces processus peuvent intervenir au cours de notre expérience et nos observations de la dynamique du PH-WEOC sont certainement le résultat de la combinaison de plusieurs d'entre eux (Kaiser & Kalbitz, 2012), avec des influences plus ou moins importantes et variables au cours

du temps. Dans cette expérience, nous savons que les deux réservoirs de C_{org}, le résidu et la MO du sol, sont dégradés. Leurs concentrations dans le sol diminuent et le suivi de la production de CO_2 dans les microcosmes, présenté dans le paragraphe suivant, montre que le C_{org} minéralisé provenait de ces deux réservoirs. Par contre, nous ne disposons pas d'informations suffisantes pour déterminer l'influence de chacun des processus énoncés précédemment sur l'évolution de la composition isotopique du PH-WEOC.

L'érosion de diversité bactérienne entraîne des différences très marquées de la composition isotopique du PH-WEOC. Le schéma commun entre les trois niveaux de diversité correspond à des concentrations en ^{13}C basses au début de l'expérience puis à une augmentation au cours du temps. La baisse de diversité provoque un ralentissement de cette dynamique car plus la diversité bactérienne est basse et plus l'augmentation du pourcentage en ^{13}C est tardive. Le fait que la valeur minimale soit également observée avec du retard pour D3 va dans le sens de ce décalage temporel de l'évolution de la composition isotopique du PH-WEOC. Ces résultats sont à mettre en relation avec des différences dans les fonctions de dégradation des communautés bactériennes issues de l'érosion de diversité. Le fait que les dynamiques observées soient similaires, mais que leur cinétique soit liée au niveau de diversité montre que les communautés bactériennes de D2 et D3 sont résilientes au cours de cette expérience. Le temps de résilience entre D2 et D3 révèle également que la communauté bactérienne ayant subi la plus grosse baisse de diversité est plus impactée et que sa résilience prend plus de temps, avec un ralentissement de la dynamique de dégradation de la MO, comme observé par Juarez et al. (2013).

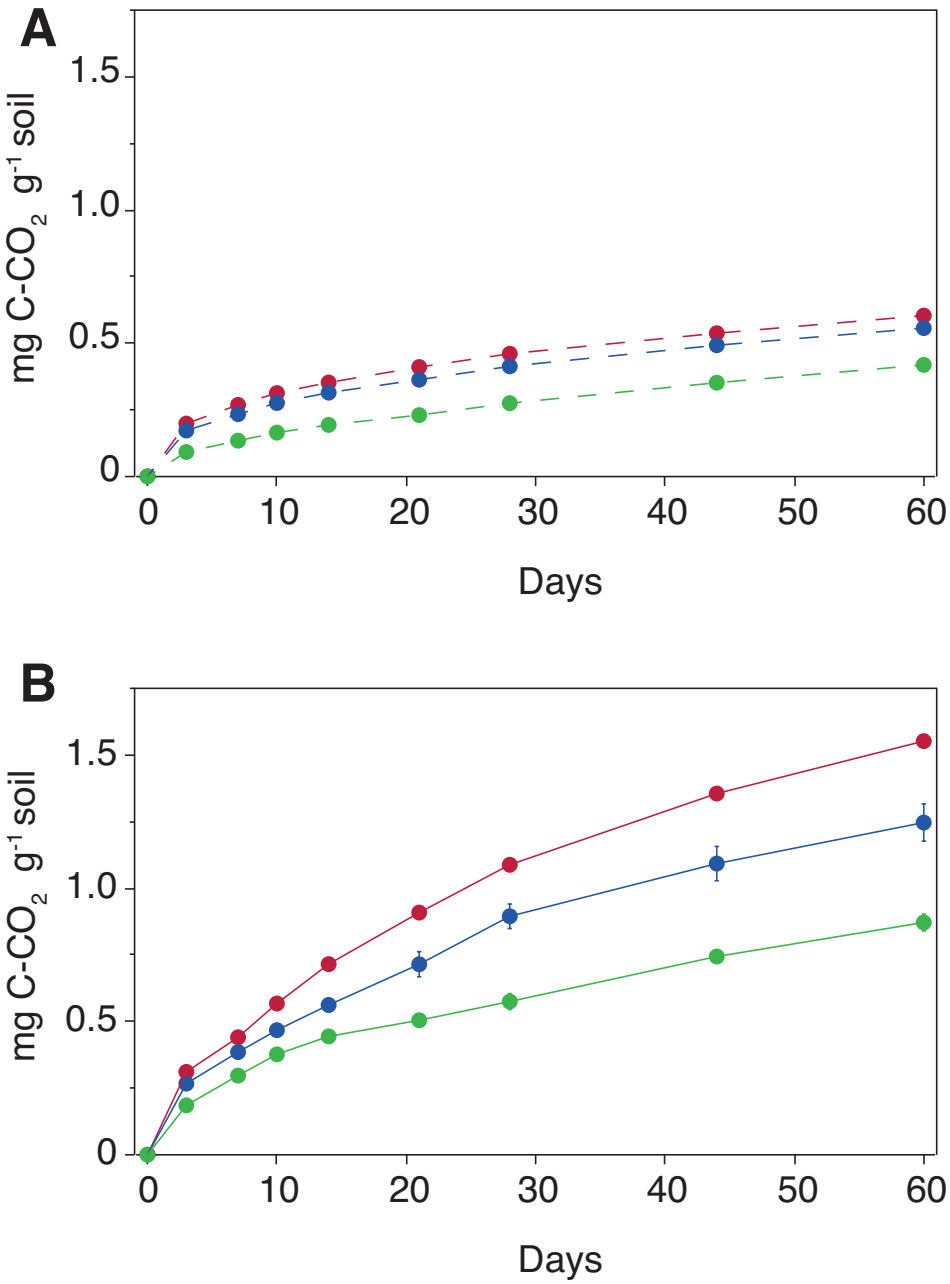

Figure 4 (A) Courbes des émissions cumulées de CO_2 (mg C-CO_2 g^{-1} de sol) au cours de l'incubation pour les trois niveaux de diversité microbienne dans les échantillons « contrôle ». (B) Courbes des émissions cumulées de CO_2 (mg C-CO_2 g^{-1} de sol) au cours de l'incubation pour les trois niveaux de diversité microbienne dans les échantillons « amendé ». Chaque point est une moyenne de trois réplicats et les barres d'erreur représentent l'erreur standard.

3.4 Minéralisation de la matière organique par l'activité des microorganismes du sol

La production de CO_2 au cours de l'expérience provient de la respiration des microorganismes au cours de la dégradation des composés organiques minéralisés. Les mesures réalisées sur les échantillons « contrôle » montrent qu'entre 0,4 et 0,6 mg de CO_2 par g de sol sont produits au cours de l'expérience (Fig. 4). L'intensité de la production de CO_2 est plus élevée pendant les premiers jours de l'expérience puis diminue et se stabilise après une dizaine de jours. Les échantillons contenant la population microbienne la moins diversifiée minéralisent moins de C, alors que pour D1 et D2, les quantités de CO_2 produites sont similaires. Cette première observation confirme l'impact de l'érosion de diversité sur la dynamique de la communauté D3 dans les échantillons « contrôle ».

L'amendement organique peut être considéré comme une perturbation, provoquant la réorganisation des communautés bactériennes, du fait de l'apparition d'une nouvelle source d'énergie avec une composition différente. L'apport du résidu favorise l'adaptation et le développement d'une partie des espèces de la communauté plus adaptée à décomposer cette source de C. Comme attendu, l'amendement provoque une augmentation des flux de CO_2, avec des flux cumulés compris entre 0,8 et 1,6 mg de CO_2 par g de sol (Fig. 4). Cet effet attendu de l'amendement avait déjà été souvent observé (e.g. Waldrop & Firestone, 2004). Les flux de minéralisation mesurés sont corrélés avec les niveaux de diversité bactérienne, correspondant à des flux plus élevés pour la diversité D1, intermédiaire pour D2 et inférieurs pour D3. Ces résultats montrent que plus la diversité microbienne est élevée, plus la communauté s'adapte aux modifications liées à l'amendement et le dégrade rapidement.

Une communauté bactérienne diversifiée est capable d'assurer des fonctions de dégradation plus variée et a une capacité d'adaptation plus élevée. Étant donné que les différentes espèces consomment des ressources trophiques sensiblement différentes, les communautés bactériennes ayant une forte richesse spécifique peuvent utiliser une plus grande proportion de l'ensemble des ressources disponibles (Bell et al., 2005). La communauté D2, qui avait montré une dynamique de minéralisation similaire à D1 dans les échantillons « contrôle », est impactée par l'amendement et des flux de CO_2 mesurés dans les échantillons « amendé » sont inférieurs à ceux de D1.

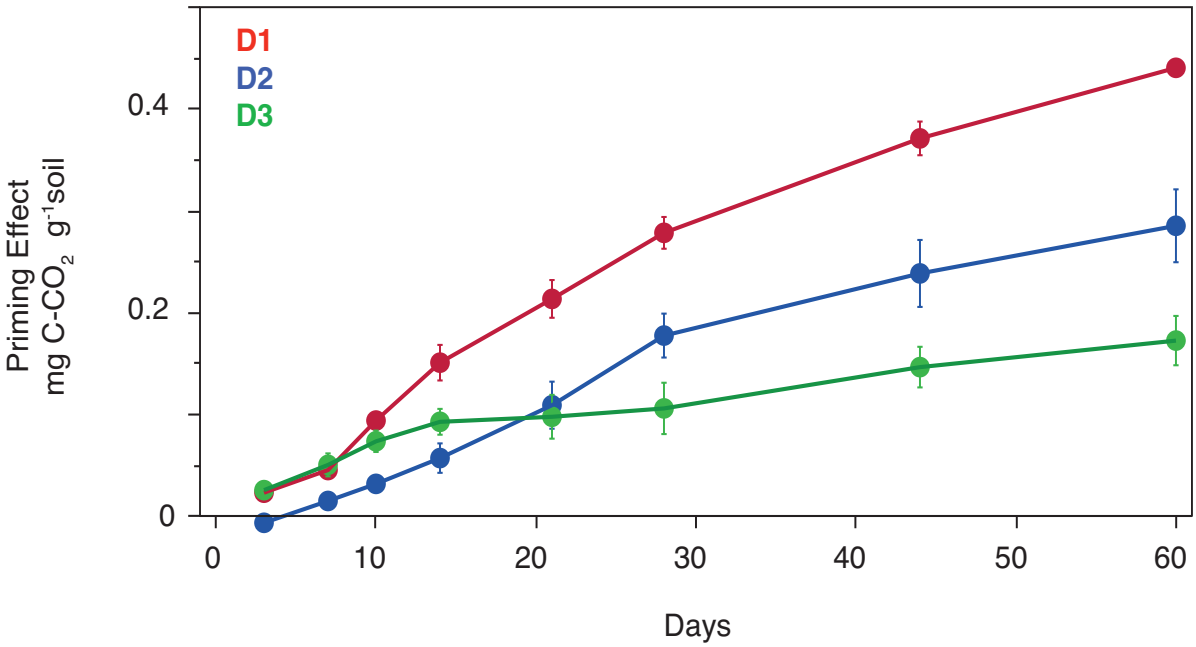

Figure 5 Courbes des émissions cumulées de CO_2 produit par le Priming Effect (mg C-CO_2 g^{-1} de sol) au cours de l'incubation pour les trois niveaux de diversité microbienne dans les échantillons « amendé ». Chaque point est une moyenne de trois réplicats et les barres d'erreur représentent l'erreur standard.

Les communautés microbiennes ont donc été perturbées par l'amendement et la dynamique de dégradation de la MO est moins efficace que pour D1, comme l'ont montré les mesures réalisées sur le sol et sur le PH-WEOC. Les flux de minéralisation de D3 sont également en accord avec les observations précédentes, qui ont montré un ralentissement de la dynamique de dégradation par les bactéries. La baisse de diversité et la période de pré-incubation semblent avoir favorisé le développement de groupes bactériens spécialisés dans la décomposition de la MO du sol : les K-stratégistes. Ils sont caractérisés par un développement lent en comparaison des r-stratégistes, qui sont eux spécialisés dans la décomposition de substrat plus labile, ont une croissance rapide, et sont plus adaptés à la décomposition du résidu dans notre expérience (Fontaine et al., 2003).

3.5 Le *priming effect* : minéralisation accrue de la matière organique du sol suite à un amendement organique

Le résidu de blé enrichi en ^{13}C (96% d'atomes de ^{13}C) permet de suivre les transferts de C_{org} depuis le résidu vers les autres compartiments de C. Les mesures de la composition isotopique du CO_2 permettent de quantifier les proportions de C minéralisé provenant du résidu marqué ou de la MO endogène du sol. En tenant compte des flux de CO_2 produits dans les échantillons « contrôle », nous avons quantifié le *priming effect* (PE) qui correspond à l'augmentation de la minéralisation de la MO du sol dans les échantillons « amendé » causée par l'apport du résidu (Löhnis, 1926).

Le PE est constaté pour les trois niveaux de diversité dans notre expérience avec des quantités de CO_2 comprises entre 0,15 et 0,45 mg C-CO_2 par g de sol à T60 (Fig. 5). Les flux de CO_2 attribués au PE correspondent à des augmentations respectives de minéralisation de la MO du sol de 73%, 41% et 31% pour D1, D2 et D3 à la fin de l'expérience. Le PE se met en place dès l'apport du résidu, à T0, pour D1 et D3 et à partir de T3 pour D2. Le phénomène de PE est plus intense pour les échantillons D1, suggérant que l'apport de MO fraîche stimule davantage la minéralisation de la MO du sol quand la diversité bactérienne est plus élevée. Jusqu'à T7, le PE dans les échantillons D3 est aussi intense que dans D1. La communauté bactérienne de D3, bien qu'elle produise moins de CO_2 (Fig. 4) semble favoriser la MO du sol comme source d'énergie. Cette communauté moins diversifiée, qui s'est établie et stabilisée en absence de MO fraîche, est davantage spécialisée dans la décomposition du pool de MO stable que les communautés D1 et D2.

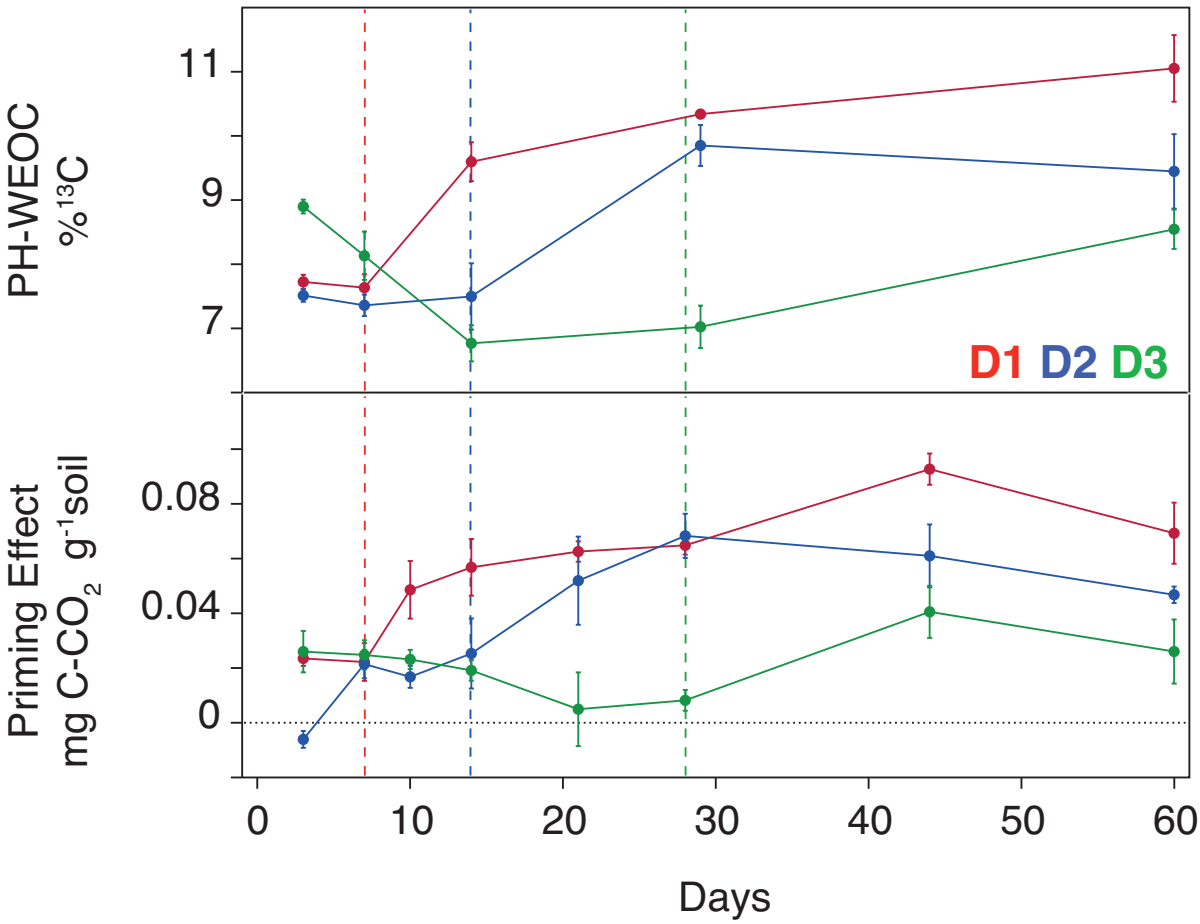

Figure 6 Lien entre la dynamique de dégradation et solubilisation du résidu enrichi en ^{13}C et le phénomène de Priming Effect. (en haut, identique à Figure 2) Evolution du pourcentage de ^{13}C dans le PH-WEOC au cours de l'incubation pour les trois niveaux de diversité microbienne dans les échantillons « amendé ». (en bas) Courbes des émissions non-cumulées de CO_2 produit par le Priming Effect (mg C-CO_2 g^{-1} de sol) au cours de l'incubation pour les trois niveaux de diversité microbienne dans les échantillons « amendé ». Chaque point est une moyenne de trois réplicats et les barres d'erreur représentent l'erreur standard.

Dans une deuxième phase, à partir de T14, le PE est moins marqué, ce qui suggèrent que la composition de la communauté bactérienne évolue avec un développement tardif des espèces r-stratégistes, décomposant le résidu. Pour la communauté D2, le PE est plus long à se mettre en place, avant de s'exprimer jusqu'à la fin de l'incubation. Pour expliquer les causes du PE, l'hypothèse principale est que les groupes bactériens K-stratégiques tirent également profit de l'apport du résidu. Ainsi les populations de K-stratégiques augmentent et une plus grande quantité d'enzymes de décomposition de la MO du sol est produite, provoquant l'augmentation de sa dégradation (Fontaine et al., 2003).

3.6 Lien entre la dynamique des matières organiques solubles et le *priming effect*

En analysant les flux d'émission de CO_2 non-cumulés correspondant au PE au cours de l'incubation, nous pouvons observer que ce phénomène n'est pas constant au cours de l'expérience. Des augmentations du PE sont ainsi constatées pour D1, D2 et D3, respectivement à T7, T14 et T28 (Fig. 6). Ces changements dans la dynamique du PE peuvent également être observés sur la Figure 5, avec de légères augmentations dans la cinétique du PE. En comparant ces changements dans la dynamique du PE avec l'évolution de la composition isotopique du PH-WEOC (Fig. 6), un synchronisme entre l'augmentation du PE et l'enrichissement en ^{13}C du PH-WEOC est observé.

En reconsidérant les différents processus pouvant expliquer les variations de la composition isotopique du PH-WEOC énoncés précédemment, ces augmentations en ^{13}C dans le PH-WEOC semblent être le résultat d'une augmentation de la minéralisation des composés solubles issus de la dégradation de la matière organique du sol et donc à une perte de ^{12}C. Ainsi, le PH-WEOC apparaît davantage comme un pool transitoire pour les matières organiques lors de la dégradation. De plus, cette relation démontre l'intérêt de l'analyse du PH-WEOC pour une meilleure compréhension de la dynamique de dégradation de la MO dans les sols.

Conclusion

Les objectifs de cette étude étaient d'estimer l'effet d'un apport de MO fraîche et l'influence de la diversité bactérienne sur la dynamique de dégradation de la MO. Nous avons mis en évidence que l'apport d'une matière organique exogène (amendement) a provoqué le *priming effect*, i.e. l'augmentation de la minéralisation de la MO du sol, et ce pour les trois niveaux de diversité étudiés. L'approche par traçage isotopique ^{13}C s'est révélée pertinente pour quantifier précisément le PE. Nous avons également pu démontrer que l'analyse du PH-WEOC offrait un moyen de compréhension de la dynamique de minéralisation de la MO.

Le gradient de diversité bactérienne utilisé a montré que la dynamique de dégradation de la MO était ralentie lorsque la diversité baissait. La baisse de diversité a entrainé une perte partielle des fonctions de dégradation de la MO et cet effet a été observé dans tous les compartiments de C des microcosmes. Ce travail a permis de montrer l'importance de la diversité microbienne pour les fonctions de dégradation de la MO. La résilience fonctionnelle des communautés bactériennes, mise en avant dans de nombreuses études ne tenant pas compte de la diversité microbienne, n'est pas systématique.

Chapitre 4

Physico-chimie des sols, matière organique soluble et abondance naturelle en ^{13}C liées à la microbiologie des sols à l'échelle régionale

Soil physico-chemistry, soluble organic matter and ^{13}C natural abundance, linked to microbiology, at the regional scale

J. Guigue[1], J. Lévêque[1], O. Mathieu[1], P. Schmitt-Kopplin[2,3], M. Lucio[2], D. Arrouays[4], C. Jolivet[4], S. Dequiedt[5], N. Chemidlin Prévost-Bouré[6] and L. Ranjard[5,7]

[1] UMR 6282 Biogéosciences, Université de Bourgogne, Dijon, France.

[2] Helmholtz Zentrum München, German Research Center for Environmental Health, Analytical BioGeoChemistry, Neuherberg, Germany

[3] Chair of Analytical Food Chemistry, Technische Universität München, Freising-Weihenstephan, Germany.

[4] INRA, US 1106, INFOSOL, Orléans, France

[5] INRA, AgroSup Dijon, Université Bourgogne, UMR 1347 Agroécologie - plateforme GenoSol, Dijon, France

[6] AgroSup Dijon, UMR 1347 Agroécologie, Dijon, France

[7] INRA, UMR 1347 Agroécologie, Dijon, France

Submitted to *Soil Biology and Biochemistry*

Résumé

Les populations microbiennes jouent un rôle clé dans la réactivité biogéochimique des sols et sont influencées par des interactions complexes des processus biotiques et abiotiques du sol, menant à une variété d'habitats et de sources d'énergie dans le sol. L'identification des relations clés entre les communautés microbiennes et leur pédo-environnement est cruciale pour une meilleure évaluation de la dynamique globale des sols. La matière organique soluble des sols est un pool sensible et réactif, et son influence sur les communautés microbiennes n'est par encore intégralement comprise.

Nous avons étudié 120 échantillons de sol prélevés dans des écosystèmes variés de la région Bourgogne, en France. La matière organique soluble (solubilité potentielle et aromaticité) a été caractérisée au moyen de la méthode PH-WEOC (extraction à haute pression et haute température). Les caractéristiques physico-chimiques des sols (pH, texture, teneurs en carbone organique et en azote total) ont été mesurées, ainsi que la composition isotopique du carbone dans les sols et dans les extraits PH-WEOC. L'abondance des bactéries et des champignons, et la structure génétique des communautés bactériennes (B-ARISA) ont été déterminées. L'influence de la roche mère et du couvert végétal, et les relations entre les communautés microbiennes et le pédo-environnement, ont été estimées au moyen d'analyses en composantes principales et d'analyse de co-inertie.

Les effets sur le pédo-environnement attribués au couvert végétal et à la roche mère sont présentés. Les caractéristiques du PH-WEOC sont contrôlées par les quantités d'argile et de matière organique. L'aromaticité du PH-WEOC et sa signature $\delta^{13}C$ reflètent des différences dans les voies de dégradation de la matière organique du sol et dans la production de composés organiques solubles, en relation avec le couvert végétal. La structure génétique des communautés bactériennes est liée au pH et à la texture du sol ainsi qu'au PH-WEOC, révélant l'importance des matières organiques solubles pour les communautés bactériennes.

Ce travail met en évidence les relations entre les populations microbiennes et le pédo-environnement à une échelle régionale. Cette étude globale conduite à une échelle large, et sur un jeu d'échantillons hétérogènes, fournit des preuves fortes des liens entre les variables biogéochimiques du sol.

Abstract

Microbial populations play a key role in soil biogeochemical reactivity and are influenced by the complex interaction of soil biotic and abiotic processes, leading to a variety of soil habitats and sources of energy. The identification of the key relationships between microbial communities and their soil environment is crucial for a better evaluation of global soil dynamics. The soluble organic matter in soils is a sensitive and reactive pool, and its influence on microbial communities is not yet fully understood.

We studied 120 soil samples collected from various ecosystems in the Burgundy region, in France. The soluble organic matter (potential solubility and aromaticity) was characterised using pressurised hot-water extraction of organic matter (PH-WEOC). The soil physico-chemical characteristics (pH, texture, soil carbon and nitrogen) were measured, as was the carbon isotope composition in soils and in the PH-WEOC. We determined the abundance of bacteria and fungi and the genetic structure of bacterial communities with the Bacterial Automated Ribosomal Intergenic Spacer Analysis (B-ARISA) technique. Assessment of the influence of parental material and land cover, and of the relationships between the microbial communities and the soil environment, was performed by means of principal component analyses and a co-inertia analysis.

We present the effects attributed to land cover and parental material on soil environment. The characteristics of PH-WEOC are controlled by soil organic matter quantity and clay content. The aromaticity of PH-WEOC and its $\delta^{13}C$ signature reflect differences in the decomposition pathways of soil organic matter and in the production of soluble organic compounds, in relation to land cover. The genetic structure of bacterial communities is related to soil texture and pH and to the PH-WEOC, revealing the importance of soluble organic matter in the dynamics of bacterial communities.

This work highlights the relationships between microbial populations and the soil environment at a regional scale. This integrated study conducted at a large scale, on a heterogeneous sample set, provides robust evidence of the links between soil biogeochemical variables.

1 Introduction

Many environmental factors interact to determine soil characteristics. Climate, soil type, geology and geomorphological context, together with vegetation and management practices, all influence soil biogeochemistry (Jenny, 1941; McBratney et al., 2003; Wiesmeier et al., 2013). Parental bedrock determines the geochemical composition of soil, while the effects of climate, vegetation and (micro)organisms impact pedogenesis, and the resulting soil characteristics (e.g. pH, mineralogical composition, quantity and quality of organic matter). The interactions between all these environmental factors make the identification of their influence on soil characteristics difficult to assess, especially with restricted sample sets.

In this context, soil-monitoring networks provide a great opportunity to investigate the special links between soil characteristics and environment. Several soil-monitoring networks have been established around the world (Morvan et al., 2008; van Wesemael et al., 2011). These programs allow the analysis of very large datasets, integrating soil diversity and the influence of environmental factors. Many studies have been conducted using the French soil quality-monitoring network (RMQS), allowing large-scale assessment of soil organic carbon stocks (Martin et al., 2011), abundance of microorganisms (Dequiedt et al., 2011), and trace metal concentrations (Saby et al., 2009), for example. Large-scale investigation of the complex variability of soil biogeochemistry becomes possible, because of the sample set available with this soil-monitoring network (n=2200). The soluble organic matter in soils is a central component of soil biogeochemistry and the RMQS project represents a great opportunity to broaden the knowledge about this pool of organic matter.

The soluble organic matter in soils generally corresponds to less than 2% of the soil organic matter but is considered as highly sensitive, due to its high solubility and turnover rate (Kaiser & Kalbitz, 2012; Chantigny et al., 2014). This pool of soil organic matter has been identified as being linked with vegetation (Kalbitz et al., 2000a; Sanderman & Amundson, 2008), soil mineralogy (Kaiser et al., 2001; Schneider et al., 2010), climate (Camino-Serrano et al., 2014) and microbial activity (Lerch et al., 2010). The soluble organic matter concentration in soil solution is controlled by its production, leaching, stabilisation and degradation (Kalbitz et al., 2000b). Molecular investigation has revealed that thousands of different

compounds compose the soluble organic matter in soils (Ohno et al., 2010). Its sources, as well as the interactions between the numerous environmental variables involved in these processes, are complex and controversial, and studies with large sample sets may help to identify general trends in the dynamics of soluble organic matter, and its relationship with other soil biogeochemical characteristics.

In this study, we analyse the 120 samples of the French soil quality monitoring network collected in the Burgundy region, an area selected for its significant diversity in geology, soil type and vegetation. We determined the physico-chemical properties of soils and the characteristics of the soluble organic matter, using pressurised hot-water extraction of organic carbon (PH-WEOC) in the laboratory. We also measured the ^{13}C natural abundance in soil organic carbon (SOC) and in PH-WEOC, and we characterised the bacterial and fungal communities. Our objectives were (i) to assess the variations in soil properties related to the regional diversity in geology and land-cover, (ii) to link the variability in soluble organic matter properties with soil physico-chemistry and biology, (iii) to discuss the ^{13}C pattern observed at the regional scale in relation to other soil biogeochemical properties. As the soluble organic matter is a highly reactive pool of soil organic matter, we also hypothesised that it might interact with the dynamics of microbial populations and we thus sought (iv) to identify the variables of soil physico-chemistry and of PH-WEOC related to the genetic structure of bacterial communities at the regional scale.

2 Materials and methods

2.1 Study area and soil samples

The Burgundy region, in the east of France, has an area of 31,582 km^2 and is characterised by an interesting environmental heterogeneity, resulting from climatic, geological, geomorphological and land-cover diversity.

There are three major geological ensembles in the region (Fig. 1). The Massif du Morvan, in the centre, is composed of Hercynian granite, Palaeozoic volcanic rocks, and metamorphic rocks (granite, basalt and gneiss) and is bordered by continental sediments (sandstone and clay). In the northern part of the region, are found marls and calcareous sedimentary rocks dating from Trias and Jurassic (marl, limestone) and younger marine sediments dating from Cretaceous (clay and chalk). In the Bressan graben floodplains, to the south-east, and the Loire and Yonne river valleys, in the south-west and the north-west of the region, Cenozoic sediments form the bedrock (recent alluvial sediment). The highest elevations are found in the Massif du Morvan (901 m a.s.l.), and the lowest in the valley of the River Yonne (50 m a.s.l.).

Three different types of climate influence the Burgundy region. The Oceanic climate is dominant and results in greater precipitation (about 1000 mm year^{-1}) in the western part of the region. Mild temperatures are however impeded by the elevation, which reinforces seasonal thermal differences. The eastern part of the region is subjected to a Continental influence from the east and north-east, while Mediterranean influence following the River Rhône corridor results in warmer temperatures in the south of the region during summer.

The land cover is a mosaic of forest (9950 km^2), permanent grassland (8000 km^2) and cropland (10580 km^2) in balanced proportions (Fig. 1). Deciduous and coniferous forests are both present. Croplands are mainly areas of intensive agriculture, and all grasslands are permanent for at least ten years.

All soil samples were collected for the RMQS project, the French soil quality-monitoring network (http://www.gissol.fr/programme/rmqs/rmqs.php).

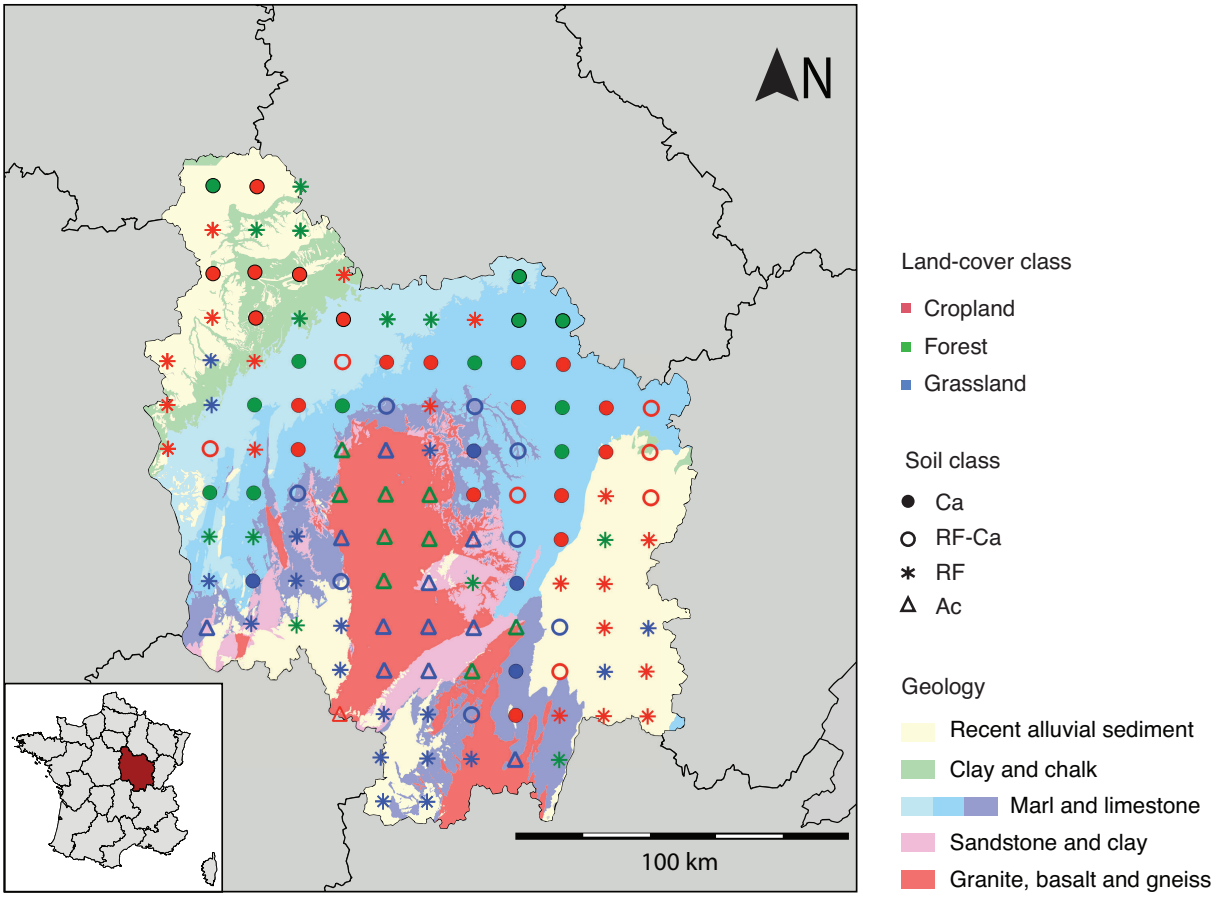

Figure 1 Simplified geological map of the Burgundy region, with the sampling locations, and indications of land cover (colour of symbol) and soil classes (form of symbol).

The RMQS project is a scientific program covering the whole of France. It consists of a systematic sampling of soils on a 16 km regular grid across the French territory, and the complete inventory includes 2,200 sites. The topsoil (0-30 cm or less for thinner soils) was sampled at the centre of each 16 x 16 km cell. The final sample is a composite of 25 core samples taken within a 20 m x 20 m area, using an unaligned sample design. Each sample was precisely geopositioned, and the soil profile and site environment were described. Soil samples were air-dried, sieved to 2 mm and stored before further analysis. More details on the sampling protocol are available in Jolivet et al. (2006). This study was conducted on the 120 topsoil samples from the Burgundy region.

We considered two categorical variables that are supposed to control the biogeochemistry of soil. The first categorical variable is land cover, grouped into three classes: cropland (n=46), forest (n=33), and grassland (n=41).

The second categorical variable corresponds to soil geochemical classes and is composed of four groups, determined with respect to bedrock type, as well as geomorphological condition, pH, carbonate and exchangeable calcium content. We built this classification considering two contrasted geochemical poles: the first dominated by calcium and the second dominated by silicon.

The first class, denoted Ca (n=35), comprised alkaline soils, developed on calcareous rock and containing more than 2% of $CaCO_3$. The soil types in this first class are Cambisols (Calcaric) and Rendzic Leptosols (IUSS Working Group WRB, 2006).

The second class, denoted Ac (n=21), includes acidic soils developed on magmatic, metamorphic rocks and acidic sandstones in the Morvan area, corresponding to Cambisols (Dystric, Eutric or Hypereutric), Cambic Umbrisols and Umbric Leptosols (IUSS Working Group WRB, 2006).

The remaining soil samples are soils developed on residual formations, such as alluvial and colluvial deposits, eolian loamy deposits or weathered soils on carbonate rocks. These samples were divided into two classes, based on their concentration in exchangeable calcium.

The class denoted RF-Ca (n=15) thus comprised the soils developed on residual formations with a high content of exchangeable Ca (arbitrary minimum threshold fixed at 150 μmol g^{-1}), corresponding to Cambisols (Hypereutric), Luvic Cambisols,

Haplic Luvisols, Haplic Albeluvisols, Fluvisols, Planosols and Gleysols (IUSS Working Group WRB, 2006).

The class denoted RF (n=49) is composed of the soil samples developed on residual formations with a low content of exchangeable Ca (less than 150 µmol.g^{-1}) and are Cambisols (Eutric) and Fluvisols (Eutric) (IUSS Working Group WRB, 2006).

2.2 Soil physico-chemical analyses

The Soil Analyses Laboratory of INRA (Arras, France, http://www6.lille.inra.fr/las) performed analyses of soils. The pH_{water} was measured in a soil:water solution (ratio 1:5) (NF ISO 10390). Soil texture was determined using the pipette Robinson method (NF X 31-107). Total carbonates were quantified by volumetric method using the Bernard calcimeter (NF ISO 10693). Total organic carbon (NF ISO 10694) and total nitrogen (NF ISO 13878) contents were measured by dry combustion.

2.3 Extraction of Pressurised Hot-Water-Extractable Organic Carbon

Pressurised hot-water-extractable organic carbon (PH-WEOC) was extracted using a solvent extractor (ASE200, Dionex Corporation, Sunnyvale, USA). A previous study by Guigue et al. (2014) has shown that this method is suitable to study water-extractable organic matter in soils. The extraction consisted of the leaching of 10-g soil samples with ultrapure water at 100° C and 10 MPa. All conditions were the same as in the study of Guigue et al. (2014). All samples were extracted at least in duplicate, and additional extractions were performed when the relative variability exceeded 10 % for the extraction parameters (volume, $SUVA_{254}$ and extraction ratio; see below).

2.4 Characterisation of PH-WEOC extracts

After extraction, the volume was determined gravimetrically; the pH was measured with a microelectrode N 5800 A (Schott Instruments); specific ultraviolet (UV) absorbance at 254 nm ($SUVA_{254}$) was measured with a Jenway 6715 spectrophotometer. After acidification, the organic C content in the extracted solutions was quantified in 5 ml subsamples with a total organic carbon analyser (TOC 5000A, Shimadzu) in NPOC mode.

The extraction ratio (ER) expressing the efficiency of the extraction procedure was then calculated as the ratio of extracted C to total soil organic C (Eq. 1).

$$(1)\ ER = (V \times [C_{PH\text{-}WEOC}]) / (P \times [C_{soil}])$$

where ER is the extraction ratio in mg of C extracted per g of soil C; V is the volume of the extracted solution in ml; $[C_{PH\text{-}WEOC}]$ is the concentration of C in the extract in μg g^{-1}; P is the weight of soil in g; and $[C_{soil}]$ is the concentration of C in the soil in mg g^{-1}

2.5 Isotopic measurements

Measurements of $\delta^{13}C$ were performed on the bulk soil samples and on PH-WEOC extracts. Before analysis, carbonates were removed from soil samples with excess of 2 M HCl. The PH-WEOC extracts were acidified to remove inorganic carbon, then freeze-dried. Isotopic analyses of the organic fraction were performed in triplicate on a Vario Micro Cube elemental analyser coupled in a continuous flow mode to an isotope ratio mass spectrometer (IsoPrime, Elementar). The USGS40 (IAEA) was used as a standard ($\delta^{13}C_{PDB}$ = -26.2 ± 0.1 ‰). All results are expressed in delta notation (Eq. 2).

$$(2)\ \delta^{13}C = [R_{sample} / R_{std}) - 1] \times 1000$$

where R_{sample} and R_{std} are the absolute $^{13}C/^{12}C$ ratios for sample and standard. $\delta^{13}C$ values are reported in parts per thousand (‰) relative to the Vienna Pee Dee Belemnite (VPDB) international reference.

2.6 Microbial community structure analysis

DNA extraction and purification

DNA was extracted from the 120 soil samples, following the procedure optimised by Ranjard et al. (2003). Briefly, 1.5 g (dry weight) of soil sample was mixed with 5 ml of a solution containing 100 mM TRIS (pH 8.0), 100mM EDTA (pH 8.0), 100mM NaCl and 2% (w/v) sodium dodecyl sulphate. Two grams of 106-mm diameter and eight 2-mm diameter glass beads were added in a bead-beater tube and were then homogenised for 30 s at 1600 r.p.m. in a mini bead-beater cell disruptor (Mikro-dismembrator S.B. Braun Biotech International). The samples were then incubated

for 30 min at 70° C, and centrifuged at 7000 g for 5 mn at 15° C. Supernatants were collected and incubated for 10 min on ice with 1/10 volume of 3 M potassium acetate (pH 5.5) and centrifuged at 14,000 g for 5 min. After precipitation with one volume of ice-cold isopropanol, the nucleic acids were washed with 70% ethanol and resuspended in 100 ml of sterile ultrapure water.

Quantification of DNA extracts

As described in Dequiedt et al. (2011), crude DNA extracts were resolved by electrophoresis in a 0.8% agarose gel, stained with ethidium bromide and photographed (Infinitycapt, Vilber Lourmat). Dilutions of calf thymus DNA (Bio-Rad) were included in each gel and a standard curve of DNA concentration was used to estimate the final DNA concentration in the crude extracts. The ethidium bromide intensity was integrated with ImageQuaNT software (Molecular Dynamics).

ARISA fingerprinting

The Bacterial Automated Ribosomal Intergenic Spacer Analysis (B-ARISA) techniques are molecular fingerprinting methods (Ranjard et al., 2001) that take advantage of the length polymorphism of bacterial ribosomal InterGenic Spacers (IGS) and of the relative abundance of the different IGS sizes to characterise the genetic structure of soil bacterial communities. The ribosomal IGS were amplified with 50 ng of DNA as template and with the primer set: S-D-Bact-1522-b-S- 20/L-D-Bact-132-a-A-18. The PCR conditions were as described by Ranjard et al. (2003). The S-D-Bact-1522-b-S-20 primer was labelled at its 5' end with the IRD800 fluorochrome to allow detection of the PCR fragments by the sequencer system (ScienceTec). The ARISA fragments were resolved on 3.7% polyacrylamide gels under denaturing conditions for 15 h at 3000 V/60W on a LiCor DNA sequencer (ScienceTec).

Data obtained from the 1D-Scan software (ScienceTec) were converted into a table summarising band presence and intensity, using the PrepRISA program. The resulting ARISA data matrix (soil samples as rows and bands as columns) takes into account the presence/absence and relative intensity of bands. Lengths, in base pairs (bp), were calculated by using a size standard with bands ranging from 200 to 742 bp for bacterial communities.

2.7 Statistical analysis

Statistical analyses were performed using the software JMP 9.0 (SAS Institute) and R 3.1.0 (R Core Team, 2012). The differences in pH, texture, SOC, TN, C/N, ER, $SUVA_{254}$ and $\delta^{13}C$ signature between the three land-cover classes and between the four soil classes were assessed using the non-parametric Steel-Dwass multiple comparison, as soil properties showed heteroscedasticity. The difference between the $\delta^{13}C$ of soil and of PH-WEOC was tested with a matched pairs *t*-test. Linear regressions were fitted using the ordinary least squares method. A multiple linear regression of the ER values against soil variables was computed with the stepwise procedure, using a bidirectional elimination of variables and a *K*-fold validation. A principal component analysis (PCA) was performed on the correlation matrix of the soil and PH-WEOC variables. A second PCA was computed on the covariance matrix of the B-ARISA profiles obtained for each soil. To estimate the relationship between soil physico-chemistry and the genetic structure of the microbial communities, we computed a co-inertia analysis, using the ade4 1.6-2 package (Dray et al., 2003). The co-inertia analysis is a symmetric multivariate method for the matching of two or more data tables. In our study, we examined co-inertia between the matrices (with samples as row and scores on retained PCA axis as columns) of (i) soil physico-chemical variables resulting from the first PCA and (ii) the ecological information from the PCA on the B-ARISA profiles. A randomisation test of 1000 permutations (Monte Carlo test) was performed to confirm the significance of the co-structure between the two data tables.

Table 1 Means and standard errors of pH, texture, soil organic carbon (SOC), total nitrogen (TN) and C/N ratio of the 120 topsoils grouped by land cover (top) and soil class (bottom). For each variable, multiple comparisons were computed separately for the effect of land cover and of soil class. For each variable, a change of letter indicates a significant difference (Steel-Dwass' test, $P < 0.05$) between the land-cover classes or between the soil classes.

	n	pH	Sand	Silt	Clay	SOC	TN	C/N
			mg g^{-1}	mg g^{-1}	mg g^{-1}	mg g^{-1}	mg g^{-1}	
Land-cover class								
Cropland	46	6.4 (0.1)a	222 (24)a	455 (18)a	323 (19)a	18.2 (1.3)a	1.8 (0.1)a	10.1 (0.3)a
Forest	33	5.0 (0.2)b	260 (35)a	424 (23)ab	316 (29)a	46.1 (5.0)b	2.8 (0.3)b	17.1 (0.6)b
Grassland	41	5.4 (0.1)b	331 (35)a	384 (23)b	285 (26)a	26.7 (2.2)c	2.4 (0.2)b	11.2 (0.3)c
Soil class								
Ca	35	6.9 (0.1)a	144 (19)a	407 (16)a	449 (18)a	40.1 (4.2)a	3.2 (0.2)a	11.9 (0.5)a
Rf-Ca	15	6.1 (0.1)b	79 (17)a	449 (26)ab	472 (31)a	31.5 (4.8)a	2.8 (0.3)ac	10.9 (0.7)a
Rf	49	5.2 (0.1)c	302 (24)b	483 (21)b	214 (11)b	17.5 (1.1)b	1.4 (0.1)b	12.4 (0.6)a
Ac	21	4.4 (0.1)d	539 (25)c	285 (20)c	176 (8)b	34.4 (5.7)a	2.2 (0.2)c	14.4 (1.1)a

Table 2 Means and standard errors of extraction ratio (ER) and $SUVA_{254}$ of the topsoils grouped by land cover (top) and soil class (bottom). For each variable, multiple comparisons were computed separately for the effect of land cover and of soil class. For each variable, a change of letter indicates a significant difference (Steel-Dwass' test, $P < 0.05$) between the land-cover classes or between the soil classes.

	n	ER	$SUVA_{254}$
		mg C g^{-1} soil C	L mg^{-1} C cm^{-1}
Land-cover class			
Cropland	46	30.9 (1.6)ab	0.016 (0.001)a
Forest	33	26.6 (1.9)a	0.011 (0.001)b
Grassland	41	35.5 (1.6)b	0.014 (0.001)a
Soil class			
Ca	35	23.2 (1.4)a	0.012 (0.003)a
Rf-Ca	15	27.2 (2.5)ab	0.014 (0.001)ab
Rf	49	37.9 (1.3)c	0.016 (0.001)b
Ac	21	32.2 (2.3)bc	0.013 (0.001)ab

3 Results

3.1 Soil physico-chemical diversity

Each sample was assigned to two distinct classifications. The first classification refers to the vegetation and is divided into three groups (cropland, forest, and grassland), while the second classification was built considering the soil abiotic environment (bedrock, geomorphology) and is divided into four groups, denoted Ca, Rf-Ca, Rf and Ac (see Materials and methods section). Unfortunately, the systematic sampling applied in the RMQS program was not developed specifically to test the effect of land-cover and soil classes at a regional scale, which therefore results in an unbalanced design if both effects are considered simultaneously. The large number of samples, however, does allow the two effects to be investigated separately.

The soil characteristics in each of these groups are listed in Table 1. Cropland soils are characterised by higher pH and lower SOC and TN contents, as well as lower C/N. The forest soils are generally enriched in SOC and TN and have higher C/N, while intermediate SOC content and C/N were found in grassland soils. The second classification based on soil characteristics leads to a more clear differentiation regarding pH and texture. Soils from the Ca group have higher pH, high clay and silt contents, as well as high SOC and TN contents. The Rf-Ca group is characterised by slightly lower pH and shows similar contents of clay and silts, as well as SOC and TN, to soils from the Ca group. The Rf class comprises soils with a siltic texture, lower pH than in the previous classes and low SOC and TN contents. The fourth group, denoted Ac, contains soils with more acidic pH, sand-rich texture and SOC and TN contents similar to those of the Ca and Rf-Ca groups. No significant differences were found in C/N between soil classes.

3.2 PH-WEOC quantity and aromaticity in relation to land-cover and soil classes

The extraction ratio (ER) expresses the yield of the extraction as the ratio of extracted C to total soil organic C. The ER values range from 10.4 to 59.5 mg C g^{-1} SOC, with a mean of 31.3 ± 1.0 mg C g^{-1} SOC. The ER is higher in grassland soils and lower in forest soils, and a significant difference was found between these two groups of samples.

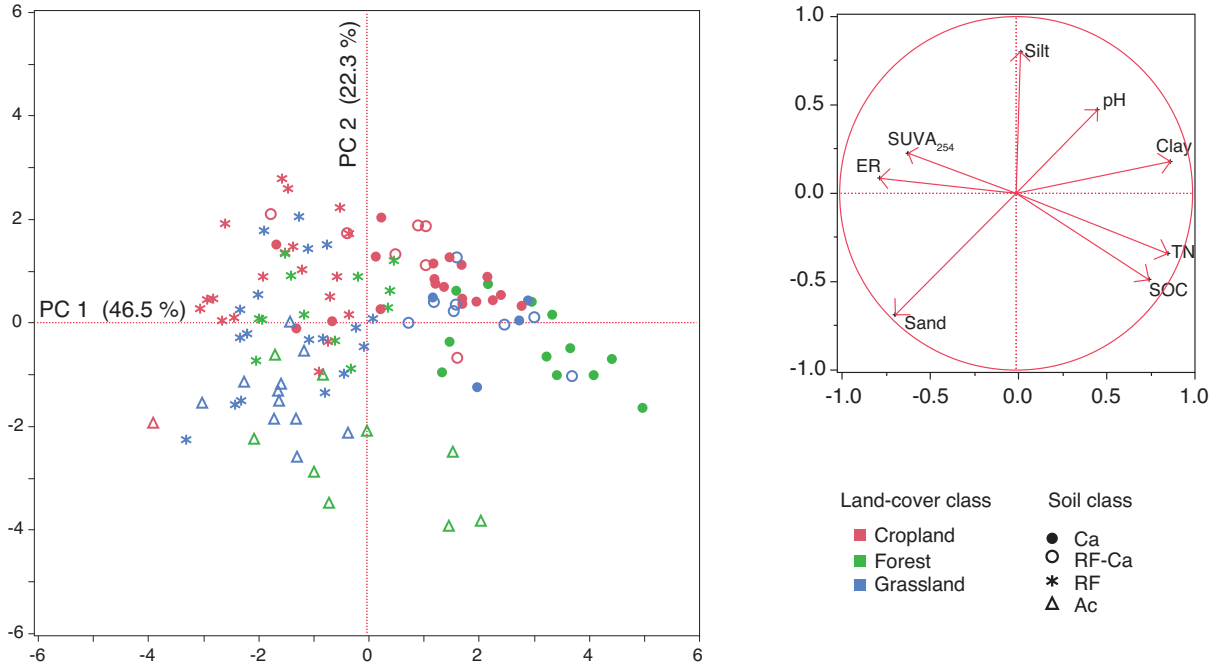

Figure 2 Score plot (a) of the principal component analysis (PCA) of the 120 soil samples from the Burgundy region, computed from the variables of soil physico-chemistry. Eight variables were investigated in the PCA (pH; clay; silt; sand; SOC; TN; $SUVA_{254}$ and ER). The first (PC 1) and second (PC 2) principal components are represented with indications of land cover (colour of symbol) and soil classes (form of symbol). The correlation coefficients (loadings) between the original variables and the first two principal components are represented in the loading plot (b). The loadings reflect the importance of the original variables in the direction of each principal component.

Intermediate values were measured for cropland soils and no significant difference was found with the other land-cover groups (Table 2). Lower ERs were measured in soils of the Ca group, while soils of the Rf group were characterised by higher ERs.

We then characterised the PH-WEOC by measuring its specific UV absorbance at 254 nm ($SUVA_{254}$). We found that the $SUVA_{254}$ is generally lower in PH-WEOC extracted from forest soils compared to grassland and cropland soils (Table 2). Significant differences were also found between soil classes, with aromaticity lower in soils of the Ca class, but higher in soils assigned to the Rf class. The $SUVA_{254}$ values of PH-WEOC from soils of the Rf-Ca and Ac classes were generally intermediate.

All variables reported in Table 1 and Table 2 (except C to N ratio) were then investigated using a PCA approach. The PCA well discriminates our sample set, when considering variables of soil physico-chemistry and of the PH-WEOC pool (extraction ratio, $SUVA_{254}$). The first two principal components explained about 69% of the total variance of the dataset. The sample scores and the variable loadings are presented in Figure 2. The projection of variables in the loading plot shows that they are ordered in two groups. The first one grouped pH and soil texture (sand, loam, and clay) and distributes the samples between bottom left and top right in the PCA space. The second group of variables scattered the samples between top left and bottom right, and groups the variables that refer to soil organic matter content and characteristics (SOC, TN, ER and $SUVA_{254}$).

3.3 $\delta^{13}C$ signature of SOC and PH-WEOC

Considering the whole sample set, we found that the $\delta^{13}C$ of soil organic carbon ranges from -28.6 ‰ to -24.4 ‰. We measured more negative $\delta^{13}C$ of SOC in grassland soils compared to the $\delta^{13}C$ in cropland and forest soils (Table 3). When comparing the $\delta^{13}C$ signatures by soil class, we found few differences between the four groups, which could be related to the occurrence of the three different land covers in each of the soil classes.

We also measured the $\delta^{13}C$ signature in the PH-WEOC pool. The $\delta^{13}C$ of PH-WEOC ranges from -28.4 ‰ to -22.4 ‰. Again, we observed clear differences in $\delta^{13}C$ signatures, in relation to the land-cover categories (Table 3). The PH-WEOC of grassland soils is isotopically lighter than the PH-WEOC of forest soils, while in cropland soils we measured

Table 3 Means and standard errors of $\delta^{13}C_{PDB}$ of SOC and of PH-WEOC and differences between $\delta^{13}C_{PH\text{-}WEOC}$ and $\delta^{13}C_{SOC}$ ($\Delta^{13}C$) of the 120 topsoils grouped by land cover (top) and soil class (bottom). For each variable, multiple comparisons were computed separately for the effect of land cover and of soil class. For each variable, a change of letter indicates a significant difference (Steel-Dwass' test, $P < 0.05$) between the land-cover classes or between the soil classes.

	n	$\delta^{13}C_{SOC}$ ‰	$\delta^{13}C_{PH\text{-}WEOC}$ ‰	$\Delta^{13}C$ ‰
		Land-cover class		
Cropland	46	-26.7 (0.1)a	-25.8 (0.2)a	0.94 (0.10)a
Forest	33	-26.7 (0.1)a	-24.2 (0.2)b	2.55 (0.15)b
Grassland	41	-27.9 (0.1)b	-27.1 (0.1)c	0.86 (0.05)a
		Soil class		
Ca	35	-26.8 (0.1)a	-25.4 (0.2)a	1.39 (0.20)a
Rf-Ca	15	-27.5 (0.2)b	-26.7 (0.2)b	0.82 (0.07)a
Rf	49	-27.2 (0.1)ab	-25.7 (0.2)ab	1.47 (0.15)a
Ac	21	-27.4 (0.2)b	-26.0 (0.3)ab	1.42 (0.18)a

Table 4 Means and standard errors of biomass abundance, bacterial and fungal densities (in base pairs) and fungal to bacterial ratio (F/B) of the 120 topsoils grouped by land cover (top) and soil class (bottom). For each variable, multiple comparisons were computed separately for the effect of land cover and of soil class. For each variable, a change of letter indicates a significant difference (Steel-Dwass' test, $P < 0.05$) between the land-cover classes or between the soil classes.

	n	Biomass µg DNA g^{-1} soil	B Dens 10^9 bp	F Dens 10^7 bp	F/B %
			Land-cover class		
Cropland	46	9.0 (0.5)a	10.0 (2.6)a	6.0 (0.9)a	1.11 (0.17)a
Forest	33	17.1 (1.9)b	9.9 (2.3)a	26.9 (7.6)b	4.07 (0.98)b
Grassland	41	10.0 (0.7)a	11.5 (2.9)a	3.9 (0.6)a	1.78 (0.91)a
			Soil class		
Ca	35	16.6 (1.7)a	18.3 (3.5)a	24.8 (7.3)a	1.81 (0.39)a
Rf-Ca	15	12.1 (1.5)ab	17.2 (7.4)a	6.2 (1.1)ab	0.78 (0.21)a
Rf	49	8.9 (0.6)b	4.7 (5.3)b	4.8 (0.7)b	1.96 (0.50)a
Ac	21	9.1 (0.7)b	5.6 (1.4)b	6.8 (2.7)b	4.28 (2.03)a

intermediate $\delta^{13}C$ signatures. As observed for SOC, there are few differences related to soil class, which seem to be primarily related to the differences in land-cover distribution.

We found that the $\delta^{13}C$ signature in PH-WEOC was significantly less negative than in bulk SOC. This difference between the $\delta^{13}C$ of PH-WEOC and the $\delta^{13}C$ of SOC is noted $\Delta^{13}C$ and is reported in Table 3. The values range between -0.9 and 4.3 ‰, with a mean ^{13}C-enrichment in PH-WEOC of about 1.4 ‰. The $\Delta^{13}C$ is significantly greater in forest soils than in grassland and cropland soils (Table 3). No differences were found between the mean values of $\Delta^{13}C$ in the four soil classes.

3.4 Microbial communities

Distribution of microbial biomass, as measured through the amount of DNA extracted from soil samples, ranged from 2.1 to 41.8 µg DNA g^{-1} soil, with significant differences between land-cover categories (Table 4). The highest mean value was measured in forest soils, with 17.1 ± 1.9 µg DNA g^{-1} soil. Lower biomass yields were measured for the other land-cover categories, and no significant differences were found between cropland and grassland, with 9.0 ± 0.5 and 10.0 ± 0.7 µg DNA g^{-1} soil, respectively. The greater abundance of microorganisms in forest soils results from the higher fungal density in these samples, with about five times more gene copy numbers per gram of dry soil detected in the forest soils compared to the samples from grassland and cropland (Table 4). No differences in bacterial densities were found between the three categories of land-cover, with a mean of 10.5×10^9 gene copies g^{-1}. The greater abundance of fungal communities in forest soils also leads to a fungal to bacteria (F/B) ratio significantly higher in the forest soils than in cropland and grassland soils (Table 4). Depending on the soil class, we found that total biomass, bacterial density and fungal density are much higher in soils of the Ca group. High values were also measured for biomass and bacterial density in samples from the Rf-Ca group, while lower abundance of microorganisms were found in samples from the Rf and Ac groups (Table 4). A great variability was observed in F/B ratio between the soil classes, but no significant difference was found.

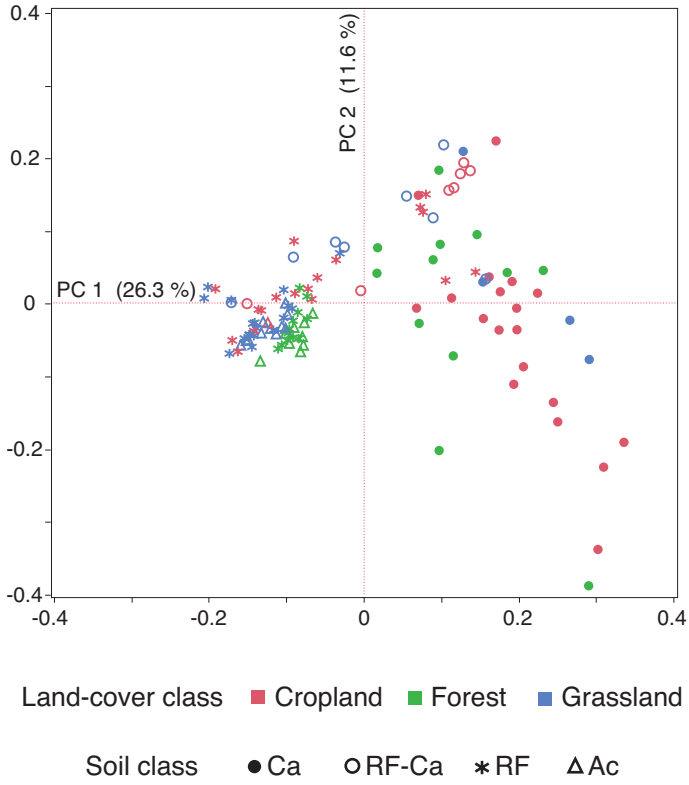

Figure 3 Score plot of the principal component analysis (PCA) of the 120 soil samples from the Burgundy region, computed from the 100 most dominant bands in the B-ARISA profiles. The first (PC 1) and second (PC 2) principal components are represented with indications of land cover (colour of symbol) and soil classes (form of symbol).

The complex B-ARISA profiles were summarised through a PCA approach, allowing a visual evaluation of the variations in the genetic structure of the bacterial community between samples. The two first principal components explain 37.9% of the total variance, and the scores of the samples are represented in Figure 3. Some of the samples have positive scores on the first axis and are well discriminated in the PCA space. We found that all samples from the Ca class were included in this group of differentiated samples. Half of the grassland soils in the Rf-Ca class and the cropland soils from the Rf-Ca and Rf classes are also included in this group of differentiated samples. Most of the samples from the Ac and Rf classes appear very close in the PCA space, with negative scores on the first axis and very slight variability on the first two axes. Investigations were also conducted considering the 3rd to 5th axes of the PCA (data not shown) but did not further discriminate our sample set, showing the limitation of this statistical approach for the investigation of the genetic structure of bacterial communities with such a large and heterogeneous sample set.

In order to detect possible relationships between soil physico-chemistry and bacterial community structure, a co-inertia analysis was computed, considering them as two distinct datasets. The Monte Carlo test confirmed a significant co-structure (RV = 0.38; $p<0.001$) between the two datasets. The samples were plotted in the resulting co-inertia space considering their ARISA profiles (Fig. 4a). The contribution of the variables of soil physico-chemistry to the co-structure is represented as a projection in this same co-inertia space in Figure 4b. The samples are well separated on the first axis, yielding 87.8 % of the variance in the co-structure. The soil variables with the heaviest canonical weights on this axis are pH, clay and sand contents, and ER. We observed a good separation of the samples in the co-inertia space according to soil class. All samples of the Ca class have positive scores on the first axis, while samples of the Ac class all have negative scores. The samples of the Rf-Ca group are more scattered along this axis and most of the Rf samples have negative scores, with the exception of five cropland soils with positive scores on this first axis. The second axis accounts for only 7.2% of the variance in the co-structure. The two variables that drive the variance on this second axis are the SOC content and the $SUVA_{254}$. The discrimination along the second axis tends to separate the samples by soil class, with more positive scores on the second axis for samples from the Ca and Ac groups.

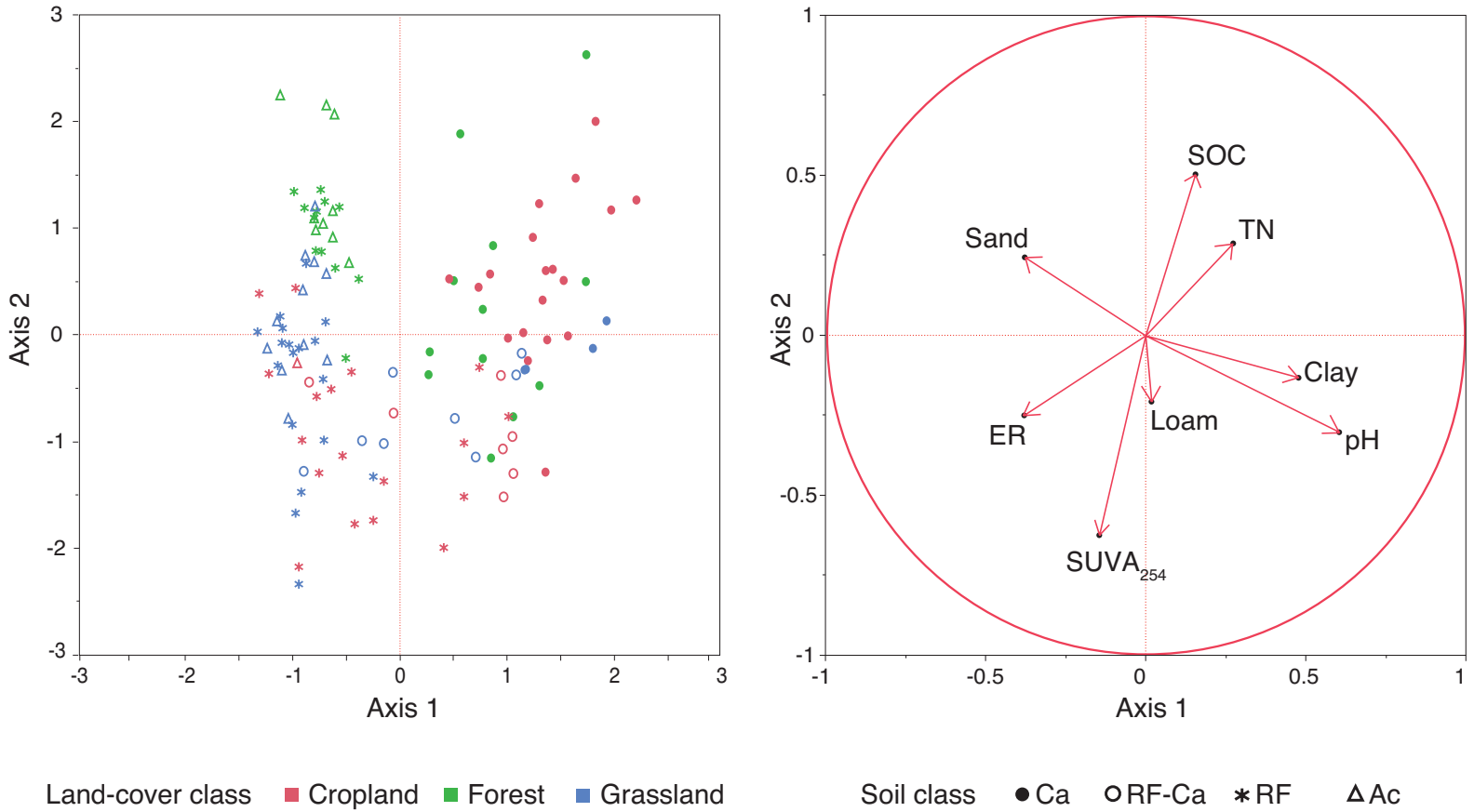

Figure 4 (a) Relative position of the samples in the first factorial plan of the co-inertia analysis with indications of land cover (colour of symbol) and soil classes (form of symbol), and (b) canonical weights of the soil physico-chemical variables in the first factorial plan of the co-inertia analysis.

4 Discussion

4.1 Linking soil diversity to land-cover and soil classes

Considering variables of soil physico-chemistry and soluble organic matter (PH-WEOC), we found that both land-cover and soil classes have an effect on soil properties and describe well the main variability observed in soils of the Burgundy region. The best investigation of soil diversity was undoubtedly the PCA (Fig. 2). The main factors controlling soil diversity are soil classes, through the different types of soil parental material. These two factors are the basis of the soil classes we determined, characterised by clear heterogeneities of texture and pH (Table 1). Following the order Ca > Rf-Ca > Rf > Ac, a clear decrease in pH was found and a transition from clayic textures to sandic textures was also observed. The diversity of bedrock in the Burgundy region (siliceous rocks, marl, limestone or recent alluvial deposits) is responsible for the great variability in soil pH measured in this study. The soil texture is also closely related to the bedrock geology and to the geomorphology of the sampling area. Previous studies on the spatialisation of soil texture (Jordan et al., 2005; Zhao et al., 2009) reported that type of parent material and topographical position are two major drivers of soil texture.

The samples of the Ca and Rf-Ca groups are found at the top right of the PCA space, in line with the high pH and the dominance of clay and silt in these soils. The similarity between the Ca and Rf-Ca groups is consistent with the results for each variable investigated individually, which revealed few differences between these samples (Table 1 and 2) and suggest the importance of exchangeable calcium and calcium carbonate in these soils. The samples of the Ac group, characterised by low pH and higher sand content, are located on the opposite side of the score plot. The samples of the Rf group have intermediate pH and texture, and their position reflects the influence of the second set of variables, belonging to soil organic matter (SOC, TN) and PH-WEOC (ER, $SUVA_{254}$). These variables reveals clear specificities for the soils of the Rf class, with generally low SOC and TN contents, and high ER and $SUVA_{254}$ (Table 1 and 2). Within each soil class, the distribution in the PCA space of the samples with different land covers is governed by this second set of variables (Fig. 2).

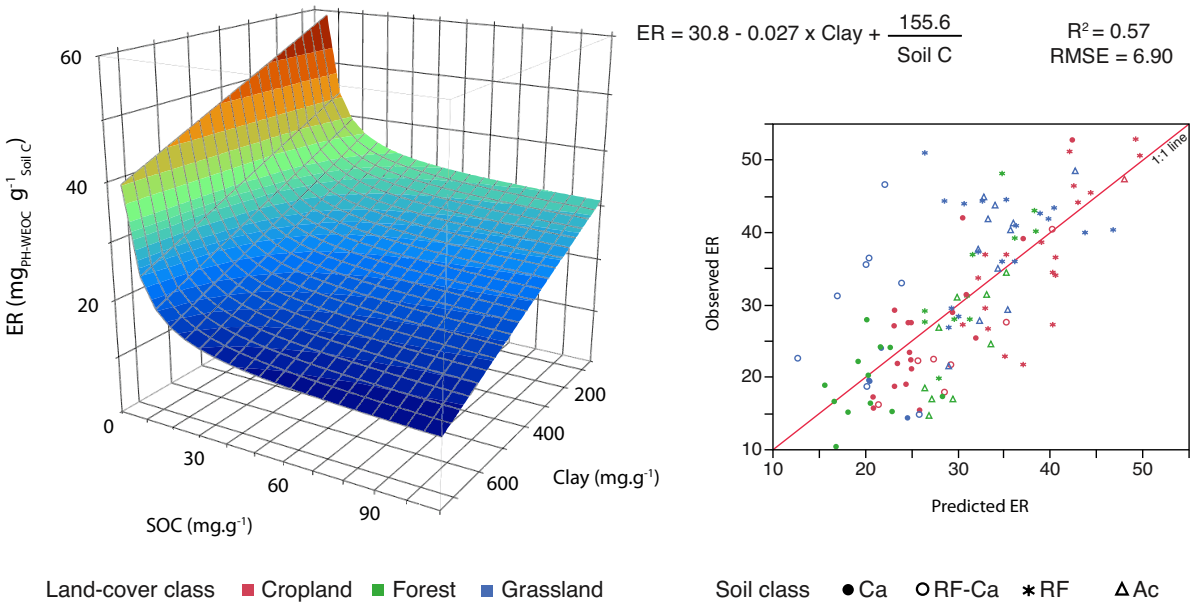

Figure 5 Multiple correlation model between extraction ratio (ER), and soil organic carbon (SOC) and clay contents. (a) Response surface plot of ER as a function of SOC and clay contents. (b) Observed vs predicted values of ER, with indications of land cover (colour of symbol) and soil classes (form of symbol).

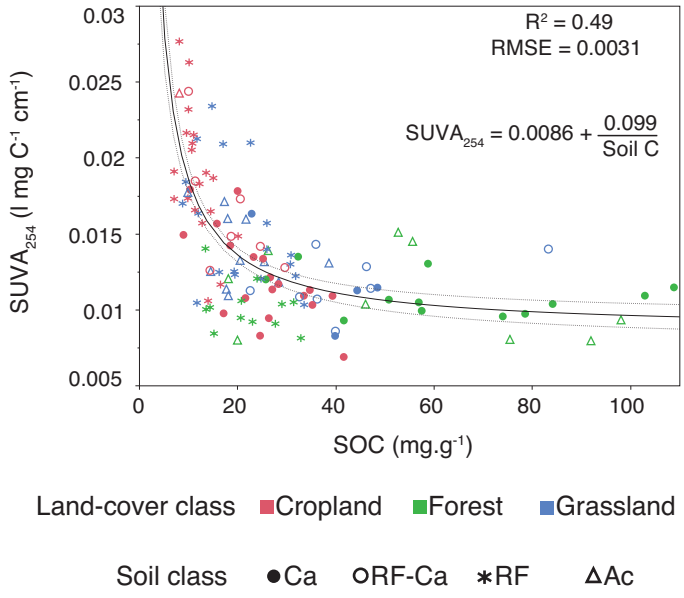

Figure 6 Correlation between $SUVA_{254}$ and SOC content with indications of land cover (colour of symbol) and soil classes (form of symbol). The solid line corresponds to the best-fitted model, and its equation and model parameters are presented on the plot.

The forest soils, characterised by high SOC content and low $SUVA_{254}$, are mostly located on the right, and the cropland soils, which showed lower SOC contents and high ER and $SUVA_{254}$, are on the left of the score plot, while the grassland soils are in intermediate positions. This pattern highlights the differences observed in organic matter properties between the soils of the three classes of land cover (Table 1 and 2). To summarise, soil diversity is primarily controlled by type of soil and parental bedrock, and the corresponding gradient in pH and texture. Nevertheless, the effect of land cover is observed in each of the soil classes. This effect is linked to the differences in organic matter quantity and PH-WEOC characteristics, and seems to be a secondary influence compared to the effect of soil class.

4.2 PH-WEOC characteristics in relation to soil diversity

Most studies reporting the results of soil C extraction relate the yield of C in the extracts to bulk soil mass (e.g. Embacher et al., 2007; Uselman et al., 2012). Here we report the amount of extracted C related to total SOC, and note this as the extraction ratio (ER). This way of calculating extraction results is rarely used in the literature (Zhao et al., 2008; Guigue et al., 2014), but it provides interesting information, as it expresses the proportion of potentially extractable SOC.

The multiple linear regression model showed that ER is controlled by both SOC and clay content (Fig. 5). The stepwise procedure for variable selection revealed that no other variables from our dataset improve the prediction of ER. This model can help to predict ER in soils from temperate ecosystems. However, even if this model describes our data quite well (R^2 = 0.57), the equation should not be used for extrapolating ER values for soils with SOC and clay contents that exceed the limits of the axes presented here, or for specific soil types not studied in our work, such as Histosols, Chernozems or Cryosols, for example. Furthermore, considerable uncertainties subsist in the prediction of ER values (RMSE = 6.9), and other large-scale studies may help to improve the prediction of ER.

The inverse relation of ER to SOC reveals that in soils with decreasing SOC content, the increase in the proportion of extractable C is more pronounced. This relation is consistent because, even for soils with low SOC content, we never extracted less than 0.25 mg of C per gram of soil, as if there was always a minimum quantity of extractable C.

The quantification of bacterial and fungal densities in the soils of the Burgundy region (Table 4) revealed that even the soils from the sub-classes characterised by low SOC and TN contents contain significant amount of microorganisms. In soils with low SOC content, microbial activity thus seems to be maintained, and it is logical that the soluble organic C pool represents a greater proportion of the total SOC, thus corresponding to greater ER values in these samples. On the other hand, in soils with a high C content, a smaller proportion of SOC is extracted. This is consistent if we consider that, when SOC is high, there is no limitation for the microorganisms to access the SOC as a substrate for energy, and the ratio of biomass to SOC is often lower, thus leading to smaller proportions of SOC being processed by microorganisms, and so to smaller ERs.

The relation of ER with clay is easier to explain. Many studies have shown that organic matter is progressively transferred to the finer fraction during stabilisation (Feng et al., 2011; Gunina & Kuzyakov, 2014). This process leads to the isolation and protection of organic matter within aggregates. It is logical that this protection mechanism is greater in soils with clayic textures, while the aggregation of organic matter is necessarily smaller in sandy soils. These different potentials of aggregation may explain why we measured higher ER in soils with low clay content, and decreasing ER values when clay content increased.

We also detected an influence of SOC content on PH-WEOC quality, with an inverse relation between $SUVA_{254}$ and the SOC content of the samples (Fig. 6). The $SUVA_{254}$ is a good indicator of aromatic carbon content in dissolved organic matter (Weishaar et al., 2003). The correlation indicates low aromaticity of PH-WEOC in organic-rich soils. High organic matter content may lead to the preferential extraction of non-aromatic and more hydrophilic compounds, such as carbohydrates, microbial metabolites and microbial decay products, explaining the decrease observed in PH-WEOC aromaticity. The high abundances of bacterial and fungal biomass (Table 4) in the forest soils support this hypothesis, as they suggest increased production of organic compounds with low aromaticity resulting from microorganism activity.

We observed a sharp increase in $SUVA_{254}$ for the samples with low SOC content. Most of these soils with high aromaticity are cropland or grassland soils of the Rf class. An explanation of this high aromaticity of PH-WEOC could be that the solubilised

compounds are mainly derived from the stabilised C pool. This is valuable for cropland soils, because of the deficit in new C entrance into agricultural soils (exportation of crops at harvest or crop residue burning). This situation promotes the mineralisation of the stable C pool that may result in the release of aromatic humified compounds into the PH-WEOC during its degradation by microorganisms. Another explanation is that smaller quantities of non-aromatic compounds are produced and preserved in these soils with low SOC content. This is supported by the low amount of microbial biomass in the Rf soils and in cropland soils, which must result in lower degradation rates of soil organic matter and in lower production of microbial metabolites and microbial decay products.

To summarise, forest soils differ from the soils of other land-cover classes, as the ER is lower for these samples, revealing that a smaller proportion of SOC is potentially soluble, and the PH-WEOC extracted from these soils is generally less aromatic. The PH-WEOC extracted from cropland soils is enriched in aromatic C, probably with an increased contribution of the more humified, stable C pool to the PH-WEOC. The effect of soil classes on ER and $SUVA_{254}$ is mainly related to SOC and clay contents.

4.3 ^{13}C dynamics in soils and in PH-WEOC

The $\delta^{13}C$ measurements of SOC have largely been used in C3/C4 environments (Balesdent et al., 1987; Jolivet et al., 2003), in soil aggregate size fractions (Gunina & Kuzyakov, 2014), and in specific soil profiles (Amiotte-Suchet et al., 2007). However, few studies present results for such large sample sets. In this study, the contribution of C4 plants is supposed to make a minor contribution to the SOC isotopic signature and is suspected for only a few cropland soils, with the $\delta^{13}C$ of SOC around -25‰. Maize cultivation is rare in the Burgundy region and might be responsible for these ^{13}C-enriched cropland soils. No other influence of C4 plants is probable, as the vegetation in the study area is exclusively composed of C3 plants.

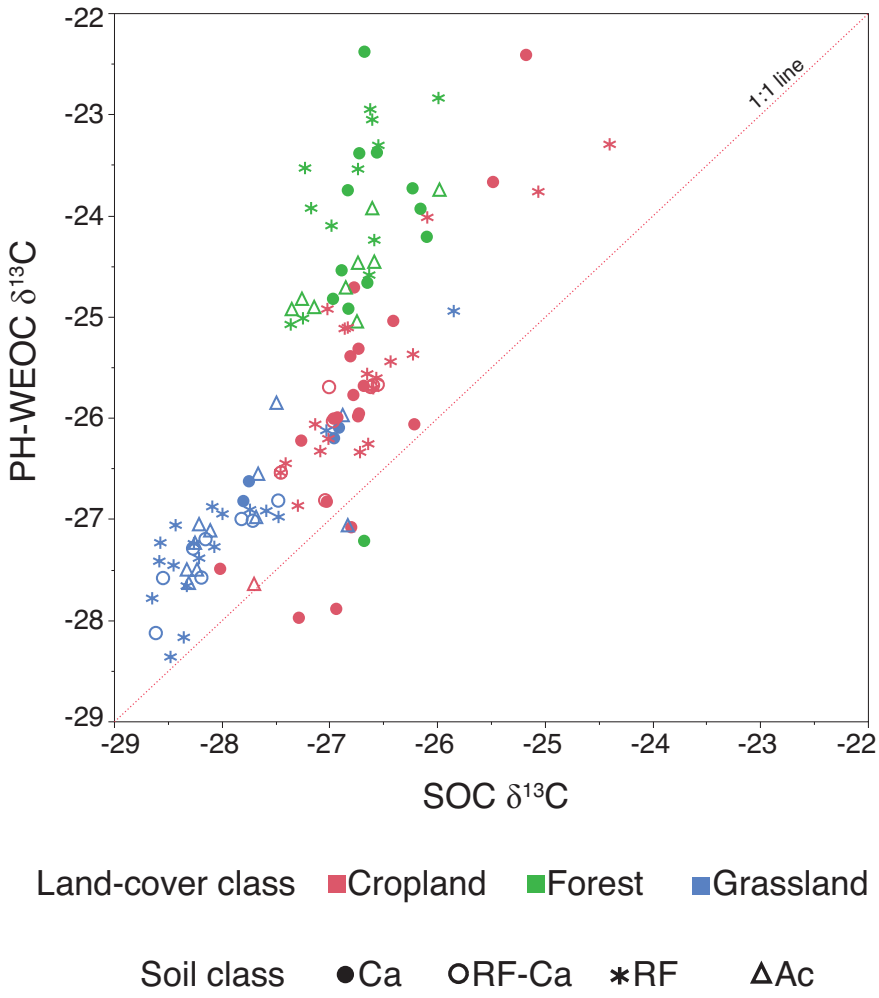

Figure 7 Biplot of the $\delta^{13}C$ signature in the SOC against the $\delta^{13}C$ signature in the PH-WEOC, with indications of land cover (colour of symbol) and soil classes (form of symbol).

To our knowledge there is no previous study reporting such a clear difference between land cover under C3 vegetation. Trends in C isotopic signatures have been detected in plants with changes in mean annual precipitations (MAP) (Diefendorf et al., 2010; Kohn, 2010) or with elevation (Sparks & Ehleringer, 1997), but these effects do not appear to have a significant influence for our study area, as the ranges in MAP and elevation are clearly smaller in our study. Our results suggest differences in composition of the bulk organic matter in relation to land cover, with a larger proportion of isotopically lighter compounds in grassland soils (Fig. 7).

The pattern of $\delta^{13}C$ signatures of soil organic matter may be influenced by differences in the proportions of the organic compounds entering the soils under contrasted vegetation. For example, lignin and lignin-derived compounds are known to be ^{13}C depleted compared to bulk SOC, while carbohydrates have been reported to have less negative $\delta^{13}C$ signatures (Benner et al., 1987). The fact that the rhizosphere is a major contributor to SOC in grassland soils is consistent with this explanation. Indeed, a greater proportion of lignin in root tissues (Fernandez et al., 2003) has been reported in previous studies. Furthermore, fungal communities are often considered to be the main drivers of lignin decomposition. In our study, we found the lowest density of fungi in grassland soils and the highest in forest soils, where it was between 5 and 10 times higher. This large difference suggests that lignin may be better preserved in grassland soils than in forest soils, supporting the pattern of $\delta^{13}C$ observed. However, we did not characterise the soil organic matter sufficiently precisely to confirm any differences in the molecular composition between the different land covers. Another explanation could be that grassland vegetation photosynthesised a depleted source of CO_2. As these soils are covered by short vegetation, and because high soil respiration rates have been reported for grassland ecosystems (Raich & Tufekcioglu, 2000; Sanderman & Amundson, 2008), we can hypothesise that a significant proportion of the CO_2 used for photosynthesis originates from soil respiration. Soil CO_2 is depleted in ^{13}C compared to atmospheric CO_2 (Lerch et al., 2010; De Troyer et al., 2011), and a greater contribution of soil CO_2 for the photosynthesis of short grassland vegetation may lead to a ^{13}C-depletion in grassland plants compared to trees, which photosynthesise CO_2 at greater heights, or to crops, where low SOC content may lead to lower soil respiration rates. This shift in ^{13}C abundance in plant tissues may thus result in the shift observed in the $\delta^{13}C$ of SOC in grassland ecosystems.

The $\delta^{13}C$ signatures of PH-WEOC show a different pattern, with differences between the three land-cover classes. We found lower values in grassland soils, intermediate in cropland soils, and higher in forest soils (Table 3). These results suggest that additional processes influence the $\delta^{13}C$ of PH-WEOC compared to SOC. We found significant differences between the $\delta^{13}C$ of PH-WEOC and of SOC, with less negative values in the PH-WEOC extracts (Fig. 7). These differences in $\delta^{13}C$ between the two pools reveal distinct molecular compositions, with a greater proportion of ^{13}C-enriched solubilised compounds, as reported by Werth & Kuzyakov (2010).

This ^{13}C enrichment of the PH-WEOC is consistent with a greater proportion of carbohydrates in the soluble pool compared to bulk SOC. The fact that carbohydrates are more hydrophilic than lipids or lignin-derived compounds supports the hypothesis for their preferential extraction. The soluble organic C in soil has been identified as the result of the microbial degradation of organic matter in soils (Fröberg et al., 2003; Hagedorn et al., 2004; Malik & Gleixner, 2013). During degradation, ^{12}C isotopes are preferentially mineralised by microorganisms, as this needs less energy than for the ^{13}C isotopes. This fractionation during SOC mineralisation thus leads to the ^{13}C-depletion of soil CO_2 and to the ^{13}C-enrichment in the degradation products released in the soluble pool, supporting the $\Delta^{13}C$ values found here. We also found greater $\Delta^{13}C$ for forest soils, with values of 2.55 ± 0.15 ‰ (Table 3). This could result from a more pronounced preferential extraction of carbohydrates in these soils. This hypothesis is coherent with the lower $SUVA_{254}$ values measured in the PH-WEOC of the forest soil (Table 2), as increases in carbohydrate proportions lead to decreasing aromaticity. Again, this increase in the proportion of non-aromatic molecules may be linked to the greater contribution of microbial metabolites and microbial decay products. We measured a greater density of fungi in the forest soils, supporting the ^{13}C-enrichment for these soils and for the PH-WEOC. As microorganisms preferentially release ^{12}C isotopes during the mineralisation of SOC, microbial tissues are enriched in ^{13}C. Regarding the involvement of fungal communities in the ^{13}C pattern observed in forest soils, we suspect that saprophytes have the greatest impact on ^{13}C fractionation because these fungi show significant ^{13}C-enrichment (Högberg et al., 1999), with $\delta^{13}C$ values ranging from -24.0 ‰ to -21.6 ‰ in their fruit bodies, while the fruit bodies of mycorrhizal fungi have $\delta^{13}C$ values varying between -29.2 ‰ and -24.3 ‰. Thus, a great abundance

of saprophyte fungi in forest soils is in line with the production of the ^{13}C-enriched organic compounds observed in the PH-WEOC.

4.4 Relationships between soil physico-chemistry and the genetic structure of bacterial communities

The relationships between soil physico-chemistry and the genetic structure of bacterial communities have been investigated in previous studies (Chemidlin Prévost-Bouré et al., 2011; Ranjard et al., 2013). In our study, the soil variable with the greatest influence on the genetic structure of bacterial communities is pH. This major influence of pH has been reported in many studies (e.g. Fierer & Jackson, 2006; Lauber et al., 2008, 2009) and is again strongly confirmed, due to the high pH range in our study. The influence of soil pH on bacterial community structures is visible with the PCA on B-ARISA profiles (Fig. 3). However, the PCA is not sufficient to discriminate all samples satisfactorily. The use of the co-inertia analysis, as a subsequent step, helped to investigate the relationships between soil parameters and bacterial community structure (Fig. 4). This analysis reveals that, in addition to pH, soil texture through clay and sand contents, also has a major influence on bacterial communities at the regional scale. Soil texture can be considered as an indicator of soil microhabitats and it is therefore coherent to observe its control on soil bacterial communities. This influence of texture has also been reported in other studies (Girvan et al., 2003; Johnson et al., 2003) and soil moisture dynamics, air and water diffusion due to pore connectivity and substrate accessibility are major soil physical processes controlled by texture that must impact bacterial community dynamics. The link between the extraction ratio (ER) and bacterial communities was more unexpected. This result is very interesting because no study had previously revealed this relationship, and the soluble organic matter pool has rarely been considered in studies of bacterial community structures. Previous research has demonstrated that soluble organic matter extracted from soils can easily be used as a source of energy by soil microorganisms (Kiikkilä et al., 2006; McDowell et al., 2006; Bowen et al., 2009). It is also known that degradation of soil organic matter by microorganisms produces soluble organic compounds (Mikutta et al., 2007; Kaiser & Kalbitz, 2012). Both of these processes confirm the close connection between the dynamics of soluble organic matter and microbial activity. Nevertheless, since the co-inertia analysis is a symmetrical approach and because soluble organic compounds

are either consumed or produced by soil microorganisms, we cannot determine whether it is the solubility of the SOC (ER) that controls the bacterial communities, or *vice-versa*, or even a combination of the two. The key variables detected here (pH, clay, sand and ER) and the discrimination of the samples in Figure 4 reveal the strong effect of soil classes on the bacterial community structure, while land cover does not appear to have a great effect, except for the forest soils of the Ac and Rf classes, which are separate from the cropland and grassland soils in the co-inertia space. For these samples, the effect of land cover on the bacterial community structure is related to the differences in SOC content and in the aromaticity of the PH-WEOC. However, this effect must be considered with caution, as it is visible along the second axis of the co-inertia space, which accounts for only a small part of the variance in the bacterial community structures.

Conclusion

This integrated study conducted at the scale of the Burgundy region reveals the effect of both land cover and soil class on soil biogeochemistry. While the soil parental material mainly controls soil pH and texture, land cover influences soil organic matter content and carbon isotope composition. The dynamics of soluble organic matter (PH-WEOC) is regulated by carbon and clay contents. The aromaticity of PH-WEOC and its $\delta^{13}C$ signature reflect differences in the decomposition pathways of soil organic matter and in the production of soluble organic compounds, in relation to land cover. Our study also demonstrates that the genetic structure of the bacterial community is related to soil physico-chemistry, revealing the major influences of soil texture and pH. The quality of soil organic matter is shown to play a major role in the structure of the bacterial community, especially its potential of solubility, and also the aromaticity of the organic compounds present in the solution. Further studies with molecular characterisation of PH-WEOC and determination of the bacterial communities at the taxonomic level are envisaged, in order to determine their close relationship, and to better constrain their role in the soil C cycle.

Acknowledgements

The RMQS soil-sampling and physico-chemical analyses were supported by a French Scientific Group of Interest on soils: the 'GIS Sol', involving the French Ministry for Ecology and Sustainable Development, the French Ministry of Agriculture, the French Agency for Energy and Environment (ADEME), the French Institute for Research and Development (IRD), the National Institute for Agronomic Research (INRA), and the National Institute of the Geographic and Forest Information (IGN). We thank all the soil surveyors and technical assistants involved in sampling the sites, and technical support from the French soil sample archive, which provided the collection of soils studied.

This work, through the involvement of technical facilities of the GenoSol platform of the ANAEE-Services infrastructure, received a grant from the French state through the National Agency for Research under the program ANR-11-INBS-0001 "Investments for the Future", as well as a grant from the Regional Council of Burgundy. We are also grateful to Yueming Lu, Ida-Fleure Ibinga and Marie-Jeanne Milloux for their assistance in the laboratory. Review comments and English editing of this paper by Carmela Chateau-Smith were also greatly appreciated.

Chapitre 5

Caractérisation moléculaire des matières organiques du sol extractibles à l'eau par spectrométrie de masse à ultrahaute résolution

Molecular characterisation of water-extractable organic matter in soils using ultrahigh-resolution mass spectrometry

J. Guigue[1], O. Mathieu[1], M. Harir[2], M. Lucio[2], D. Arrouays[3], C. Jolivet[3], J. Lévêque[1] and P. Schmitt-Kopplin[2,4]

[1] UMR 6282 Biogéosciences, Université de Bourgogne, Dijon, France.

[2] Helmholtz Zentrum München, German Research Center for Environmental Health, Analytical BioGeoChemistry, Neuherberg, Germany

[3] INRA, US 1106, INFOSOL, Orléans, France

[4] Chair of Analytical Food Chemistry, Technische Universität München, Freising-Weihenstephan, Germany.

Résumé

La matière organique dissoute (MOD) est un réservoir de carbone des sols hautement réactif, et est donc une composante essentielle du cycle global du carbone. Un grand défi pour une meilleure compréhension de la réactivité de la MOD, repose sur sa caractérisation au niveau moléculaire. La spectrométrie de masse par résonance cyclotronique ionique à transformée de Fourier (FTICR-MS) émerge depuis peu comme une méthode très puissante pour la caractérisation moléculaire des matières organiques naturelles provenant d'environnements variés, et apparaît donc comme une technique adéquate pour la caractérisation moléculaire de la MOD des sols.

Dans cette étude, nous avons analysé les matières organiques extraites extraite à 100° C et 10 MPa (PH-WEOM) de 120 sols prélevés en région Bourgogne. Le PH-WEOM représente la fraction la plus labile de la matière organique du sol et est étudié comme proxy de la MOD présente dans la solution du sol. La composition moléculaire du PH-WEOM a été déterminée par FTICR-MS et des analyses statistiques multivariées et sans *a priori* ont été utilisées pour tester si la résolution moléculaire ultrafine du WEOM révélait des groupes d'échantillons ayant une signature moléculaire commune.

Au total, 3629 formules moléculaires ubiquistes dans le PH-WEOM ont été identifiées. Leur représentation dans un diagramme de van Krevelen et des analyses « Kendrick mass » révèlent la grande hétérogénéité de cette mixture organique. Ces composés peuvent être attribués à de nombreuses classes, telles que les tannins, les lignines, les lipides ou les carbohydrates, par exemple. Ces composés sont organisés en séries d'homologues, signifiant que la complexité du WEOM résulte d'un continuum dans la décomposition des biomolécules d'origine, en suivant les voies de réactions chimiques variées.

L'investigation des données au moyen des analyses statistiques multivariées et sans *a priori* révèle que le PH-WEOM des sols de forêt a une composition moléculaire clairement distincte, avec une contribution majeure de composés du type des lignines et des tannins, et avec une aromaticité plus ou moins importante, en lien avec les caractéristiques du sol, en particulier le pH. Le PH-WEOM est plus similaire entre les sols de culture et de prairie. Le rôle du pH a également été identifié pour ces échantillons et correspond à des motifs moléculaires en lien avec l'activité microbienne, tels que la présence de composés avec des ratios H/C élevés pouvant être attribués à des lipides, des carbohydrates et des acides

nucléiques. Un groupe d'échantillons provenant de sols de culture, développés sur des formations résiduelles, est caractérisé par une composition moléculaire très spécifique, riche en composés aliphatiques contenant du souffre, et met en évidence l'influence de processus spécifiques dans les sols sur la composition moléculaire du PH-WEOM. Cette étude confirme le grand potentiel de la FTICR-MS pour résoudre l'extrême complexité du PH-WEOM des sols.

Abstract

Dissolved organic matter (DOM) is a highly sensitive and reactive reservoir of carbon (C) in soils, and is therefore a crucial component of the global C cycle. A great challenge to better understand its reactivity, and to detect the effects of the factors controlling DOM, relies on its characterisation at the molecular level. Fourier transform ion cyclotron resonance-mass spectrometry (FTICR-MS) has recently emerged as a highly powerful method for molecular characterisation of natural organic matter from various environments and thus appeared as an adequate technique for the characterisation of soil DOM at the molecular level.

In this study, we analysed water-extracted organic matter at elevated pressure and temperature (PH-WEOM) obtained from 120 Burgundy soils. The PH-WEOM represents the most labile fraction of soil organic matter and is studied to approximate the DOM found in the soil solution. We used FTICR-MS to determine PH-WEOM molecular composition, and unsupervised multivariate statistical analyses to test if the ultrafine molecular resolution of PH-WEOM reveals groups of samples with a common molecular fingerprint.

A total of 3,629 molecular formulas ubiquitous in the PH-WEOM were identified. Their representation in a van Krevelen diagram and Kendrick mass analyses reveal the great heterogeneity of this organic mixture. Compounds can be assigned to many different chemical classes, such as tannins, lignins, lipids or carbohydrates, for example. These compounds are arranged in homologous series, meaning that the complexity of the PH-WEOM results from a continuum in the decomposition of original biomolecules, following various paths of chemical reaction.

The data investigation using unsupervised multivariate statistics reveal that PH-WEOM from forest soils has a clearly distinct molecular composition, with major contributions from lignin- and tannin-like compounds, and with a more or less pronounced aromaticity related to soil characteristics, especially the soil pH. The PH-WEOM is more similar for cropland and grassland soils. The role of pH was also identified in the PH-WEOM samples from cropland and grassland soils and corresponds to molecular patterns related to microbial activity, with the presence of compounds with high H/C, presumably corresponding to lipids, carbohydrates and nucleic acids. A group of samples from cropland soils developed on residual formations is characterised by a very specific molecular composition, rich in S-containing aliphatic compounds, highlighting the importance of specific soil processes in the molecular

composition of PH-WEOM. This study confirms the great potential of FTICR-MS to resolve the high complexity of PH-WEOM in soils.

1 Introduction

Soils are the greatest reservoir of organic matter in terrestrial ecosystems. Dissolved organic matter (DOM) is a highly sensitive and reactive reservoir of carbon (C) in soils (Marschner & Kalbitz, 2003; Kaiser & Kalbitz, 2012), and is therefore a crucial component of the global C cycle. The chemical properties of DOM are related to important soil processes, such as the speciation and transport of plant nutrients and metals, and the transfer of organic matter to deeper horizons or to water systems.

Many factors controlling DOM chemical properties have been reported. Vegetation type (i.e. forest, grassland or agricultural fields) was presented as the most dominant factor for DOM fluxes and composition, while climate and soil texture are considered to have less impact (Chantigny, 2003). Many studies also demonstrate the significant effect of vegetation change on DOM, with general increases in DOM fluxes and aromaticity as responses to environmental perturbations (Kalbitz et al., 2000a; Li et al., 2014). The solubility of soil organic matter (SOM) is known to be controlled by ionic strength and pH (Kalbitz et al., 2000b). The (de)sorption processes, via interaction with the soil mineral phase, especially with clay and Fe- and Al-oxides, control DOM composition, due to the specific affinities of different organic compounds with these minerals (Kaiser et al., 2001). Both the quantity and the composition of DOM in soil are controlled by a combination of these factors, and DOM production results from biotic and abiotic mechanisms, including the microbial processing of SOM and variations in temperature and moisture.

The effects of all these factors are variable in space and time, and the great diversity of soils often makes general statements appear unreasonable (Chantigny, 2003). Soil-monitoring networks provide a great opportunity to detect general trends between soil characteristics and environment. These programs allow the analysis of very large datasets, integrating soil diversity and the influence of environmental factors (van Wesemael et al., 2011; Ranjard et al., 2013).

A great challenge to better understand DOM reactivity, and to detect the effects of these controlling factors, relies on the characterisation of DOM at the molecular level (Kaiser & Kalbitz, 2012). However, due to the complexity of this mixture of organic molecules, most of the analytical procedures employed to describe soil DOM only partially succeed in resolving such high diversity.

Fourier transform ion cyclotron resonance-mass spectrometry (FTICR-MS) has recently emerged as a highly powerful method for molecular characterisation of natural organic matter from various environments (Schmitt-Kopplin et al., 2010a; b; Mosher et al., 2010; Ohno et al., 2010). The ultrahigh resolution of FTICR-MS makes molecular identification possible, and is ideal for the desired molecular-level characterisation of soil DOM. Structural interpretation of FTICR-MS data is possible with the use of graphical analysis (van Krevelen, 1950; Kendrick, 1963; Kim et al., 2003a), and the calculation of specific indexes, such as the aromaticity index (Koch & Dittmar, 2006) and the double bond index (Yassine et al., 2014).

In this study, we analysed water-extracted organic matter (WEOM) obtained from 120 Burgundy soils. The WEOM represents the most labile fraction of SOM and is studied to approximate the DOM found in the soil solution. The Burgundy region presents an interesting diversity in land-cover and soil parent material, which is reflected in our sample set, thus providing the opportunity to investigate the relationships between soil properties and WEOM molecular composition. We used FTICR-MS to determine WEOM molecular composition, and unsupervised multivariate statistical analyses to test if the ultrafine molecular resolution of WEOM reveals groups of samples with a common molecular fingerprint.

2 Materials and methods

2.1 Soil samples

All soil samples were collected in the Burgundy region for the RMQS project, the French soil quality-monitoring network. Based on a systematic sampling of soils on a 16 km regular grid, the topsoil (0-30 cm or less for thinner soils) was sampled at the centre of each 16 x 16 km cell. The final sample is a composite of 25 core samples from a 20 m x 20 m area. Soil samples were air-dried and sieved to 2 mm. More details on the sampling protocol are available in Jolivet et al. (2006).

This study was conducted on the 120 topsoil samples from the Burgundy region, in the east of France, which is characterised by an interesting environmental heterogeneity. The land cover is a mosaic of forest (9,950 km^2) with both deciduous trees and conifers, permanent grassland (8,000 km^2) and cropland (10,580 km^2), which are mainly areas of intensive agriculture. Three major geological ensembles composed the region (see Figure 1 in Chapter 4).

The Massif du Morvan, in the centre, composed of Hercynian granite, Palaeozoic volcanic rocks and metamorphic rocks, is bordered by continental sediments (sandstones and marls). In the northern part of the region, are found marls and calcareous sedimentary rocks dating from Trias and Jurassic and younger marine sediments (clay and chalk) dating from Cretaceous. In the Bressan graben floodplains, to the south-east, and the Loire and Yonne river valleys, in the south-west and the north-west of the region, Cenozoic alluvial sediments form the bedrock.

The Oceanic climate, from the west, is dominant. The eastern part of the region is subjected to a Continental influence from the east and north-east, while Mediterranean influence from the south results in warmer temperatures along the Bressan graben floodplains during summer.

We considered two categorical variables that are supposed to control the biogeochemistry of soil. The first categorical variable is land cover, grouped into three classes: cropland (n=46), forest (n=33), and grassland (n=41). The second categorical variable is based on soil geochemistry and is composed of four classes, determined with respect to bedrock type, as well as geomorphological condition, carbonate and exchangeable calcium content.

The class Ca (n=35) comprised soils developed on calcareous rock and containing more than 2% of $CaCO_3$. The soil types are Cambisols (Calcaric) and Rendzic Leptosols (IUSS Working Group WRB, 2006).

The class Ac (n=21) includes acidic soils developed on magmatic, metamorphic rocks and acidic sandstones, corresponding to Cambisols (Dystric, Eutric or Hypereutric), Cambic Umbrisols and Umbric Leptosols (IUSS Working Group WRB, 2006).

The remaining soil developed on residual formations, such as alluvial and colluvial deposits, eolian loamy deposits or are weathered soils on carbonate rocks.

The class Rf-Ca (n=15) comprised the soils developed on residual formations with a high content of exchangeable calcium (arbitrary minimum threshold fixed at 150 µmol g^{-1}), corresponding to Cambisols (Hypereutric), Luvic Cambisols, Haplic Luvisols, Haplic Albeluvisols, Fluvisols, Planosols and Gleysols (IUSS Working Group WRB, 2006).

The class Rf (n=49) is composed of the soil samples developed on residual formations with a low content of exchangeable Ca (less than 150 µmol g^{-1}) and are Cambisols (Eutric) and Fluvisols (Eutric) (IUSS Working Group WRB, 2006).

The Soil Analyses Laboratory of INRA (Arras, France, http://www6.lille.inra.fr/las) and the GISMO analytical platform (Dijon, France) performed analyses of soils.

2.2 Extraction of Pressurised Hot-Water-Extractable Organic Matter

Pressurised hot-water-extractable organic matter (PH-WEOM) was extracted using a solvent extractor (ASE200, Dionex Corporation, Sunnyvale, USA). The extraction consisted of the equilibration and leaching of 10-g soil samples with ultrapure water at 100° C and 10 MPa. All conditions were the same as in the study of Guigue et al. (2014). All samples were extracted at least in duplicate, and additional extractions were performed when the relative variability exceeded 10 % for the extraction parameters (volume, $SUVA_{254}$ and extraction ratio; see Materials and methods in Chapter 4), to ensure that we obtain a good representativeness for each sample.

2.3 Electrospray ionisation - Fourier transform ion cyclotron resonance - mass spectrometry (ESI–FTICR–MS)

FTICR–MS principle

The principle of FTICR–MS is based on ion cyclotron resonance and is described in detail in Amster (1996) and Marshall et al. (1998), for example.

In this study, the first step corresponds to the electrospray ionisation of the molecules (Cole, 2000). This technique is often retained for ionisation of NOM samples, as it is a soft ionisation method, which is efficient for the ionisation of the various classes of chemical compounds. Briefly, the sample is pumped through a metal capillary, to which a high potential relative to a counter electrode is applied (The potential depends on the distance between the capillary and the electrode, usually an electric field of 1 kV cm^{-1} is applied). It produces a charged solution, which is then dispersed into a mist of very fine droplets when it exists the capillary. Heating and collisions with an inert gas (e.g. N_2), between the capillary and the counter electrode, lead to the desolvation of the charged droplets. Charged ions are formed by Coulombic explosions (Cole, 2000; Tremblay, 2006) and enter the mass analyser through an orifice in the counter electrode.

Ions are then guided through two ion funnels and transferred through two quadrupoles. The first quadrupole acts as an ion buncher, while the second can be seen as a mass filter prior to linear ion acceleration and collision with a target gas inside the hexapole, before their entrance into the ICR cell under high vacuum (10^{-9} – 10^{-10} mbar) for high-resolution detection (Kanawati et al., 2012).

The ions are trapped in the ICR cell under the combined influence of an electric field and a strong homogeneous magnetic field. Ions orbit with motion perpendicular to the magnetic field, at a frequency determined by their mass to charge ratio (m/z). The cyclotron frequency of ions is inversely related to their m/z (Equation 1). The orbital radius of the ions is increased with radiofrequency excitation pulses, without modification of their frequency, in order to enhance their detection precision.

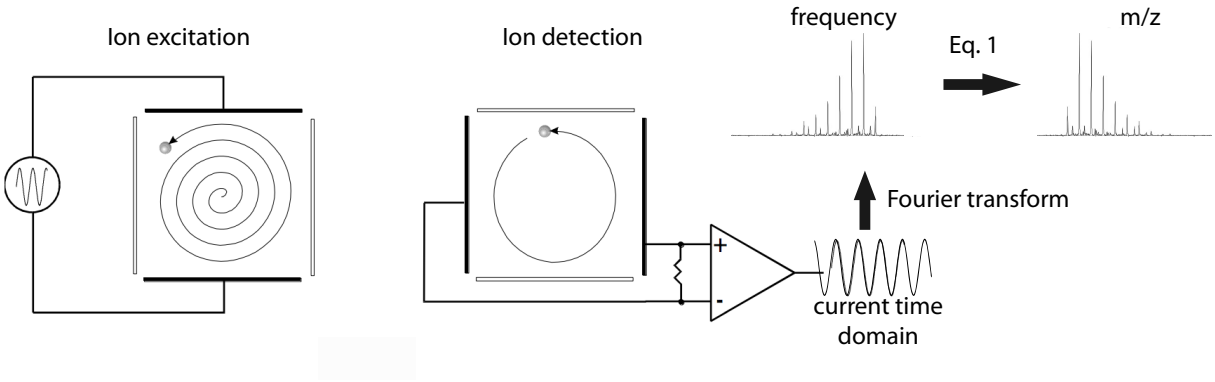

Figure 1 A simplified view of the successive steps involved in FTICR-MS measurements. The magnetic field is perpendicular to the plan of the figure. On the left side, the scheme shows an ion orbiting in the ICR cell, submitted to an excitation by radiofrequency pulses resulting in the increase of its orbital radius. The cyclotron frequency, inversely proportional to the m/z of the ion, is then captured by the detector plates, which record a current time domain signal. This time-domain signal is Fourier-transformed and a frequency spectrum is obtained. The frequency spectrum is finally converted on a mass spectrum by the mean of the Eq. 1 (see text).

The motion of ions produces a time-dependent signal, recorded with the detection plates as an oscillating electric voltage over time, corresponding to the time-domain spectrum of all detected ions. This spectrum is deconvoluted into a frequency spectrum using Fourier transformation. The ultrahigh-resolution mass spectrum is obtained using Equation 1 for the conversion of the frequency spectrum. Figure 1 illustrates the sequential steps from ion excitation in the ICR cell to the acquisition of the mass spectrum.

(Eq. 1) $f_c = B(z/m)$

where fc is the cyclotron frequency, B is the magnetic field strength, z is the charge of the ion, and m is the mass of the ion.

Because of the ultrahigh mass accuracy and resolution of this technique, FTICR mass spectra allow the identification of thousands of peaks, for which unique molecular formula can be unambiguously assigned. The FTICR-MS has proven its potential for investigating the great complexity of natural organic matter (NOM) in various environments, from freshwater to deep-sea (Mosher et al., 2010; Lechtenfeld et al., 2014), in soils and sediment (Wu et al., 2004; Ohno et al., 2010), and also in aerosols or extra-terrestrial material (Schmitt-Kopplin et al., 2010a; 2010b), for example. This technique can be used to determine the composition of organic mixtures, and to elucidate chemical and biological transformations, at the molecular level and with an extremely high resolution.

However, FTICR-MS also presents some limitations. Molecule selectivity during sample preparation, such as the desalting step with C_{18} columns, for example, leads to the loss of the non-polar molecules that could represent up to 40% of the mixture (Kim et al., 2003b; Perminova et al., 2014). The different ionisation processes, due to variable ionisation efficiencies of individual compounds, also lead to a loss of information, making rigorous quantification impossible (Hertkorn et al., 2007; Nebbioso et al., 2010). Moreover, isomer differentiation is difficult when not combined with techniques providing structural information, such as NMR and infrared spectroscopy, or with fractionation techniques before the FTICR-MS measurements (Hertkorn et al., 2007; Yassine et al., 2014). Accordingly, the mass peak intensities integrate all isomers with the same m/z value.

FTICR–MS measurements

The PH-WEOM samples were desalted on solid phase extraction (SPE) columns before Fourier transform ion cyclotron resonance mass spectrometry measurements. Filtered WEOM samples were acidified to pH 2 with CH_2O_2 (formic acid, p.a. grade, Merck) and the DOM was extracted using SPE cartridges (Bakerbond C_{18}, 100 mg / 1 g, J.T.Baker). The cartridges were rinsed with 1 ml of methanol (Hypersolv, Prolabo), followed by 1 ml of acidified MilliQ water (1% CH_2O_2). Then 1 ml of acidified PH-WEOC extracts (pH 2) was gravity passed through the cartridge. Subsequently, remaining salts were removed with 1 ml of acidified MilliQ water (1% CH_2O_2) and DOM was eluted with 1 ml methanol and stored at 4° C.

FTICR mass spectra were acquired in negative ion mode on a Bruker Solarix 12 Qe FTICR mass spectrometer, equipped with a 12 T superconducting magnet and a APOLLO II electrospray source (Agilent sprayer), at a flow rate of 120 µL h^{-1} with a nebulizer gas pressure of 20 psi and a drying gas pressure of 15 psi. A total of 500 scans were added for each mass spectrum. The spectra were acquired with a time domain of 4 megawords over a mass range of m/z 147–1000 and were externally calibrated based on arginine clusters (5.10^{-5} M). Internal calibration was performed to achieve an error <0.2 ppm, using known exact mass peaks between 200 and 950 Da that are ubiquitous in NOM samples.

For each peak with a signal to noise ratio superior to 3, the plausible elemental formulas were calculated in batch mode using FormCalc, homemade software. Formulas were assigned from the m/z peaks based on $C_{0\text{-}100}$, $H_{0\text{-}\infty}$, $O_{0\text{-}80}$, $N_{0\text{-}2}$ and $S_{0\text{-}1}$, with a tolerance <0.5 ppm between experimental and theoretical masses. The generated formulas were validated by setting sensible chemical constraints (nitrogen rule, positive double bond equivalent, O/C ratio ≤ 1, H/C ratio ≤ 2.5).

2.4 Data treatments and statistics

Only the assigned molecular formulas with m/z from 147 to 800 were considered for the data analysis. We did not take into account the peaks with m/z higher than 800, as the resolving power of the technique is known to decrease with increasing m/z, and formula assignment becomes no longer unique within experimental mass measurement error (Kunenkov et al., 2009a). A matrix with samples in columns, m/z in rows, and peak intensity

in each cell was computed. All m/z that were present in less than 5 of the 120 samples were removed, and peak magnitude was transformed into relative magnitude for each sample. This matrix revealed that, considering the 120 samples, a total of 15,751 different m/z with assigned molecular formulas was found. For each sample, an average of about 8,200 m/z was detected. To explore this large dataset, we applied unsupervised multivariate approaches, using principal component analysis (PCA) and hierarchical cluster analysis (HCA) (Sleighter et al., 2010).

Using PCA allows the visualisation of multivariate dataset variance, by reducing it to fewer dimensions, with principal components (PCs) as the new variables (Hotelling, 1933). It makes the most informative viewpoint visible by using only the first few PCs, so that the dimensionality of the transformed data is reduced. The first PC is the linear combination of the standardised original variables that has the greatest possible variance. Each subsequent PC is the linear combination of the variables explaining the greatest possible proportion of the residual variance and is orthogonal to all previously defined components. To examine how the molecular composition of our samples differs, a PCA was computed using raw peak intensities, with SIMCA 11 software.

As a second step, HCA was used to identify natural groups of samples, based on their molecular signature, out of the heterogeneous sample set. These groups, or clusters, should be as homogeneous as possible and the differences among the clusters as large as possible. Here, HCA was performed with normalised m/z intensities (centred and reduced by row). A similarity matrix built on Pearson's correlation coefficients was computed, and the average linkage method was chosen to build the head map, using Hierarchical Cluster Explorer 3.5 software.

2.5 Data visualisation

The ESI–FTICR mass analyses of PH-WEOM, and more generally of NOM, produce extremely complex spectra, with several thousands of peaks and dozens of molecules detected at the same nominal mass. Their graphical presentation and structural interpretation are therefore very complicated. In this study, the tools used to present our data and to obtain structural information are van Krevelen diagrams, Kendrick mass-defect analyses, together with the calculation of double bond equivalence, aromaticity index and double bond index.

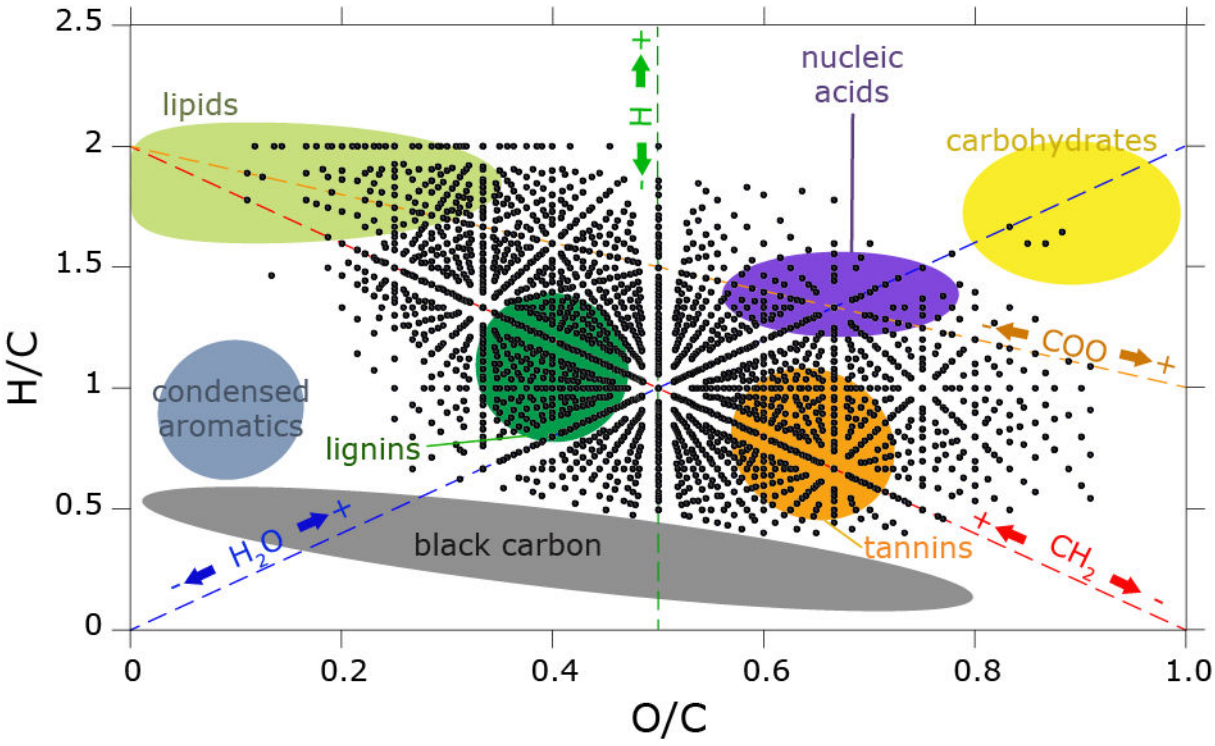

Figure 2 The van Krevelen diagram with the molecular formulas ubiquitous in the PH-WEOM of the 120 soils of the Burgundy region. The coloured domains indicate the regions characteristics for the main compound classes. It must be noted that the precise region for these classes varies in the literature. The four coloured dotted lines connect molecular species that differ by a specific molecular group. At a unique position in the van Krevelen diagram, compounds with different molecular formulas can be found (e.g. $C_{10}H_{11}O_6$ with m/z = 227.05573 and $C_{30}H_{33}O_{18}$ with m/z = 681.16720 fall exactly in the same position). Isomers are also projected in the same coordinates in this plot, and Hertkorn et al. (2007) announce up to 10^8 possible isomers for a single molecular formula. Some extensions of this diagram can be used for a visual evaluation of the molecular composition, such as projection showing the H/C values as a function of m/z.

van Krevelen diagrams

The van Krevelen diagram was developed by Dirk Willem van Krevelen, in order to assess the origin and maturity of kerogen and petroleum (van Krevelen, 1950). This diagram consists of a biplot of the hydrogen-to-carbon atomic ratio (H/C) as a function of the oxygen-to-carbon atomic ratio (O/C) of organic compounds, thus facilitating the retrieval of information from the assigned formulas.

Since classes of compounds present in natural organic matter (NOM) are found in characteristic regions of the van Krevelen diagram, this diagram is adequate as a first step for data interpretation. Indeed, the projection onto this diagram of formulas corresponding to lignin, condensed hydrocarbons, tannins or polysaccharides fell into distinct regions (Kim et al., 2003a; Wu et al., 2004). Thus, the patterns observed for NOM can be linked to the source material, but also to trends linked to the degradation and reactivity of NOM compounds. To illustrate this graphical tool, Figure 2 presents a van Krevelen diagram with the regions characteristic of various compound classes, and clearly distinct lines corresponding to chemical reactions.

Kendrick mass defect (KMD)

The KMD analysis provides a closer examination of the molecular formulas and their relationships. As highlighted in Figure 2, series of molecular formulas are aligned along straight lines in the van Krevelen diagram, and these lines correspond to differences in the number of C, H and O atoms. Such differences can be related to (de)methylation (CH_3 against H), or (de)carboxylation (O=C–OH against H), for example.

The KMD analysis can sort series of compounds with formulas that differ by a chosen functional group or molecule, thus helping the identification of series of homologous compounds (Kendrick, 1963). In our study, we conducted a CH_2-based KMD analysis (Eq. 2 and 3), which is the most frequently used, and seems relevant in our situation, as the methyl groups are consumed during the biodegradation of NOM by soil microorganisms. We also explored COO-based KMD plots (Eq. 4 and 5), as (de)carboxylation is also a major process in organic matter decomposition (Grinhut et al., 2011).

The following equations (Eq. 2–5) are used to calculate the Kendrick mass defect for CH_2– and COO–homologous compounds:

(Eq. 2) Kendrick mass (CH_2) = IUPAC mass × (14 / 14.01565)

(Eq. 3) KMD (CH_2) = nominal mass – Kendrick mass (CH_2)

(Eq. 4) Kendrick mass (COO) = IUPAC mass × (44 / 43.989829)

(Eq. 5) KMD (COO) = nominal mass – Kendrick mass (COO)

The KMD values are then plotted as a function of the nominal Kendrick mass. In the resulting KMD plot, series of homologous compounds are projected onto the same horizontal lines and differ on the x-axis by the nominal mass of the chosen functional group (e.g. a difference of 14 Da for one CH_2 group, or 44 Da for one COO group).

Double bond equivalence (DBE) and Aromaticity index (AI)

Another way to sort the identified compounds for interpretation is the calculation of DBE. The DBE indicates the sum of rings and double bonds present in a single molecule and is calculated from the molecular formula, according to Equation 6.

(Eq. 6) $DBE = 1 + 0.5 \times (2C - H + N)$

As a result, higher DBE values are found for less saturated molecules (decrease in H content). A means to estimate the degree of unsaturation is the determination of double-bond density, by normalising the DBE to the total number of C (DBE/C). The DBE is perfectly appropriate to measure the number of C=C and rings in pure hydrocarbons (Koch & Dittmar, 2006).

This index is independent of the number of O and S in a molecule. However, the O atoms present in carbonyl groups, but also the N–C π-bonds or C=S structures, reduce the potential number of C=C. For this reason, Koch & Dittmar (2006) developed the aromaticity index (AI), considering the possibility that heteroatoms (in particular O) can form double bonds not contributing to aromaticity. For the calculation of AI, considering Equation 6, the total number of heteroatoms is subtracted from C, and the number of N atoms is subtracted from H, because the addition of one N atom requires the addition of one H atom (Eq. 7).

(Eq. 7) $$AI = DBE_{AI} / C_{AI} = (1 + C - O - S - 0.5H) / (C - O - S - N)$$

If $DBE_{AI} \leq 0$ or $C_{AI} \leq 0$, then AI = 0

The AI therefore provides a measure of C=C double bond density in a molecule after removing the π-bond contribution from O, N and S atoms. For this reason, we use the AI for the evaluation of our results, as it provides more reliable information than DBE. A threshold value of AI ≥ 0.5 indicates the presence of aromatic structures. A second threshold of AI ≥ 0.67 unambiguously provides a minimum criterion for the presence of condensed aromatic structures in a molecule.

Double bond index (Xc)

The determination of AI for molecules with aromatic cores but only a short alkyl chain is greatly informative. However, aromatics with long alkyl chains will not be identified as aromatic structures and the proportion of aromatic compounds in a mixture will be underestimated. To overcome this limitation, Yassine et al. (2014) recently developed the double bond index (*Xc*) and proposed a general equation for its calculation (Equation 8). This index considers the fraction of O and S involved in π-bonds structures, so that the *Xc* value is not affected by the length of the alkyl chain.

(Eq. 8) $$Xc = 3 \times \{[DBE - (mO + nS) - 2\} / [DBE - (mO + nS)]$$

where m and n are the respective fractions of O and S involved in π-bond structures

If $DBE \leq mO + nS$, then $Xc = 0$

It must be specified, nevertheless, that the fraction of O and S involved in π-bond structures can be estimated only if the functional groups present in the molecule and their ratios are determined, mainly using NMR or infrared spectroscopy. This information would allow a more precise estimation of the aromatic structures in the molecules. In the absence of this information, we chose the values of m = 1 and n = 1. With this hypothesis, we assumed that all O and S atoms are involved in π-bond structures. Therefore the content of aromatic and condensed aromatic structures is greatly underestimated, but allows the determination of the lowest possible fraction of the aromatic and condensed aromatic structures of a molecule. Yassine et al. (2014) proposed a threshold value of Xc ≥ 2.5000 as the minimum criterion for the presence of aromatic structures in a molecule and a second threshold value of Xc ≥ 2.7143 for the presence of condensed aromatic structures.

Lastly, the AI and Xc values are complementary, as their comparison gives an estimation of the aromatic (AROM) and condensed aromatic structures (CARS) with long or short alkyl chains. In this study, the different fractions are estimated as follows:

$CARS_{short}$ = AI ≥ 0.67

$CARS_{long}$ = Xc ≥ 2.7143 and AI < 0.67

$AROM_{short}$ =0.5 ≤ AI < 0.67

$AROM_{long}$ = Xc ≥ 2.5000 and AI < 0.50

3 Results and Discussion

3.1 FTICR mass spectrum

All of the PH-WEOM samples produced highly complex FTICR mass spectra. As a representative example, the mass spectrum of the PH-WEOM obtained from a forest soil developed on a calcareous parent material is shown in Figure 3A, with subsequent expansions of the m/z axis in the mass window m/z = 357–386 (Fig. 3B), m/z = 369.9–370.4 (Fig. 3C) and 368.9–369.3 (Fig. 3D). More than 22,000 peaks with a signal to noise ratio > 3 were detected in the mass range from 147 to 800 m/z. The peak resolving power (m / δm at 50% peak height) is calculated to be over 400,000 at m/z = 400. A total of 14,630 unique molecular formulas was found, corresponding to a formula assignment for about 2/3 of the peaks. Data filtration, using the chemical constraints described in the Materials and methods section, results in the reduction to 8,342 unique molecular formulas. The shape of the complete mass spectrum (Fig. 3A) is in line with the NOM spectra reported in previous studies (Kujawinski et al., 2009; Schmitt-Kopplin et al., 2010b), showing that peaks were continuously detected along the whole range of m/z, with higher peak intensities around 300–350 m/z. Such mass distribution was described as being probably governed by two opposite chemically imposed trends (Schmitt-Kopplin et al., 2012). Firstly, the probability for the building of isomeric structures with identical compositions increases for higher masses, explaining the rise in relative intensity observed from 154 m/z to 350 m/z. In contrast, molecules with higher mass are less volatile and are thus less easily ionised, resulting in the decrease in intensity at higher m/z, from 350 m/z to 800 m/z. The largest molecular weights detected using FTICR-MS are below those measured using size exclusion chromatography (SEC) (e.g. Reemtsma & These, 2003) for humic and fulvic acids. Kujawinski et al. (2002) proposed that non-covalently bonded complexes, which would remain intact during SEC analysis, might be disaggregated during electrospray ionisation.

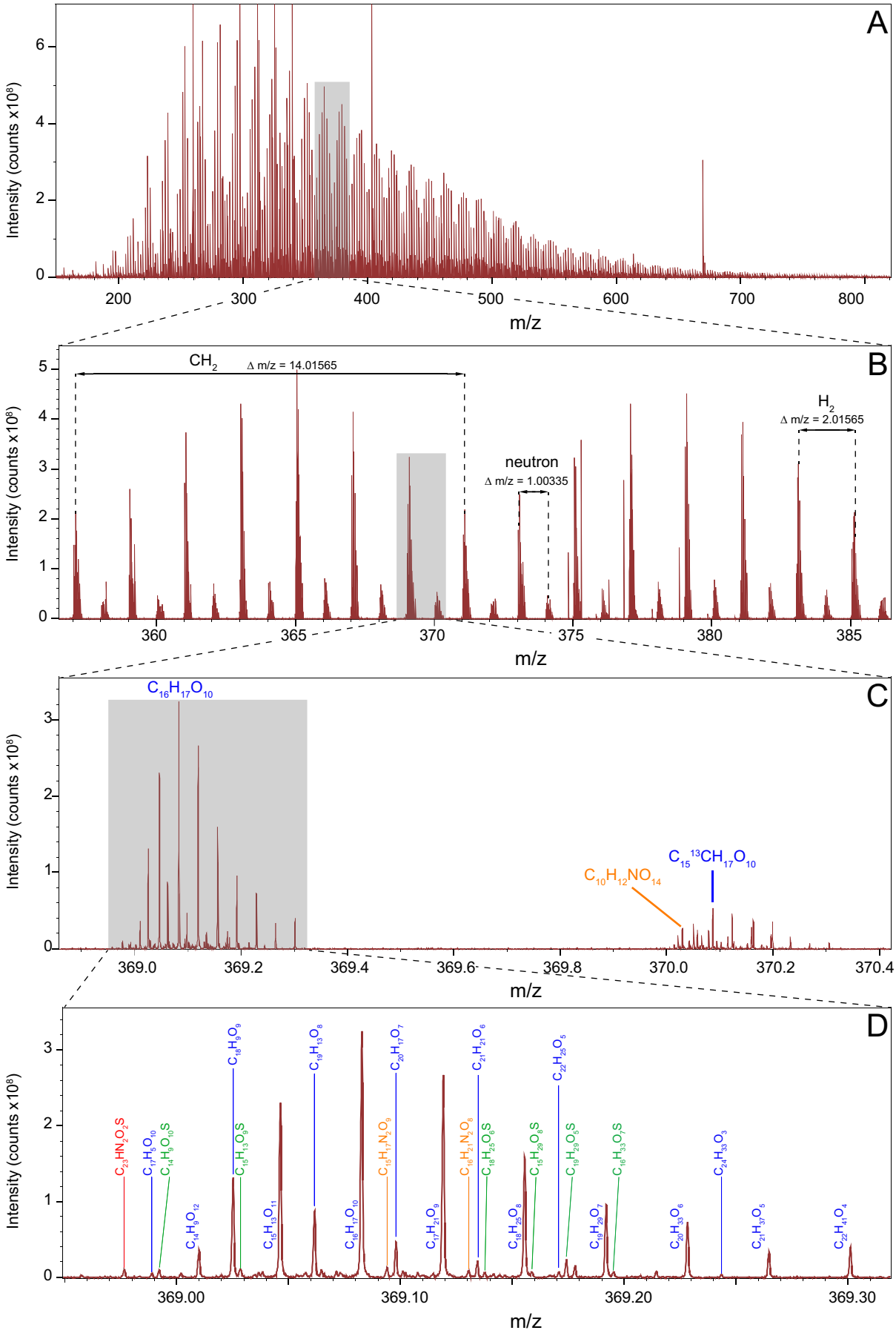
A
Intensity (counts x10⁸)
m/z
B
CH2 Δ m/z = 14.01565
neutron
Δ m/z = 1.00335
H2
Δ m/z = 2.01565
C
C16H17O10
C10H12NO14
C15 13CH17O10
D
C23HN2O2S
C17H5O10
C14H9O10S
C14H9O12
C18H9O9
C15H13O9S
C15H13O11
C19H13O8
C16H17O10
C15H17N2O9
C20H17O7
C17H21O9
C21H21O6
C16H21N2O8
C18H25O8S
C18H25O8
C15H29O8S
C22H25O6
C19H29O5S
C19H29O7
C16H33O7S
C20H33O6
C24H33O3
C21H37O5
C22H41O4

Figure 3 Negative electrospray 12 T FTICR mass spectrum of a forest soil from the Ca class, shown as example, with m/z 160−825 Da. (B) Enlargement of the mass range m/z 357−386 Da (Δm = 29 Da) with groups of peaks detected at each nominal mass showing that only singly charged peaks were detected. (C) Enlargement of the mass range 369.9−370.4 Da (Δm = 10.5 Da) to highlight the presence of isotopologues and compounds with an odd number of N atoms at even m/z. (D) Enlargement of the mass range 368.9–369.3 (Δm = 0.4 Da) with annotation of the assigned molecular formulas. The resolving power is about 350,000 in this mass range. A regular spacing of 0.03639 Da matching with the exchange of CH_4 against oxygen is observed between peaks. Molecular formulas containing S atoms or an even number of N atoms are also found at this odd nominal mass.

On enlarging the mass spectra presented in Figure 3B, we clearly observed the dominance in intensity of the peaks in the vicinity of odd nominal m/z. The molecules found at odd nominal masses contain C, O and an odd number of H atoms. The S-containing molecules are also found at odd nominal masses, while molecules containing one N atom are found at even masses, due to the fact that incorporation in a molecule of one N atom (valence = 3) requires the removal of one H atom.

The low intensities measured at even nominal masses thus indicate the presence of molecules containing one N atom but also molecules containing one ^{13}C isotope (Fig. 3C) with a Δm of exactly 1.00335 Da, corresponding to the mass of one neutron. Most of the peaks at even m/z can be assigned to the ^{13}C isotope of peaks at odd m/z. The absence of peak clusters between odd and even masses indicates that the ions are singly charged.

The enlargement of the nominal mass 369 shows two series of CHO molecular formulas, with a regular spacing of 0.00364 m/z, corresponding to the exchange of CH_4 against oxygen. The peak distribution at the nominal mass 369 shows a Gaussian distribution. The peak intensities here should be regarded as resulting from the integration of all isomers for a unique molecular formula. The peaks with the highest intensities correspond to molecular formulas that exhibit average H/C and O/C elemental ratios, for which a greater number of possible isomers can be found (Hertkorn et al., 2007).

In the following sections, we will present the ubiquitous molecular fingerprint detected in at least 95% of the 120 PH-WEOM samples obtained from the soils of the Burgundy region. A total of 3,629 different molecular formulas were detected in at least 114 PH-WEOM samples. These molecules are composed of CHO (64.9%), CHON (31.9%) and CHOS (3.2%). Such omnipresence of specific organic compounds was also observed in 60 samples of marine DOM (Lechtenfeld et al., 2014). Our sample set being likewise very large, the significance of these ubiquitous molecules in PH-WEOM is therefore greatly strengthened.

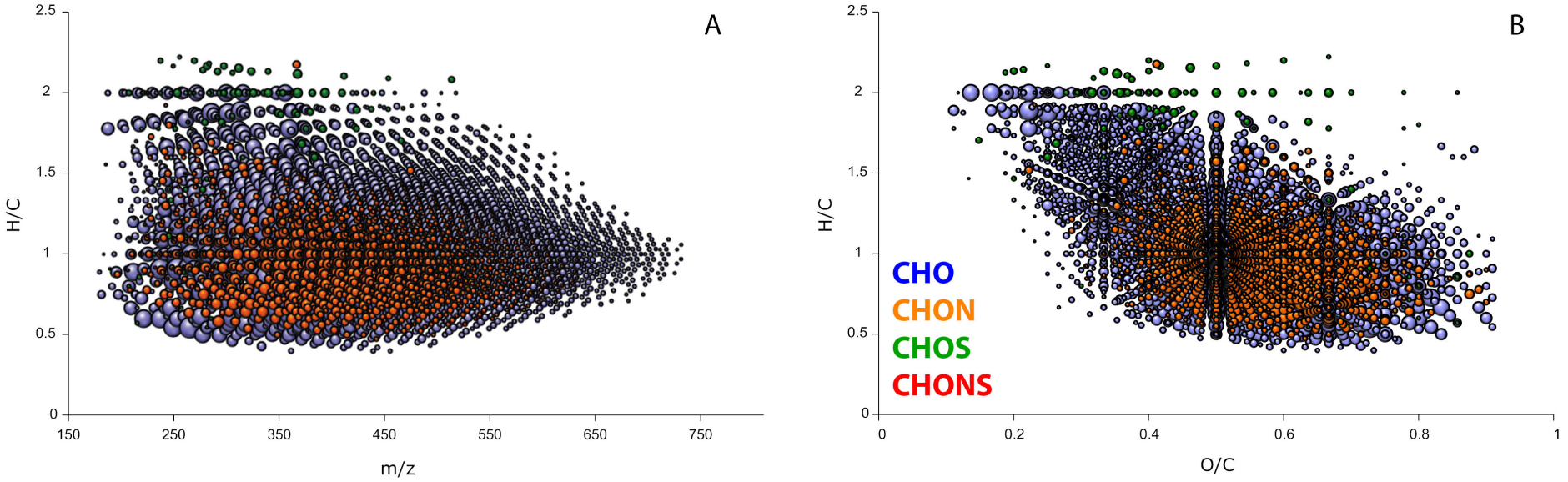

Figure 4 (A) Graph of the H/C ratio as a function of m/z and (B) van Kevelen diagram for the representation of the ubiquitous 3629 molecular formulas detected at least in 95% of the PH-WEOM samples. (colour code: blue for CHO compounds, orange for CHON compounds and green for CHOS compounds).

3.2 Ubiquitous molecular formulas in the PH-WEOC

van Krevelen diagram

The ubiquitous masses are shown in a graph of the H/C ratio as a function of m/z (Fig. 4A) and in a van Krevelen diagram (Fig. 4B). The projected formulas fill a large space in the two graphs, highlighting the great diversity of the ubiquitous molecular formulas.

The CHO formulas fully cover the mass range from 200 to 700 m/z, with a decreasing abundance of formulas with m/z > 500. The van Krevelen diagram shows that these CHO compounds have H/C comprised between 0.4 and 2.0, and O/C comprised between 0.15 and 0.85. The CHON formulas cover a large but more restricted range of m/z, from 250 to 650. These compounds are also more concentrated in the van Krevelen plot, with H/C ranging from 0.5 to 1.4 and O/C ranging from 0.4 to 0.75. Lastly, the few CHOS compounds are characterised by high H/C of about 2 and a wide range of O/C (0.2–0.7).

Generally, the interpretation based on van Krevelen diagrams refers to regions characteristic of a specific class of compounds, as previously presented in Figure 2. Referring to these regions, different types of compounds are ubiquitous in the PH-WEOM for this study. The regions of the van Krevelen diagram corresponding to lignins and tannins are completely filled (Fig. 4B). Molecular formulas that can be assigned to lipids and nucleic acids are also partly filled, and few carbohydrates are detected. The molecules projected in these areas of the van Krevelen diagram highlight the importance of plant-derived material in the bulk composition of PH-WEOM, but also of microbially derived molecules, especially for those with high H content (lipids and nucleic acids).

Interestingly we also identified molecules filling areas between the regions characteristic of specific classes of compounds. Indeed, no disconnection was observed in the continuum of molecules along the range of H/C and O/C ratios, thus revealing that PH-WEOM is much more complex than a “simple” mixture of plant-derived compounds. The molecules linking the different regions identified are aligned in the van Krevelen diagram, following the straight lines presented in Figure 2 and corresponding to specific chemical reactions, such as (de)methylation or (de)hydratation, for example.

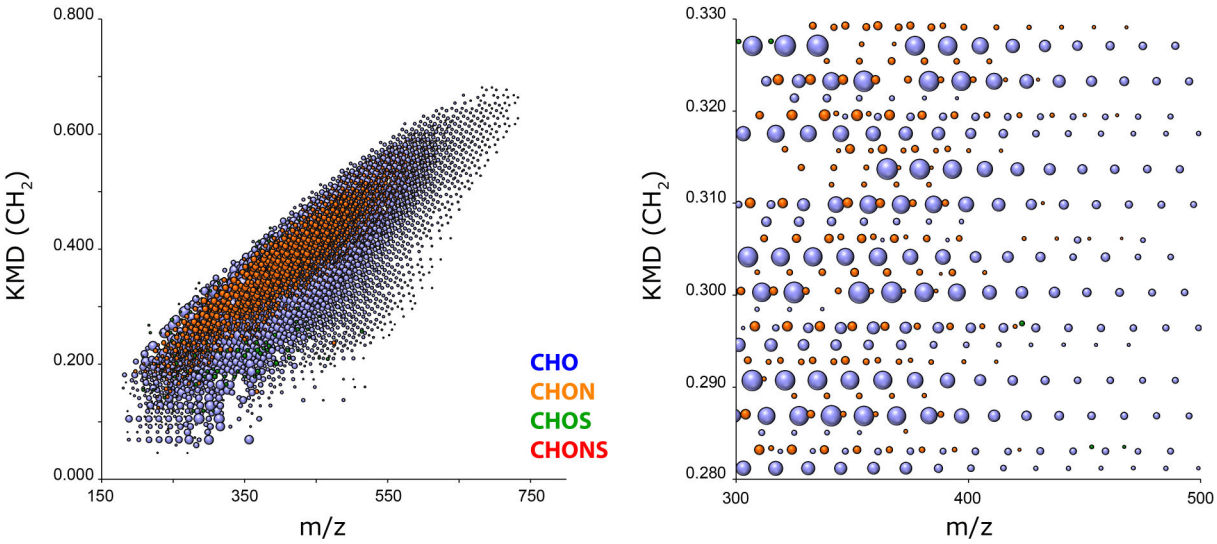

Figure 5 CH_2-based Kendrick mass defect analysis of the molecular formulas ubiquitous in PH-WEOM. The compounds with the same KMD value are aligned horizontally and and CH_2-homologous series reveal a systematic mass difference of 14 Da.

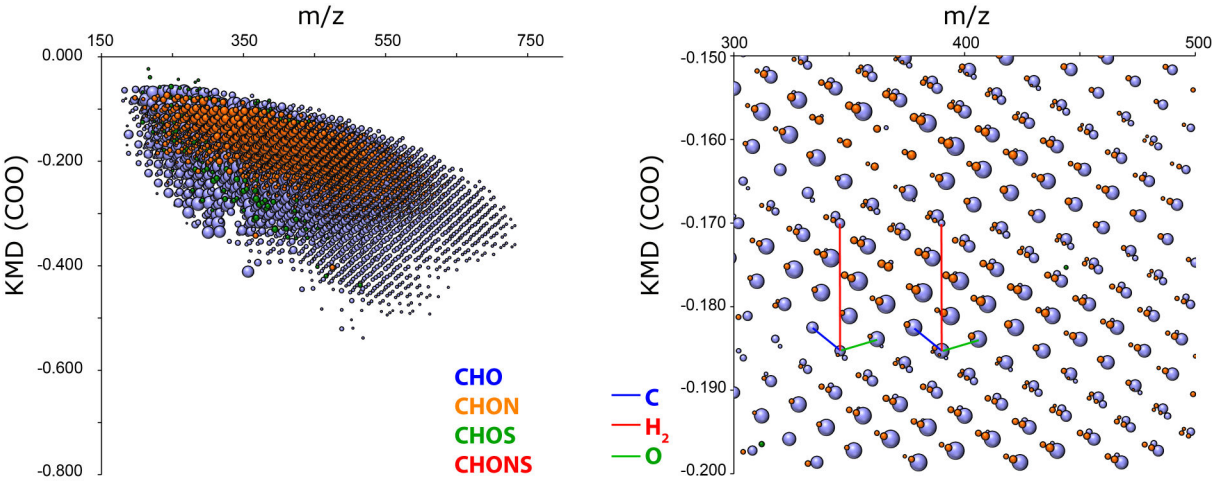

Figure 6 COO-based Kendrick mass defect analysis of the molecular formulas ubiquitous in PH-WEOM. The compounds with the same KMD value are aligned horizontally and and COO-homologous series reveal a systematic mass difference of 44 Da. Coloured lines in the enlarged plot indicate the exchange of one atom of C (blue), one atom of O (green) or two atom of H (red)

The trends observed along these lines might be indicative of structural relationships amongst series of compounds differing by the release or the incorporation of specific chemical groups. This complexity of the PH-WEOM, and more generally of DOM and SOM, derives from the fact that these mixtures originate from a multitude of different natural compounds synthesised by plants. The numerous paths for the degradation and transformation of these compounds lead to the great molecular diversity observed here, and in other studies of DOM and SOM molecular characterisation (e.g. D'Andrilli et al., 2010; Mosher et al., 2010; Ohno et al., 2014).

Kendrick mass defect (KMD)

Series of peaks following the trends along the lines in the van Krevelen diagram reveal specific chemical reactions that can be investigated by Kendrick mass defect analysis. The KMD plots allow the visualisation of homologous series of compounds differing by a selected group. Considering the mass defects from the nominal mass of C (12.00000 amu), H (1.007825 amu), and O (15.994915 amu) and because OM is primarily composed of these elements, the molecules that correspond to the peaks near nominal masses, which have a low mass defect, must have a small number of hydrogen atoms and a relatively larger proportion of oxygen atoms. In contrast, high mass defects correspond to O-deficiency and thus to a relatively larger proportion of H atoms.

Figures 5 and 6 allow the examination of the molecular series differing by CH_2 and COO groups, respectively. In the CH_2-based KMD plots, the CH_2-homologous molecular series are arranged in horizontal patterns. We found up to twenty CH_2-homologous molecules for a unique series, as clearly shown in the enlarged section of the plot. This CH_2 continuum was also found for N- and S-containing compounds, and reveals the overall importance of the CH_2 group as a building block of PH-WEOM molecules.

The carboxyl group is another major building block of NOM and (de)carboxylation reactions correspond to the addition/removal of one COO group. To investigate the importance of (de)carboxylation on the composition of PH-WEOM, COO-based KMD plots (Fig. 6) were computed. As observed in CH_2-based KMD plots, COO-homologous molecular series are aligned along horizontal lines.

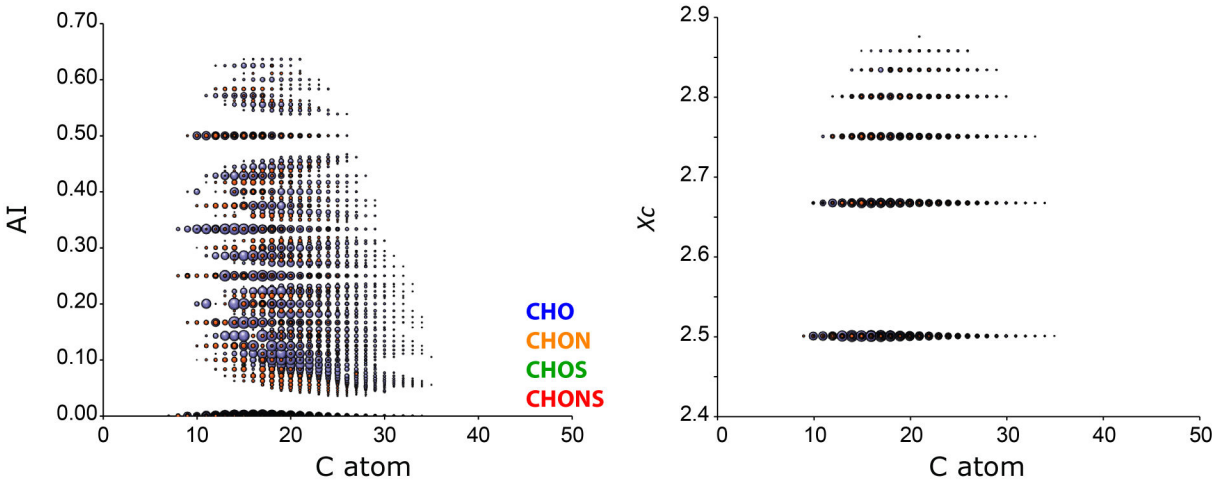

Figure 7 Plots of the AI (left) and Xc (right) as a function of carbon number for the identification of aromatic and condensed aromatic structures.

Due to the larger mass spacing (44 Da for COO and 14 for CH_2), COO-homologous series are shorter and generally no more than eight COO-homologous molecules are found in the enlarged section of the COO-based KMD plot.

We also found that CHON compounds are aligned in the COO-homologous series, while the S-containing compounds are not. The importance of COO as a key building block for NOM has already been shown in previous studies (Hertkorn et al., 2008; Grinhut et al., 2011; Smith et al., 2013).

Diagonal alignments of compounds can also be seen in the KMD plots. These alignments correspond to other homologous series, based on different reactions. The exchange of two H atoms for one O atom corresponds to homologous series diagonally aligned in the CH_2-based KMD plot, while the addition/removal of one C atom, one O atom, or two H atoms produced molecular series alignment easily detected in the COO-based KMD plot (Fig. 6). With these representations of the ubiquitous molecular formulas, we observed well-defined and complete homologous series, supporting the argument that PH-WEOM molecular characteristics are governed by a continuum in the decay processes responsible for its molecular rearrangement.

Aromaticity index (AI) and Double bond index (Xc)

An additional approach to characterise the molecular complexity of the ubiquitous molecules detected in the PH-WEOM is to estimate their proportion of aromatic structures. The aromaticity index (AI), developed by Koch & Dittmar (2006), and the double bond index (*Xc*), developed by Yassine et al. (2014), both help to provide structural information about the molecules (Fig. 7). Using the AI index, we classified 6% of the ubiquitous molecules as aromatic structures (AI ≥ 0.50), while no condensed aromatic structures (AI ≥ 0.67) were found (Fig. 7). However, using AI, as previously stated in the Materials and methods section, aromatics with long alkyl chains will not be identified as aromatic structures, leading to possible underestimation of the proportion of aromatic compounds in a mixture.

The *Xc* index, taking into consideration the fraction of heteroatoms involved in π-bond structures, remains similar when the length of the alkyl chain changes. Using the Xc index to classify the ubiquitous molecular formulas (Fig. 7), we found 18.8 % of aromatic structures (*Xc* ≥ 2.5000) and 14.1 % of condensed aromatic structures (*Xc* ≥ 2.7143). These fractions have to be considered as the smallest possible fraction

of aromatic and condensed aromatic structures in the mixture, as we make the assumption that all S and O atoms are involved in π-bond structures, leading to underestimation of the *Xc* values.

Suggestions of the molecular structures related to this *Xc* index can be found in Yassine et al. (2014). The authors show that *Xc* values of 2.5000 and 2.7143, respectively, indicate the presence of one, or two aromatic cores in a molecule. Each double bond and each aromatic core corresponds to an increase in the *Xc* value.

Comparing the results obtained using the two indexes, we can estimate the fractions of aromatic and condensed aromatic structures with short or long alkyl chains. Most of the compounds with an aromatic structure were classified as molecules with long alkyl chains (17.7% of aromatic structures containing extended alkylation and only 1.0% with little alkylation), while all condensed aromatic structures have an extended alkyl chain. The aromaticity of organic compounds was shown to be an indication of the refractory behaviour of molecules against biodegradation, and thus these estimates give an indication of the bulk reactivity of PH-WEOM (McDowell et al., 2006; Zhao et al., 2008). Our results thus reveal that a significant fraction of PH-WEOM is composed of molecular structures that would not easily be decomposed and might be preserved, either stabilised in the soil or transferred in solution.

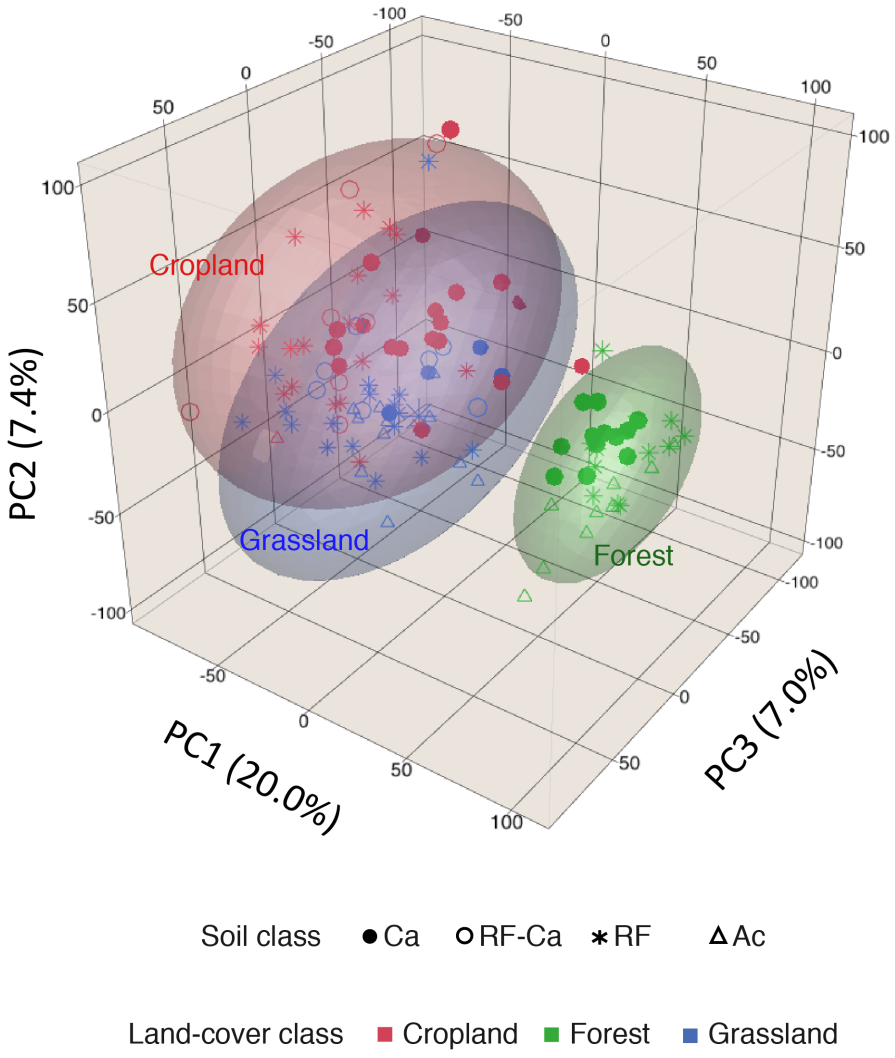

Figure 8 Principal Component Analysis showing clusters corresponding to the 3 land-cover classes, symbolised with the ellipsoids representing the confidence interval of 0.5.

3.3 Linking molecular information with soil characteristics

The primary objective of this research was to characterise the PH-WEOM in the 120 samples obtained from soils of the Burgundy region, with the aim of determining which soil characteristics, such as texture, pH, organic matter content, or even land cover and soil type, regulate the molecular composition of PH-WEOM.

Principal component analysis.

Variability in the molecular composition of the sample set was first evaluated by computing a PCA from the raw intensity of the 15,751 m/z detected by FTICR-MS. The PCA summarised about 20% of the explained variance with the first three PCs. When plotting the scores of the samples on a three-dimensional plot (Fig. 8), we observed a clear distinction along PC1 of the PH-WEOM samples obtained from forest soils, revealing that the molecular composition of PH-WEOM has a vastly different composition in these samples. Moreover, these samples are observed in a more restricted volume of the plot than those of the other classes, highlighting their greater similarity. Looking in more detail at this forest class, we observed that the samples gathered according to soil classes, suggesting the influence, at a lower level, of soil characteristics on the molecular composition of PH-WEOM. The PH-WEOM samples from cropland and grassland soils occupied a larger volume in the PCA plot and were not clearly separated, revealing greater variability in the PH-WEOM composition and no clearly different patterns for these two classes. The samples are distributed according to soil class in the PCA plot, suggesting that PH-WEOM molecular composition is controlled by soil characteristics.

Hierarchical cluster analysis

To complete this initial investigation, a second unsupervised approach was used in order to identify groups with strong similarities. A hierarchical clustering analysis (HCA) was computed from the relative intensity of the 15,751 m/z detected by FTICR-MS in the 120 PH-WEOM samples. Based on a similarity threshold of 0.518, the sample set was divided into five different clusters, which regroup the PH-WEOM samples with a significant resemblance in their molecular composition (Fig. 9).

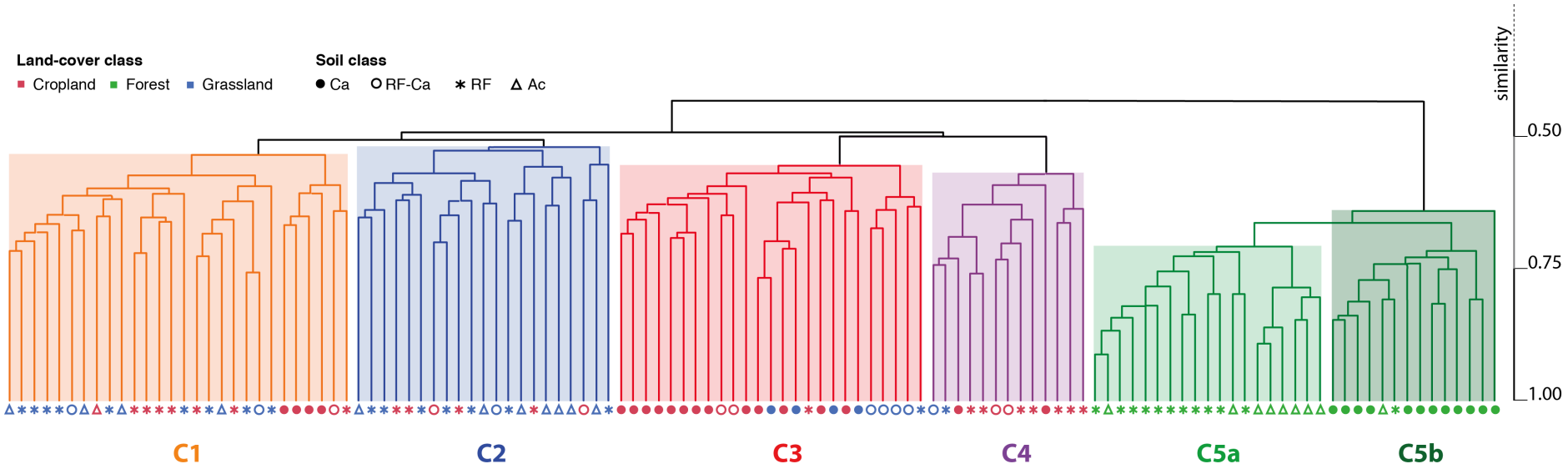

Figure 9 Dendrogram from the cluster analysis using the relative magnitudes of the 15,751 formulas in each sample. The similarity threshold was set at 0.518, thus giving five different clusters, which are shown in the separate coloured rectangles. Indications of the land cover and soil class for each sample are provided below the dendrogram. The cluster C5 was arbitrary divided in two sub-clusters for the subsequent investigations as we observed a well-defined distribution of the samples of the different soil classes in two sub-groups.

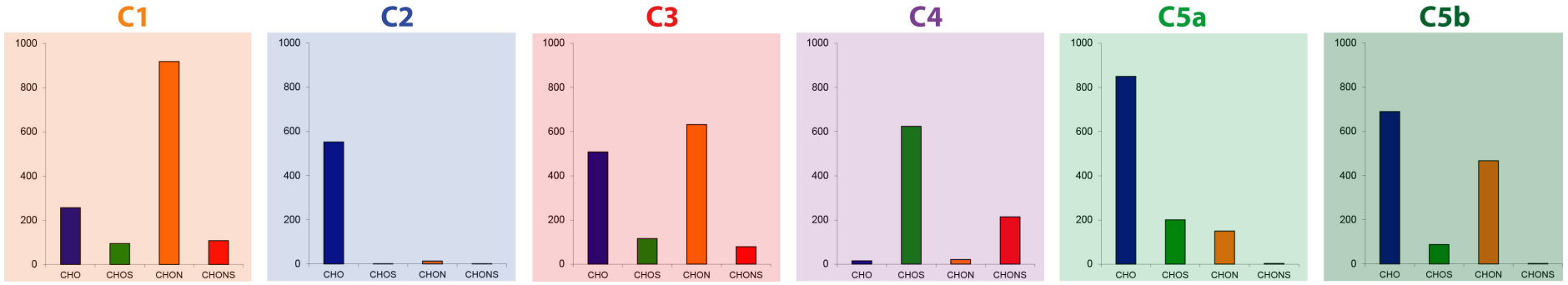

Figure 10 Counts of elemental compositions of assigned molecular formulas characteristics for each cluster (threshold of R > 0.7) according to CHO (blue), CHOS (green), CHON (orange) and CHONS (red) compounds.

As with the PCA, the outcome primarily observed in the HCA is that the samples from forest soil are grouped together and show greater similarity than all other clusters. The forest cluster can be divided into two sub-groups. We thus considered cluster 5a, which is composed of the forest samples belonging to the two classes of acidic soils (Ac) and soils containing low quantities of exchangeable calcium, developed on residual formations (Rf). The second sub-cluster, 5b, contains almost exclusively the PH-WEOM samples from forest soil developed on calcareous parent material, which are enriched in organic carbon and total nitrogen and have a texture rich in clay and silt.

The other four clusters (C1–C4) contain both cropland and grassland PH-WEOM samples. Cluster C1 regroups samples from all soil classes, with a majority from the Rf class, and balanced proportions from cropland and grassland. Cluster C2 also contains samples from most soil classes, with a greater proportion from grassland areas. When investigating soil parameters, we found that neither texture, nor organic matter content differ between C1 and C2. The main differences are higher pH, a higher extraction ratio of organic C and higher aromaticity (ER and $SUVA_{254}$, see Chapter 4) of the samples in C1 than in C2. Cluster C3 contains more cropland than grassland samples, and all but one are assigned to the soil classes Ca and Rf-Ca, which are characterised by high pH values and SOC content, and textures rich in silt and clay. Cluster C4 contains PH-WEOM samples from cropland, plus two from grassland, which correspond to soils developed on residual formations (both Rf and Rf-Ca classes), and one from a cropland soil developed on calcareous rock. These soils are all rich in silt particles.

The molecular formulas with greater intensities in each cluster, governing the classification, were extracted, based on a minimum threshold of $R > 0.7$, and the counts of CHO, CHOS, CHOS and CHONS compounds are presented in Figure 10. We found clear dissimilarities in the proportion of compound classes for the six clusters. A great proportion of CHON species characterise cluster C1, while CHO compounds were found almost exclusively for C2. Both CHON and CHO species dominate for the discrimination of C3, with a small contribution of S-containing species. Cluster C4 is mostly composed of both CHOS and CHONS compounds. Lastly, the forest samples are characterised by a great number of CHO compounds, plus CHON and CHOS. A greater number of CHON compounds was found as significant in cluster C5b than in C5a. The characteristics of soil and PH-WEOM grouped by cluster are summarised in Table 1.

Table 1 Means and standard errors of pH, soil organic carbon (SOC in mg per g of soil), total nitrogen (TN in mg per g of soil), aromaticity ($SUVA_{254}$ in L per mg of C per m) and extraction ratio (ER in mg of C extracted per g of soil C) in the six different clusters.

		pH	SOC	TN	$SUVA_{254}$	ER	Texture
C1	mean (SE) range	5.8 (0.1) 4.8–7.2	17.6 (1.8) 7.1–46.2	1.7 (0.1) 0.8–3.7	18.1 (0.8) 12.1–27.7	43.1 (1.2) 29.0–55.7	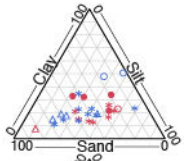
C2	mean (SE) range	5.0 (0.1) 4.3–6.5	20.7 (1.9) 7.1–38.5	1.9 (0.2) 0.7–3.5	14.1 (0.6) 10.3–21.5	32.6 (2.1) 14.9–50.7	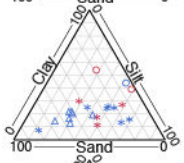
C3	mean (SE) range	6.7 (0.1) 5.0–7.3	32.5 (2.9) 10.8–83.2	2.9 (0.2) 1.0–4.5	11.8 (0.6) 6.9–21.0	23.4 (1.3) 14.4–43.3	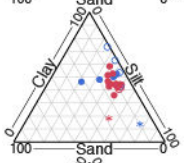
C4	mean (SE) range	6.1 (0.2) 5.2–7.3	14.9 (1.9) 9.9–36.2	1.5 (0.1) 1.1–2.9	15.6 (1.1) 9.8–23.2	30.9 (2.1) 21.7–46.5	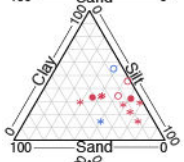
C5a	mean (SE) range	4.1 (0.1) 3.5–5.2	35.4 (6.1) 13.4–98.0	1.8 (0.3) 0.6–5.0	10.6 (0.5) 8.0–15.1	31.1 (2.7) 14.8–59.5	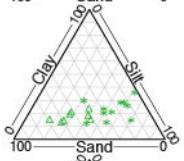
C5b	mean (SE) range	6.3 (0.2) 4.0–7.2	60.6 (6.9) 25.7–108.8	4.1 (0.4) 1.8–6.4	10.9 (0.3) 9.3–13.5	20.4 (1.5) 10.4–29.2	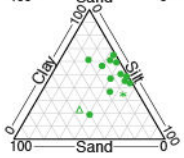

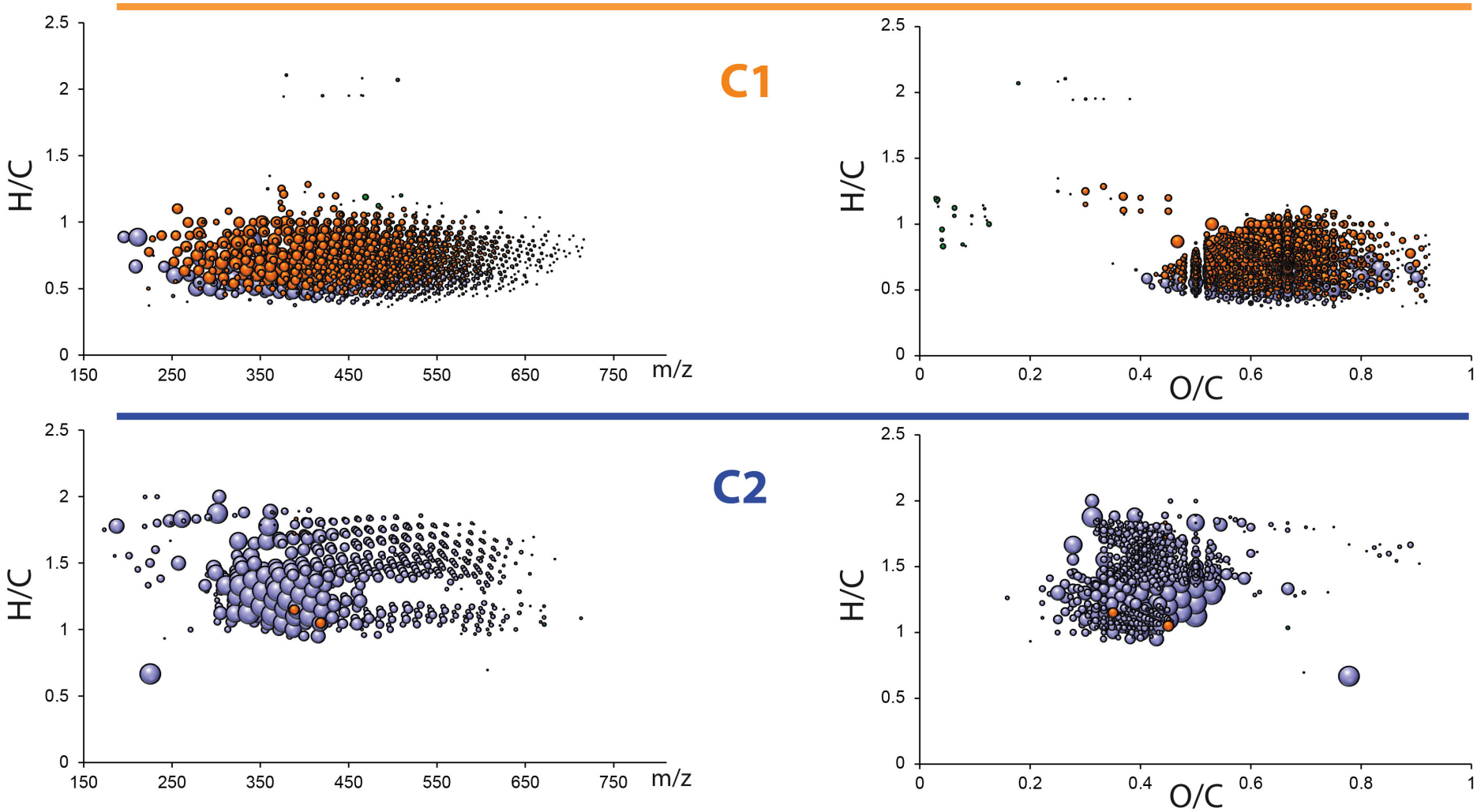

Figure 11 Representation of the assigned molecular formulas characteristic of clusters C1 and C2 in plots of H/C as a function of m/z and in van Krevelen diagrams (H/C as a function of O/C). The size of the bubbles is proportional to the mean intensity of the peaks in the PH-WEOM samples assigned to the corresponding cluster. The colour code indicates the presence of CHO (blue), CHOS (green), CHON (orange) and CHONS (red) compounds.

van Krevelen diagram analyses

The molecular formulas characteristic of each cluster are plotted on graphs of H/C ratio, as a function of m/z, and on van Krevelen diagrams (Fig. 11, 13 & 14). These representations are rich in information and reveal clear differences in the molecular fingerprint responsible for the cluster discrimination. Interestingly, the compounds identified are grouped and precisely aligned on these graphs, suggesting that they correspond to molecular series of homologous compounds, which differ by a specific chemical group, as previously shown with the KMD analyses of the ubiquitous formulas.

The molecular formulas characteristic of cluster C1 cover a wide range of m/z (250–650) and have low H/C and high O/C. These compounds are CHO and CHON species that overlap on both graphs. These compounds fall in the region of the diagram assigned to tannins, but are also observed beyond this region, towards areas with lower H/C. The pronounced unsaturation and oxidation suggest that these compounds are related to humified substances, with pronounced dehydration and dehydrogenation reactions.

The high proportion of N-containing molecules is in line with the presence of humified material. Considering that humic substances are supramolecular aggregations including biomolecules (Piccolo, 2001; Simpson et al., 2002), the association of amide groups derived from peptides, or amino-acids with various organic compounds, such as tannins, can be responsible for the great abundance of N-containing compounds in the PH-WEOM samples of cluster C1. Another explanation for these unsaturated N-containing molecules could be the presence of heterocyclic N functional groups, which can be formed abiotically during advanced humification (Knicker et al., 2002). Nevertheless, Sutton & Sposito (2005), in a review addressing this issue, suggest that the dominant chemical form of N in humic substances is amide N, derived from peptide transformation, while heterocyclic N is a less significant contributor to humic composition.

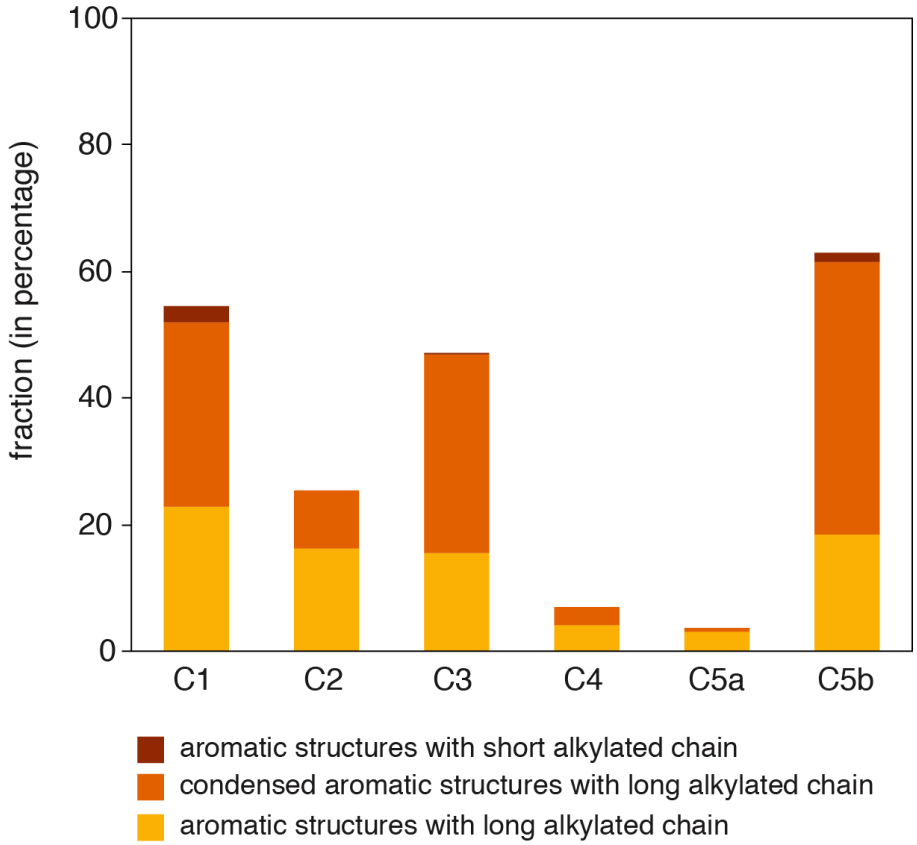

Figure 12 Fraction of compounds classified as aromatic structures in the six clusters. The different classes of aromatic structures are based on the calculation of the aromaticity index (AI) and the double-bond equivalent index (*Xc*).

The aromaticity of these compounds was assessed using the AI and *Xc* index. More than half of these compounds were classified as aromatic structures, mainly assigned to aromatic and condensed aromatic structures containing extended alkyl chains (Fig. 12). Only 2.5% of the molecular formulas correspond to aromatic structures with little alkylation, while no condensed aromatic structures with little alkylation were found.

Although cluster C2 contains PH-WEOM samples from soils that are similar to the soils of C1, especially in land cover and soil class, very different patterns are observed in Figure 11. The molecular formulas characteristic of C2 are almost exclusively composed of CHO, with greater peak intensities around 380 m/z and smaller peak intensities up to 650 m/z. The molecular formulas are grouped in a region with intermediate H/C (1.0–1.8) and O/C (0.25–0.55). This region of the van Krevelen diagram is attributed to lignins and lignin-like compounds. The presence of molecules with H/C > 1.5 is also characteristic of C2. An explanation for these H-rich compounds could be that lignins and lignin-derived molecules react and associate with aliphatic compounds, thus leading to the formation of alkylated lignin-derived molecules. We found fewer molecules with aromatic structures in C2 than in C1, with 16.2% of aromatic and 9.2% of condensed aromatic structures, all with long alkyl chains (Fig. 12).

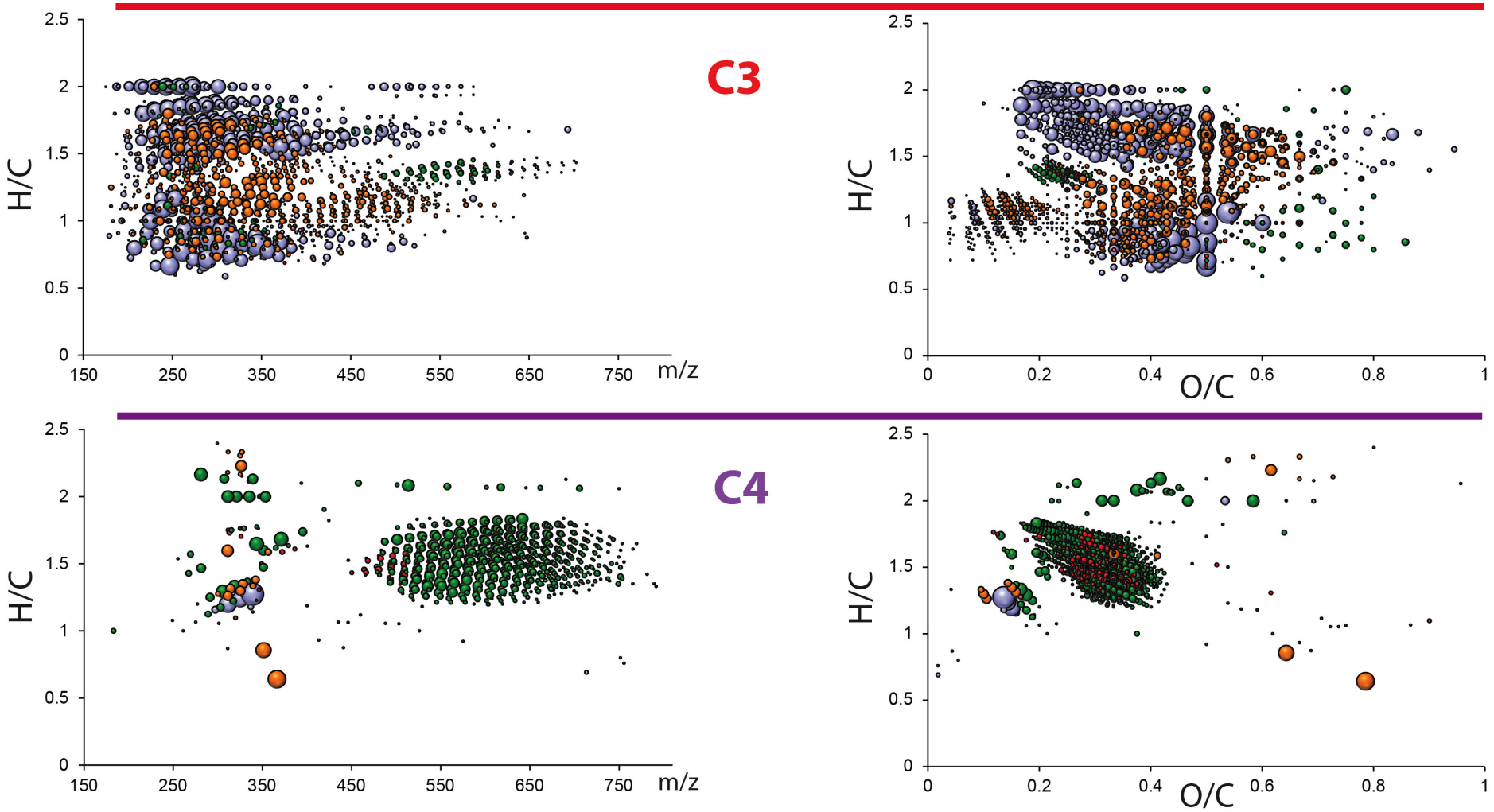

Figure 13 Representation of the assigned molecular formulas characteristic of clusters C3 and C4 in plots of H/C as a function of m/z and in van Krevelen diagrams (H/C as a function of O/C). The size of the bubbles is proportional to the mean intensity of the peaks in the PH-WEOM samples assigned to the corresponding cluster. The colour code indicates the presence of CHO (blue), CHOS (green), CHON (orange) and CHONS (red) compounds.

The molecular fingerprint observed in cluster C3 indicates the specific molecular composition of PH-WEOM for alkaline soils (Fig. 13). The plot of H/C against m/z, and the van Krevelen diagram both show that molecular specificities of C3 are much more complex than those of the other clusters. The molecular formulas identified covered very wide ranges of m/z, H/C and O/C, and several distinct groups of compounds can be identified in the van Krevelen diagram.

The first group is projected in the area attributed to lignins, with less H and more O than in C2. Both CHO and CHON species are found in this group. Many CHO compounds with high H/C are found, presumably corresponding to lipids and aliphatics. This result is in line with a contribution of microbially derived molecules, consistent with the high pH measured in the soils of cluster C3. As discussed in the previous chapter, a high abundance of microorganisms is often found in alkaline soils, and it is therefore logical to have a greater contribution of organic compounds derived from microbial activity, such as lipids and aliphatics, but also nucleic acids and carbohydrates. The N-containing compounds are found near the domain of nucleic acids, while few molecules are observed near the area of the diagram corresponding to carbohydrates. However, it is well known that the C_{18} extraction used to remove inorganic species during sample preparation is highly selective for carbohydrates. Due to their non-polarity, many carbohydrates are lost during this step. Despite this limitation, the greatest contribution of carbohydrates is observed in this cluster.

Another group of CHO and CHON compounds with very low O/C (≤ 0.2), and H/C around 1.0 is also observed. This region of the van Krevelen diagram corresponds to condensed hydrocarbons, suggesting the contribution of a C pool at an advanced stage of maturation to the PH-WEOM pool. Humified pools of soil C were suggested as a source for DOM in soils (Hagedorn et al., 2004; De Troyer et al., 2011). The great abundance of aromatic structures (Fig. 12) corresponds to the molecular formulas attributed to condensed hydrocarbons and lignins. Lastly, few CHOS and CHONS molecular formulas are projected in a very close region of the diagram and have large m/z (450–700). These compounds are relatively similar to the S-containing molecular formulas presented in cluster C4.

Cluster C4 is characterised by a very particular group of molecular formulas (Fig. 13). These formulas are almost exclusively CHOS and CHONS, with high m/z (450–750), grouped in the van Krevelen diagram in an area with H/C of 1.5 and O/C of 0.3. These compounds are arranged in continuous CH_2- and COO-homologous series, and were not classified as aromatic structures (Fig. 12).

The formation of organic S in soils is mainly due to the incorporation of sulphate in SOM, mediated by soil microorganisms, via the formation of covalent linkages (Strickland & Fitzgerald, 1984). Applications of cattle manure to fertilise agricultural land, or pesticide spreading are other sources of organic S in soils. Moreover, the incorporation of S-containing amino acids, i.e. cysteine and methionine, may also account for the organic S pool (Fitzgerald et al., 1984). This latter possibility is not very consistent with the compounds identified in C4, which are not projected in an area of the van Krevelen plot attributed to amino acids. We thus hypothesised that these compounds correspond to aliphatic structures associated with these S-containing moieties, which can be achieved via sulphatation or sulphonation.

Contamination by surfactants was envisaged, as this type of S-containing molecules, found in wastewater using FTICR-MS measurements, appeared in a nearby region of the van Krevelen diagram (Gonsior et al., 2011; Tseng et al., 2013). The presence of linear alkyl sulphonates, with high peak intensities, corresponding to surfactants, was detected in all samples by scrutinising the mass spectra. However, these compounds, probably indicating contamination by the detergents used for cleaning the PH-WEOM extraction cells or laboratory vessels, have m/z values around 300. This would indicate that the large S-containing molecules found in cluster C4 do not derive from such contamination, but are characteristic of specific soil ecosystems.

The soils corresponding to this cluster are mostly from agricultural fields located at low elevations, and developed on residual formations. These soils are rich in silt particles and have low organic C content. Such common features therefore strongly suggest that the S-rich molecular pattern observed in cluster C4 is the result of specific soil ecosystem functionalities.

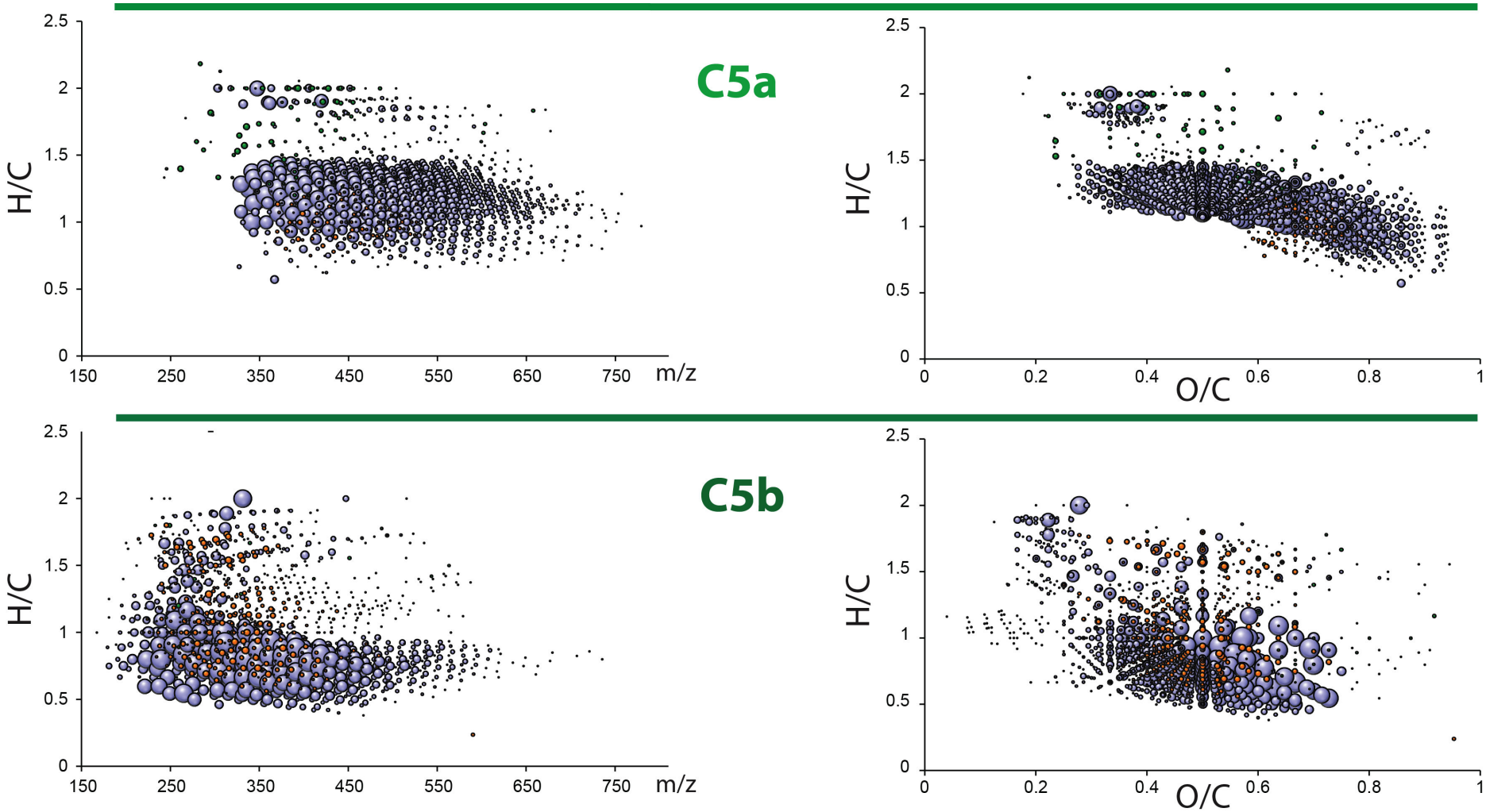

Figure 14 Representation of the assigned molecular formulas characteristic of clusters C5a and C5b in plots of H/C as a function of m/z and in van Krevelen diagrams (H/C as a function of O/C). The size of the bubbles is proportional to the mean intensity of the peaks in the PH-WEOM samples assigned to the corresponding cluster. The colour code indicates the presence of CHO (blue), CHOS (green), CHON (orange) and CHONS (red) compounds.

For clusters C5a and C5b, grouping PH-WEOM samples from forest soils, CHO compounds dominate in abundance but especially at peak intensities, so that CHOS and CHON formulas are difficult to identify on the graphs. Differences were observed in the molecular fingerprints of the two clusters, with higher m/z in C5a, and lower H/C in C5b (Fig. 14).

The CHO formulas found for C5a are distributed over a very wide range of O/C, with relatively small variations in H/C. These compounds appeared in regions attributed to tannins and lignins. The CHON formulas have more restricted O/C variation (0.6–0.8) and fall in the region characteristic of tannins. These N-containing compounds, with low peak intensities, show characteristics very similar to the CHON compounds described in C1, attributed to molecular associations leading to N preservation in soils. The CHOS compounds have higher H/C, suggesting their microbial origin.

The lignin signature in PH-WEOM is consistent with previous studies, reporting that lignins and lignin-derived compounds represent a major fraction of DOM or WEOM in the upper horizons of soils and that these compounds are preserved due to their low biodegradability (Kalbitz & Kaiser, 2008; Roth et al., 2013). The contribution of tannins was also mentioned as having considerable influence on the molecular composition of DOM in forest ecosystems (Roth et al., 2014).

However, calculations based on AI and *Xc* indexes reveal that fewer than 4% of these compounds are classified as aromatic structures (Fig. 12). This result is highly contradictory with the presence of lignin- and tannin-like compounds, as phenols are a key structural group for these compounds. Thus, these molecular formulas may correspond to other species, which could be non-aromatic molecular fragments of degraded lignins and tannins. This appears to be the more reasonable assumption, while associations of these molecular fragments with aliphatics or carbohydrates could also be envisaged and is consistent with the relatively high H/C range for lignins and tannins.

The O-rich compounds, with O/C up to 0.95, constitute COO-homologous series, revealing a very high abundance of carboxyl functional groups in these molecules. Few other compounds with high H/C are observed, in the region attributed to aliphatics, and in the region of carbohydrates, in line with a contribution of molecules derived from microbial activity or plant residues.

Cluster 5b also contains compounds with high H/C, which should correspond to aliphatics and carbohydrates. Again this observation is consistent with a contribution of soluble compounds from microbial activity and the decay of plant residues. We also found formulas with very low O/C, which fall in the region of condensed hydrocarbons. Interestingly, the presence of these compounds was detected for the two clusters regrouping the PH-WEOM samples obtained from soils with high pH values. It suggests that this type of compounds, contributing to the great fractions of aromatic structures identified in clusters C3 and C5b, are representative of the PH-WEOM of alkaline soils.

The main group of molecular formulas in cluster C5b fall in the region of tannins and lignins, but with lower m/z, H/C and O/C than the compounds found in C5a. The decrease in m/z may indicate that lignin-like and tannin-like compounds are more decomposed in C5b than in C5a. This assumption is in line with the decrease in H/C and O/C, as decreases in both ratios are expected with the condensation of organic matter during the humification process. More than 60% of the compounds were classified as aromatic and condensed aromatic structures, mostly with long alkyl chains (Fig. 12), which must correspond to phenols and polyphenols derived from lignin and tannin biomolecules.

Conclusion

The ultrahigh-resolution FTICR-MS data reveal the presence of more than 3,000 molecular formulas ubiquitous in the PH-WEOM obtained from the 120 soil samples of the Burgundy region. This common pool of organic compounds is composed of molecules with various molecular weights and compositions, as revealed by the large range of H/C and O/C found. The visualisation of this information in the van Krevelen diagram indicates the great diversity of this complex mixture, with formulas attributed to many different compound classes (lignins, tannins and aliphatics). Compounds found in regions intermediate to those attributed to known compounds are also found, revealing that PH-WEOM is composed of a molecular mixture resulting from a continuum of biomolecule decay processes. The Kendrick mass defect analysis confirms this continuity by revealing that series of homologous compounds constitute the PH-WEOM pool, and that (de)methylation and (de)carboxylation are major reactions in the decomposition of soil organic matter.

The molecular characterisation of the 120 samples of PH-WEOM has allowed the identification of groups of samples with common features. The classification using the hierarchical clustering approach shows that samples are not distributed randomly, but that this distribution is related to soil classes and land cover. The molecular composition of PH-WEOM from forest soils is clearly distinct, with major contributions from lignin- and tannin-like compounds, and with a more or less pronounced aromaticity related to soil characteristics, especially the soil pH. The PH-WEOM is more similar for cropland and grassland soils. The role of pH was also identified in the PH-WEOM samples from cropland and grassland soils and corresponds to molecular patterns related to microbial activity, with the presence of compounds with high H/C, presumably corresponding to lipids, carbohydrates and nucleic acids. A group of samples from cropland soils developed on residual formations is characterised by a very specific molecular composition, rich in S-containing aliphatic compounds, highlighting the importance of specific soil processes in the molecular composition of PH-WEOM.

This study confirms the great potential of FTICR-MS to resolve the high complexity of PH-WEOM in soils. Other on-going investigations of this dataset have already identified the molecular formulas correlated with the $\delta^{13}C$ variability in these samples, presented in the previous chapter. These formulas were extrapolated from robust PLS models

for each land-cover class, and we are able to distinguish the molecular formulas related to $\delta^{13}C$ increase (or decrease), specific to each type of land cover and those which are common to all of the land-cover classes. Further research can be envisaged with this dataset, such as investigations of the molecular information related to the aromaticity ($SUVA_{254}$) of PH-WEOM, but also the specificities of samples from soils rich in clay or SOC, for example.

Acknowledgements

The RMQS soil-sampling and physico-chemical analyses were supported by a French Scientific Group of Interest on soils: the 'GIS Sol', involving the French Ministry for Ecology and Sustainable Development, the French Ministry of Agriculture, the French Agency for Energy and Environment (ADEME), the French Institute for Research and Development (IRD), the National Institute for Agronomic Research (INRA), and the National Institute of the Geographic and Forest Information (IGN). We thank all the soil surveyors and technical assistants involved in sampling the sites, and technical support from the French soil sample archive, which provided the collection of soils studied.

This work, through the involvement of technical facilities of the GenoSol platform of the ANAEE-Services infrastructure, received a grant from the French state through the National Agency for Research under the program ANR-11-INBS-0001 "Investments for the Future", as well as a grant from the Regional Council of Burgundy. A travel grant from the doctoral school ES of the University of Burgundy facilitated the collaborative work. Review comments and English editing of this paper by Carmela Chateau-Smith were also greatly appreciated.

Conclusion générale et perspectives

Au cours de cette thèse, l'étude quantitative et qualitative des matières organiques extractibles à l'eau (WEOM) a été mise en relation avec les propriétés physico-chimiques des sols, ainsi qu'avec l'abondance et les caractéristiques des communautés microbiennes. Cette approche avait pour but de déterminer l'importance des différents facteurs, biotiques et abiotiques, sur les quantités de WEOM et surtout sur ses propriétés.

La première étape de ce travail, présentée dans le chapitre 2, portait sur la comparaison de méthodes d'extraction de WEOM. Cette étude a permis de démontrer que les différentes méthodes utilisées avaient une influence sur les quantités de matières organiques extraites et sur leurs propriétés. Les solutions obtenues au moyen des différents protocoles sont toutefois caractérisées par un potentiel de biodégradabilité et des propriétés de fluorescence assez proches. La comparaison réalisée sur cinq sols aux différences bien marquées a révélé que l'effet du sol est largement supérieur à l'effet de la méthode d'extraction sur les propriétés du WEOM, et qu'il y a une interaction significative entre ces deux effets. La méthode d'extraction à haute pression et haute température (PH-WEOC) est plus rapide, plus reproductible et a un meilleur rendement d'extraction. Pour ces raisons, la suite des travaux de cette thèse a été réalisée en utilisant cette méthode d'extraction.

Les études comparatives sur les méthodes d'extraction sont nécessaires, étant donné le grand nombre de méthodes utilisées dans les différents laboratoires. L'enjeu serait de normaliser au maximum ces différentes méthodes et d'identifier le rôle écologique des MO qu'elles permettent d'isoler. Beaucoup d'autres comparaisons sont envisageables, comme la comparaison des différents solvants utilisés pour l'extraction (eau, $CaCl_2$, K_2SO_4… à différentes concentrations), ou la comparaison avec les méthodes de prélèvements *in situ* (bougies poreuses, systèmes lysimétriques). Nos travaux ont montré qu'il est primordial de réaliser ces comparaisons en intégrant la diversité des sols dans les études.

En revenant désormais aux questions posées au début de ce manuscrit, nous allons rappeler les principales réponses apportées par ce travail, et proposer les perspectives associées à chacune d'entre elles.

Existe-t-il un lien entre l'activité microbienne et la dynamique des matières organiques ?

Un des objectifs initiaux de cette thèse était de déterminer les liens entre les communautés microbiennes et la dynamique des matières organiques du sol (MOS). Une première expérimentation, présentée dans le chapitre 3, a permis d'étudier l'impact d'une baisse de diversité bactérienne sur la décomposition de la MO. Le gradient de diversité bactérienne créé artificiellement a montré que la cinétique de dégradation de la matière organique était ralentie par la baisse de diversité. Ces modifications ont été observées sur les vitesses de dégradation de la MOS et de la matière organique fraîche, ainsi que sur la dynamique du PH-WEOC et sur les flux de CO_2 produits par la respiration microbienne.

L'utilisation d'une source de matière organique fraîche enrichie en ^{13}C a permis d'estimer le CO_2 produit par le *priming effect* (PE). Les flux de CO_2 attribués au PE sont corrélés au niveau de diversité bactérienne, avec une diminution du PE liée à la baisse de diversité. Cette approche par traçage isotopique a également permis de détecter une relation entre le PE et l'enrichissement isotopique du PH-WEOC. La composition isotopique du PH-WEOC nous informe sur les proportions de C provenant de la solubilisation de la MOS (99% de ^{12}C) et de la matière organique fraîche (96% de ^{13}C). Pour les trois niveaux de diversité bactérienne, des intensifications du PE synchrones avec des augmentations de la proportion de ^{13}C dans le PH-WEOC ont été mesurées. L'hypothèse émise suite à ces observations est que l'augmentation de la proportion en ^{13}C résulte d'une baisse en ^{12}C, due à la minéralisation des matières organiques solubles issues de la dégradation de la MOS (riche en ^{12}C). Ce lien entre la dynamique du PH-WEOC et le PE n'avait jamais été montré précédemment et il sera intéressant de confirmer cette relation avec un plus grand nombre de sols.

Les travaux présentés dans le chapitre 4 ont ensuite permis de montrer un lien entre les propriétés du PH-WEOC et la structure génétique des communautés bactériennes. Dans cette étude réalisée sur un grand nombre d'échantillons de sol hétérogènes (n=120), nous avons mis en évidence l'importance du pH et de la texture des sols sur la structure des communautés bactériennes. Ces facteurs de contrôle sur la structure des communautés avaient déjà été souvent identifiés dans d'autres études. Par contre, le lien entre la structure des communautés et le pool soluble de matière organique est un résultat nouveau.

Nous avons mis en évidence la relation entre la structure des communautés bactérienne et le potentiel de solubilité de la matière organique du sol (ER : *extraction ratio*). Cette relation avec la structure des communautés a un niveau de significativité similaire à ceux observés pour le pH et la texture. Ce résultat est renforcé par le fait qu'il a été déterminé sur une large gamme d'échantillons hétérogènes. Cependant l'approche par co-inertie ne permet pas de conclure sur le lien de cause à effet entre ces deux variables et la perspective évidente de ce travail est de mettre en place de nouvelles expériences afin de déterminer si le potentiel de solubilité de la matière organique du sol contrôle – ou est contrôlée par – la structure des communautés bactériennes.

Quelles sont les caractéristiques des sols qui contrôlent les propriétés de la MOD ?

Dans ce chapitre 4, nous avons également pu mettre en évidence des corrélations entre les propriétés du PH-WEOC et différents paramètres du sol. Le ratio d'extraction (ER), correspondant au potentiel de solubilisation de la MOS, est expliqué en grande partie par les teneurs en carbone organique (C_{org}) et en argile granulométrique des sols. Une plus grande proportion de la MOS étant soluble dans les sols avec des concentrations basses en C_{org}. L'effet conjoint de la proportion d'argile fait qu'une plus faible proportion de la MOS est solubilisée dans les sols avec les textures plus fines, qui proposent plus de sites de liaisons fortes entre la fraction minérale et la MOS. Nous avons également montré que l'aromaticité ($SUVA_{254}$) du PH-WEOC était inversement proportionnelle au taux de C_{org} du sol.

Les sols pauvres en C_{org} sont donc généralement caractérisés par une matière organique plus soluble et enrichie en composés aromatiques, alors que dans les sols caractérisés par des teneurs en C_{org} plus élevées, notamment les sols de forêt, le PH-WEOC contient une plus grande proportion de composés peu aromatiques. La signature isotopique enrichie en ^{13}C dans les sols forestiers suggère une plus forte abondance de carbohydrates, en accord avec la baisse de l'aromaticité du PH-WEOC.

Les analyses isotopiques du C ont clairement mis en évidence les différences de signature en fonction du couvert végétal, avec des valeurs de $\delta^{13}C$ plus négatives en prairie, intermédiaires pour les zones de culture et moins négatives pour les échantillons de forêt. La comparaison des valeurs de $\delta^{13}C$ du sol avec celle du PH-WEOC montre un enrichissement en ^{13}C dans la fraction soluble. Cet enrichissement révèle que le PH-WEOC a une composition chimique globalement différente de la MOS, et suggère une plus grande proportion de carbohydrates dans la fraction soluble. Cet enrichissement en ^{13}C plus marqué pour les échantillons de forêt supporte l'hypothèse d'une plus grande proportion de carbohydrates dans le PH-WEOC pour ces échantillons.

Les résultats montrant une différence de la signature isotopique en fonction du couvert végétal sont relativement surprenants et ne peuvent être irréfutablement expliqués par nos analyses. Plusieurs processus peuvent en être à l'origine. Une différenciation due aux variations d'abondance des classes de composés organiques (notamment en lignines, en carbohydrates ou en lipides) semble être l'hypothèse la plus raisonnable. Cette distinction en fonction du couvert végétal pourrait également être le résultat de l'assimilation d'une source de C ayant une signature isotopique appauvrie en ^{13}C dans les écosystèmes de prairie mais cette hypothèse nécessite des investigations supplémentaires. L'explication des différences dans la signature isotopique du C en fonction du couvert végétal suscite un grand intérêt car, à notre connaissance, aucune étude à ce jour n'avait révélé une telle influence de la végétation dans des écosystèmes exclusivement composés de plantes à mécanisme photosynthétique de type C3.

Quels sont les facteurs de contrôle de la composition moléculaire de la MOD ?

La caractérisation moléculaire à haute résolution du PH-WEOM présentée dans le chapitre 5 a confirmé la distinction claire de la composition chimique du PH-WEOC des sols de forêt par rapport aux échantillons provenant des prairies et des zones de culture. La spécificité des échantillons de forêt est principalement gouvernée par l'abondance de molécules composées uniquement des éléments C, H et O et attribuées à des molécules du type des tannins et des lignines. L'effet du couvert végétal ne permet pas de différencier les échantillons de PH-WEOC pour les sols de prairie et de culture.

Les caractéristiques des sols qui se distinguent en fonction des groupes d'échantillons formés sur la composition moléculaire du PH-WEOM sont la texture et les concentrations en C_{org}, comme mis en évidence par des indicateurs plus simples (ER et $SUVA_{254}$) dans le chapitre 4, ainsi que le pH des sols. Cette caractérisation moléculaire du PH-WEOC réalisée en intégrant la diversité des sols à l'échelle régionale a permis d'identifier six groupes d'échantillons aux signatures moléculaires clairement différenciées, notamment par la présence de composés azotés ou soufrés, par des différences de poids moléculaire, de ratio atomique (H/C et O/C) et d'abondance en structures aromatiques.

La précision des analyses, permettant de travailler en intégrant des milliers de formules moléculaires différentes, permet de fournir des informations exceptionnelles pour l'étude des effets des différents facteurs sur la composition moléculaire des matières organiques solubles. Ces effets pourraient être également étudiés individuellement au moyen de régression PLS (*partial least squares*) sur chaque variable (par exemple pH, $SUVA_{254}$ ou type de couvert végétal). La suite de ces recherches, actuellement en cours avec ce jeu de données, permettra de présenter les informations moléculaires directement corrélées à la variation du signal isotopique du C dans chacune des catégories de couvert végétal. L'objectif est de déterminer la (dis)similarité des molécules corrélées à la variation isotopique pour les différents types d'occupation du sol.

Deux perspectives excitantes peuvent être envisagées pour compléter les travaux présentés dans le chapitre 5. La première est de réaliser des mesures en résonance magnétique nucléaire (RMN), afin d'avoir des informations sur la structure des molécules qui composent

le PH-WEOC. Cependant, cela correspond à une charge de travail analytique et des temps d'acquisition des spectres RMN considérables. La deuxième perspective ne nécessiterait pas de mesures analytiques supplémentaires. Elle consisterait à confronter les données obtenues sur la composition moléculaire des 120 échantillons à des données sur la caractérisation des communautés microbiennes au niveau taxonomique, acquises par des techniques de pyroséquençage. Cette approche pourrait permettre d'identifier les liens entre les communautés microbiennes et la composition moléculaire du PH-WEOC à un niveau de résolution inégalable.

L'étude de la composition chimique des matières organiques dissoutes réalisée au cours de cette thèse, et les relations avec les différents paramètres biotiques et abiotiques du sol, ont été présentées et ces résultats contribuent aux connaissances sur les matières organiques solubles dans les sols et à leur implication dans le cycle biogéochimique du C.

Références bibliographiques

A

Akagi, J., Zsolnay, Á., & Bastida, F. 2007. Quantity and spectroscopic properties of soil dissolved organic matter (DOM) as a function of soil sample treatments: air-drying and pre-incubation. *Chemosphere* **69**, 1040–1046.

Amiotte-Suchet, P., Linglois, N., Lévêque, J., & Andreux, F. 2007. ^{13}C composition of dissolved organic carbon in upland forested catchments of the Morvan Mountains (France): Influence of coniferous and deciduous vegetation. *Journal of Hydrology* **335**, 354–363.

Amster, I.J. 1996. Fourier transform mass spectrometry. *Journal of Mass Spectrometry* **31**, 1325–1337.

Andersson, C.A., & Bro, R. 2000. The N-way Toolbox for MATLAB. *Chemometrics and Intelligent Laboratory Systems* **52**, 1–4.

Andreasson, F., Bergkvist, B., & Bååth, E. 2009. Bioavailability of DOC in leachates, soil matrix solutions and soil water extracts from beech forest floors. *Soil Biology & Biochemistry* **41**, 1652–1658.

Angers, D.A., Recous, S., & Aita, C. 1997. Fate of carbon and nitrogen in water-stable aggregates during decomposition of $^{13}C^{15}N$-labelled wheat straw in situ. *European Journal of Soil Science* **48**, 295–300.

Artz, R.R.E., Chapman, S.J., Jean Robertson, A.H., Potts, J.M., Laggoun-Défarge, F., Gogo, S., Comont, L., Disnar, J.-R., & Francez, A.-J. 2008. FTIR spectroscopy can be used as a screening tool for organic matter quality in regenerating cutover peatlands. *Soil Biology & Biochemistry* **40**, 515–527.

B

Balaria, A. 2011. Effects Of Calcium Addition On Structure And Bioavailability Of Soil Organic Matter. Doctoral dissertation, Syracuse University.

Baldock, J.A., & Nelson, P.N. 2000. Soil Organic Matter. p. 1–63. *In* Handbook of Soil Science. CRC Press. Boca Raton, USA.

Balesdent, J., Mariotti, A., & Guillet, B. 1987. Natural ^{13}C abundance as a tracer for studies of soil organic matter dynamics. *Soil Biology & Biochemistry* **19**, 25–30.

Barančíková, G., Senesi, N., & Brunetti, G. 1997. Chemical and spectroscopic characterization of humic acids isolated from different Slovak soil types. *Geoderma* **78**, 251–266.

Batjes, N.H. 1996. Total carbon and nitrogen in the soils of the world. *European Journal of Soil Science* **47**, 151–163.

Baumann, K., Dignac, M.-F., Rumpel, C., Bardoux, G., Sarr, A., Steffens, M., & Maron, P.-A. 2012. Soil microbial diversity affects soil organic matter decomposition in a silty grassland soil. *Biogeochemistry* **114**, 201–212.

Bell, T., Newman, J.A., Silverman, B.W., Turner, S.L., & Lilley, A.K. 2005. The contribution of species richness and composition to bacterial services. *Nature* **436**, 1157–1160.

Benner, R., Fogel, M.L., Sprague, E.K., & Hodson, R.E. 1987. Depletion of ^{13}C in lignin and its implication for stable carbon isotope studies. *Nature* **329**, 708–710.

Bowen, S.R., Gregorich, E.G., & Hopkins, D.W. 2009. Biochemical properties and biodegradation of dissolved organic matter from soils. *Biology and Fertility of Soils* **45**, 733–742.

Boyer, J.N., & Groffman, P.M. 1996. Bioavailability of water extractable organic carbon fractions in forest and agricultural soil profiles. *Soil Biology & Biochemistry* **28**, 783–790.

C

Camino-Serrano, M., Gielen, B., Luyssaert, S., Ciais, P., Vicca, S., Guenet, B., De Vos, B., Cools, N., Ahrens, B., Arain, M.A., Borken, W., Clarke, N., Clarkson, B., Cummins, T., Don, A., Graf Pannatier, E., Laudon, H., Moore, T., Nieminen, T.M., Nilsson, M.B., Peichl, M., Schwendenmann, L., Siemens, J., & Janssens, I.A. 2014. Linking variability in soil solution dissolved organic carbon to climate, soil type, and vegetation type. *Global Biogeochemical Cycles* **28**, 497–509.

Cammack, W.K.L., Kalff, J., Prairie, Y.T., & Smith, E.M. 2004. Fluorescent dissolved organic matter in lakes: Relationships with heterotrophic metabolism. *Limnology and Oceanography* **49**, 2034–2045.

Carney, K.M., & Matson, P.A. 2005. Plant communities, soil microorganisms, and soil carbon cycling: does altering the world belowground matter to ecosystem functioning? *Ecosystems* **8**, 928–940.

Chantigny, M.H. 2003. Dissolved and water-extractable organic matter in soils: a review on the influence of land use and management practices. *Geoderma* **113**, 357–380.

Chantigny, M.H., Harrison-kirk, T., Curtin, D., & Beare, M. 2014. Temperature and duration of extraction affect the biochemical composition of soil water-extractable organic matter. *Soil Biology & Biochemistry* **75**, 161–166.

Chemidlin Prévost-Bouré, N., Maron, P.-A., Ranjard, L., Nowak, V., Dufrêne, E., Damesin, C., Soudani, K., & Lata, J.-C. 2011. Seasonal dynamics of the bacterial community in forest soils under different quantities of leaf litter. *Applied Soil Ecology* **47**, 14–23.

Chemidlin Prévost-Bouré, N., Soudani, K., Damesin, C., Berveiller, D., Lata, J.-C., & Dufrêne, E. 2010. Increase in aboveground fresh litter quantity over-stimulates soil respiration in a temperate deciduous forest. *Applied Soil Ecology* **46**, 26–34.

Chen, H., Zhou, J., Huang, W., Yu, W., & Wan, Z. 2009. Biodegradability of dissolved organic matter derived from rice straw. *Soil Science* **174**, 143–150.

Chin, Y.-P., Aiken, G.R., & O'Loughlin, E. 1994. Molecular weight, polydispersity, and spectroscopic properties of aquatic humic substances. *Environmental Science & Technology* **28**, 1853–1858.

Chow, A.T., Tanji, K.K., Gao, S., & Dahlgren, R.A. 2006. Temperature, water content and wet–dry cycle effects on DOC production and carbon mineralization in agricultural peat soils. *Soil Biology & Biochemistry* **38**, 477–488.

Ciais, P., Sabine, C., Bala, G., Bopp, L., Brovkin, V., Canadell, J., Chhabra, A., DeFries, R., Galloway, J., Heimann, M., Jones, C., Le Quéré, C., Myneni, R.B., Piao, S., & Thornton, P. 2013. Carbon and Other Biogeochemical Cycles. *In* Climate Change 2013: The Physical Science Basis. Contribution of Working Group I to the Fifth Assessment Report of the Intergovernmental Panel on Climate Change. Cambridge University Press. Cambridge, United Kingdom and New York, NY, USA.

Coble, P.G. 1996. Characterization of marine and terrestrial DOM in seawater using excitation-emission matrix spectroscopy. *Marine Chemistry* **51**, 325–346.

Coble, P.G., Del Castillo, C.E., & Avril, B. 1998. Distribution and optical properties of CDOM in the Arabian Sea during the 1995 Southwest Monsoon. *Deep Sea Research Part II: Topical Studies in Oceanography* **45**, 2195–2223.

Cole, R.B. 2000. Some tenets pertaining to electrospray ionization mass spectrometry. *Journal of Mass Spectrometry* **35**, 763–772.

Corvasce, M., Zsolnay, Á., D'Orazio, V., Lopez, R., & Miano, T.M. 2006. Characterization of water extractable organic matter in a deep soil profile. *Chemosphere* **62**, 1583–1590.

Cory, R.M., & McKnight, D. 2005. Fluorescence spectroscopy reveals ubiquitous presence of oxidized and reduced quinones in dissolved organic matter. *Environmental Science & Technology* **39**, 8142–8149.

D

D'Andrilli, J., Chanton, J.P., Glaser, P.H., & Cooper, W.T. 2010. Characterization of dissolved organic matter in northern peatland soil porewaters by ultra high resolution mass spectrometry. *Organic Geochemistry* **41**, 791–799.

Dalenberg, J.W., & Jager, G. 1981. Priming effect of small glucose additions to 14C-labelled soil. *Soil Biology & Biochemistry* **13**, 219–223.

Dequiedt, S., Saby, N.P.A., Lelièvre, M., Jolivet, C., Thioulouse, J., Toutain, B., Arrouays, D., Bispo, A., Lemanceau, P., & Ranjard, L. 2011. Biogeographical patterns of soil molecular microbial biomass as influenced by soil characteristics and management. *Global Ecology and Biogeography* **20**, 641–652.

Dequiedt, S., Thioulouse, J., Jolivet, C., Saby, N.P.A., Lelièvre, M., Maron, P.-A., Martin, M.P., Chemidlin Prévost-Bouré, N., Toutain, B., Arrouays, D., Lemanceau, P., & Ranjard, L. 2009. Biogeographical patterns of soil bacterial communities. *Environmental Microbiology Reports* **1**, 251–255.

Derrien, D., Marol, C., Balabane, M., & Balesdent, J. 2006. The turnover of carbohydrate carbon in a cultivated soil estimated by ^{13}C natural abundances. *European Journal of Soil Science* **57**, 547–557.

Desjardins, T., Andreux, F., Volkoff, B., & Cerri, C.C. 1994. Organic carbon and ^{13}C contents in soils and soil size-fractions, and their changes due to deforestation and pasture installation in eastern Amazonia. *Geoderma* **61**, 103–118.

Diefendorf, A.F., Mueller, K.E., Wing, S.L., Koch, P.L., & Freeman, K.H. 2010. Global patterns in leaf ^{13}C discrimination and implications for studies of past and future climate. *Proceedings of the National Academy of Sciences of the United States of America* **107**, 5738–5743.

Dippold, M.A., & Kuzyakov, Y. 2013. Biogeochemical transformations of amino acids in soil assessed by position-specific labelling. *Plant and Soil* **373**, 385–401.

Dray, S., Chessel, D., & Thioulouse, J. 2003. Co-inertia Analysis and the Linking of Ecological Data Tables. *Ecology* **84**, 3078–3089.

Dray, S., Dufour, A.B., & Thioulouse, J. 2013. Analysis of Ecological Data : Exploratory and Euclidean methods in environmental sciences. CRAN version 1.6-2.

E F

Ellerbrock, R.H., & Kaiser, M. 2005. Stability and composition of different soluble soil organic matter fractions–evidence from $\delta^{13}C$ and FTIR signatures. *Geoderma* **128**, 28–37.

Embacher, A., Zsolnay, Á., Gattinger, A., & Munch, J.C. 2007. The dynamics of water extractable organic matter (WEOM) in common arable topsoils: I. Quantity, quality and function over a three year period. *Geoderma* **139**, 11–22.

Fellman, J.B., Miller, M.P., Cory, R.M., D'Amore, D. V, & White, D. 2009. Characterizing dissolved organic matter using PARAFAC modeling of fluorescence spectroscopy: a comparison of two models. *Environmental Science & Technology* **43**, 6228–6234.

Feng, W., Plante, A.F., & Six, J. 2011. Improving estimates of maximal organic carbon stabilization by fine soil particles. *Biogeochemistry* **112**, 81–93.

Fernandez, I., Mahieu, N., & Cadisch, G. 2003. Carbon isotopic fractionation during decomposition of plant materials of different quality. *Global Biogeochemical Cycles* **17**

Field, C.B., Lobell, D.B., Peters, H.A., & Chiariello, N.R. 2007. Feedbacks of Terrestrial Ecosystems to Climate Change. *Annual Review of Environment and Resources* **32**, 1–29.

Fierer, N., & Jackson, R.B. 2006. The diversity and biogeography of soil bacterial communities. *Proceedings of the National Academy of Sciences of the United States of America* **103**, 626–631.

Fitzgerald, J.W., Andrew, T.L., & Swank, W.T. 1984. Availability of carbon-bonded sulfur for mineralization in forest soils. *Canadian Journal of Forest Research* **14**, 839–843.

Flessa, H., Amelung, W., Helfrich, M., Wiesenberg, G.L.B., Gleixner, G., Brodowski, S., Rethemeyer, J., Kramer, C., & Grootes, P.M. 2008. Storage and stability of organic matter and fossil carbon in a Luvisol and Phaeozem with continuous maize cropping: A synthesis. *Journal of Plant Nutrition and Soil Science* **171**, 36–51.

Fontaine, S., Bardoux, G., Abbadie, L., & Mariotti, A. 2004. Carbon input to soil may decrease soil carbon content. *Ecology Letters* **7**, 314–320.

Fontaine, S., Mariotti, A., & Abbadie, L. 2003. The priming effect of organic matter: a question of microbial competition? *Soil Biology & Biochemistry* **35**, 837–843.

Fröberg, M., Berggren, D., Bergkvist, B., Bryant, C., & Knicker, H. 2003. Contributions of Oi, Oe and Oa horizons to dissolved organic matter in forest floor leachates. *Geoderma* **113**, 311–322.

G

Girvan, M.S., Bullimore, J., Pretty, J.N., Osborn, A.M., & Ball, A.S. 2003. Soil type is the primary determinant of the composition of the total and active bacterial communities in arable soils. *Applied and environmental microbiology* **69**, 1800–1809.

Girvan, M.S., Campbell, C.D., Killham, K., Prosser, J.I., & Glover, L.A. 2005. Bacterial diversity promotes community stability and functional resilience after perturbation. *Environmental Microbiology* **7**, 301–313.

Gleixner, G., Poirier, N., Bol, R., & Balesdent, J. 2002. Molecular dynamics of organic matter in a cultivated soil. *Organic Geochemistry* **33**, 357–366.

Gonsior, M., Zwartjes, M., Cooper, W.J., Song, W., Ishida, K.P., Tseng, L.Y., Jeung, M.K., Rosso, D., Hertkorn, N., & Schmitt-Kopplin, P. 2011. Molecular characterization of effluent organic matter identified by ultrahigh resolution mass spectrometry. *Water Research* **45**, 2943–2953.

Gregorich, E.G., Beare, M.H., Stoklas, U., & St-Georges, P. 2003. Biodegradability of soluble organic matter in maize-cropped soils. *Geoderma* **113**, 237–252.

Griffiths, B.S., Ritz, K., Wheatley, R., Kuan, H.L., Boag, B., Christensen, S., Ekelund, F., Sørensen, S.J., Muller, S., & Bloem, J. 2001. An examination of the biodiversity–ecosystem function relationship in arable soil microbial communities. *Soil Biology & Biochemistry* **33**, 1713–1722.

Grinhut, T., Hertkorn, N., Schmitt-Kopplin, P., Hadar, Y., & Chen, Y. 2011. Mechanisms of humic acids degradation by white rot fungi explored using ^{1}H NMR spectroscopy and FTICR mass spectrometry. *Environmental Science & Technology* **45**, 2748–2754.

Guenet, B., Juarez, S., Bardoux, G., Abbadie, L., & Chenu, C. 2012. Evidence that stable C is as vulnerable to priming effect as is more labile C in soil. *Soil Biology & Biochemistry* **52**, 43–48.

Guigue, J., Mathieu, O., Lévêque, J., Mounier, S., Laffont, R., Maron, P.-A., Navarro, N., Chateau-Smith, C., Amiotte-Suchet, P., & Lucas, Y. 2014. A comparison of extraction procedures for water-extractable organic matter in soils. *European Journal of Soil Science* **65**, 520–530.

Gunina, A., & Kuzyakov, Y. 2014. Pathways of litter C by formation of aggregates and SOM density fractions: Implications from ^{13}C natural abundance. *Soil Biology & Biochemistry* **71**, 95–104.

H

Hagedorn, F., Saurer, M., & Blaser, P. 2004. A ^{13}C tracer study to identify the origin of dissolved organic carbon in forested mineral soils. *European Journal of Soil Science* **55**, 91–100.

Hamer, U., & Marschner, B. 2005. Priming effects in different soil types induced by fructose, alanine, oxalic acid and catechol additions. *Soil Biology & Biochemistry* **37**, 445–454.

Heim, A., & Schmidt, M.W.I. 2007. Lignin turnover in arable soil and grassland analysed with two different labelling approaches. *European Journal of Soil Science* **58**, 599–608.

Hertkorn, N., Frommberger, M., Witt, M., Koch, B.P., Schmitt-Kopplin, P., & Perdue, E.M. 2008. Natural organic matter and the event horizon of mass spectrometry. *Analytical Chemistry* **80**, 8908–8919.

Hertkorn, N., Ruecker, C., Meringer, M., Gugisch, R., Frommberger, M., Perdue, E.M., Witt, M., & Schmitt-Kopplin, P. 2007. High-precision frequency measurements: indispensable tools at the core of the molecular-level analysis of complex systems. *Analytical and Bioanalytical Chemistry* **389**, 1311–27.

Högberg, P., Plamboeck, A.H., Taylor, A.F., & Fransson, P.M. 1999. Natural ^{13}C abundance reveals trophic status of fungi and host-origin of carbon in mycorrhizal fungi in mixed forests. *Proceedings of the National Academy of Sciences of the United States of America* **96**, 8534–8539.

Hopkins, F.M., Torn, M.S., & Trumbore, S.E. 2012. Warming accelerates decomposition of decades-old carbon in forest soils. *Proceedings of the National Academy of Sciences of the United States of America* **109**, 1753–1761.

Hotelling, H. 1933. Analysis of a complex of statistical variables into principal components. *Journal of Educational Psychology* **24**, 417–441.

Hudson, N., Baker, A., Ward, D., Reynolds, D.M., Brunsdon, C., Carliell-Marquet, C., & Browning, S. 2008. Can fluorescence spectrometry be used as a surrogate for the Biochemical Oxygen Demand (BOD) test in water quality assessment? An example from South West England. *Science of the Total Environment* **391**, 149–158.

I J

IUSS Working Group WRB. 2006. World Reference Base for Soil Resources 2006. World Soil Resources Report No 103, FAO, Rome.

Jenny, H. 1941. Factors of soil formation - A system of quantitative pedology. McGraw-Hill, New York.

Johnson, M.J., Lee, K.Y., & Scow, K.M. 2003. DNA fingerprinting reveals links among agricultural crops, soil properties, and the composition of soil microbial communities. *Geoderma* **114**, 279–303.

Jolivet, C., Arrouays, D., Lévêque, J., Andreux, F., & Chenu, C. 2003. Organic carbon dynamics in soil particle-size separates of sandy Spodosols when forest is cleared for maize cropping. *European Journal of Soil Science* **54**, 257–268.

Jolivet, C., Boulonne, L., & Ratié, C. 2006. Manuel du Réseau de Mesures de la Qualité des Sols. (Handbook of soil quality monitoring network). http://www.gissol.fr/programme/rmqs/RMQS_manuel_31032006.pdf (in French).

Jordan, G., Rompaey, A. Van, Szilassi, P., Csillag, G., Mannaerts, C., & Woldai, T. 2005. Historical land use changes and their impact on sediment fluxes in the Balaton basin (Hungary). *Agriculture, Ecosystems & Environment* **108**, 119–133.

Juarez, S., Nunan, N., Duday, A.-C., Pouteau, V., & Chenu, C. 2013. Soil carbon mineralisation responses to alterations of microbial diversity and soil structure. *Biology and Fertility of Soils* **49**, 939–948.

K

Kaiser, K., & Guggenberger, G. 2007. Sorptive stabilization of organic matter by microporous goethite: sorption into small pores vs. surface complexation. *European Journal of Soil Science* **58**, 45–59.

Kaiser, K., Guggenberger, G., & Zech, W. 2001. Isotopic fractionation of dissolved organic carbon in shallow forest soils as affected by sorption. *European Journal of Soil Science* **52**, 585–597.

Kaiser, K., & Kalbitz, K. 2012. Cycling downwards – dissolved organic matter in soils. *Soil Biology & Biochemistry* **52**, 29–32.

Kalbitz, K., Geyer, S., & Gehre, M. 2000a. Land use impacts on the isotopic signature (^{13}C, ^{14}C, ^{15}N) of water-soluble fulvic acids in a German fen area. *Soil Science* **165**, 728–736.

Kalbitz, K., & Kaiser, K. 2008. Contribution of dissolved organic matter to carbon storage in forest mineral soils. *Journal of Plant Nutrition and Soil Science* **171**, 52–60.

Kalbitz, K., Schmerwitz, J., Schwesig, D., & Matzner, E. 2003. Biodegradation of soil-derived dissolved organic matter as related to its properties. *Geoderma* **113**, 273–291.

Kalbitz, K., Schwesig, D., Rethemeyer, J., & Matzner, E. 2005. Stabilization of dissolved organic matter by sorption to the mineral soil. *Soil Biology & Biochemistry* **37**, 1319–1331.

Kalbitz, K., Solinger, S., Park, J.H.., Michalzik, B., & Matzner, E. 2000b. Controls on the dynamics of dissolved organic matter in soils: a review. *Soil Science* **165**, 277–304.

Kanawati, B., Wanczek, K.P., Gebefügi, I., & Schmitt-Kopplin, P. 2012. Prefocusing inside a linear ion beam guide—A SIMION study. *International Journal of Mass Spectrometry* **325-327**, 25–29.

Kendrick, E. 1963. A mass scale based on CH_2 = 14.00000 for high resolution mass spectrometry of organic compounds. *Analytical Chemistry* **35**, 2146–2154.

Kiem, R., & Kögel-Knabner, I. 2003. Contribution of lignin and polysaccharides to the refractory carbon pool in C-depleted arable soils. *Soil Biology & Biochemistry* **35**, 101–118.

Kiikkilä, O., Kitunen, V., & Smolander, A. 2005. Degradability of dissolved soil organic carbon and nitrogen in relation to tree species. *FEMS microbiology ecology* **53**, 33–40.

Kiikkilä, O., Kitunen, V., & Smolander, A. 2006. Dissolved soil organic matter from surface organic horizons under birch and conifers: Degradation in relation to chemical characteristics. *Soil Biology & Biochemistry* **38**, 737–746.

Kim, S., Kramer, R.W., & Hatcher, P.G. 2003a. Graphical method for analysis of ultrahigh-resolution broadband mass spectra of natural organic matter, the van Krevelen diagram. *Analytical Chemistry* **75**, 5336–5344.

Kim, S., Simpson, A.J., Kujawinski, E.B., Freitas, M.A., & Hatcher, P.G. 2003b. High resolution electrospray ionization mass spectrometry and 2D solution NMR for the analysis of DOM extracted by C18 solid phase disk. *Organic Geochemistry* **34**, 1325–1335.

Kindler, R., Siemens, J., Kaiser, K., Walmsley, D.C., Bernhofer, C., Buchmann, N., Cellier, P., Eugster, W., Gleixner, G., Grũnwald, T., Heim, A., Ibrom, A., Jones, S.K., Jones, M., Klumpp, K., Kutsch, W., Larsen, K.S., Lehuger, S., Loubet, B., Mckenzie, R., Moors, E., Osborne, B., Pilegaard, K., Rebmann, C., Saunders, M., Schmidt, M.W.I., Schrumpf, M., Seyfferth, J., Skiba, U., Soussana, J.-F., Sutton, M.A., Tefs, C., Vowinckel, B., Zeeman, M.J., & Kaupenjohann, M. 2011. Dissolved carbon leaching from soil is a crucial component of the net ecosystem carbon balance. *Global Change Biology* **17**, 1167–1185.

Kleber, M. 2010. What is recalcitrant soil organic matter? *Environmental Chemistry* **7**, 320–332.

Knicker, H., Hatcher, P.G., & González-Vila, F.J. 2002. Formation of heteroaromatic nitrogen after prolonged humification of vascular plant remains as revealed by nuclear magnetic resonance spectroscopy. *Journal of environmental quality* **31**, 444–449.

Koch, B.P., & Dittmar, T. 2006. From mass to structure: an aromaticity index for high-resolution mass data of natural organic matter. *Rapid Communications in Mass Spectrometry* **20**, 926–932.

Kögel-Knabner, I. 1997. ^{13}C and ^{15}N NMR spectroscopy as a tool in soil organic matter studies. *Geoderma* **80**, 243–270.

Kögel-Knabner, I. 2002. The macromolecular organic composition of plant and microbial residues as inputs to soil organic matter. *Soil Biology & Biochemistry* **34**, 139–162.

Kögel-Knabner, I., Guggenberger, G., Kleber, M., Kandeler, E., Kalbitz, K., Scheu, S., Eusterhues, K., & Leinweber, P. 2008. Organo-mineral associations in temperate soils: Integrating biology, mineralogy, and organic matter chemistry. *Journal of Plant Nutrition and Soil Science* **171**, 61–82.

Kohn, M.J. 2010. Carbon isotope compositions of terrestrial C3 plants as indicators of (paleo)ecology and (paleo)climate. *Proceedings of the National Academy of Sciences of the United States of America* **107**, 19691–19695.

Kracht, O., & Gleixner, G. 2000. Isotope analysis of pyrolysis products from Sphagnum peat and dissolved organic matter from bog water. *Organic Geochemistry* **31**, 645–654.

Kramer, C., & Gleixner, G. 2006. Variable use of plant- and soil-derived carbon by microorganisms in agricultural soils. *Soil Biology & Biochemistry* **38**, 3267–3278.

van Krevelen, D.W. 1950. Graphical-statistical method for the study of structure and reaction processes of coal. *Fuel* **29**, 269–284.

Kujawinski, E.B., Freitas, M.A., Zang, X., Hatcher, P.G., Green-Church, K.B., & Jones, R.B. 2002. The application of electrospray ionization mass spectrometry (ESI MS) to the structural characterization of natural organic matter. *Organic Geochemistry* **33**, 171–180.

Kujawinski, E.B., Longnecker, K., Blough, N. V., Vecchio, R. Del, Finlay, L., Kitner, J.B., & Giovannoni, S.J. 2009. Identification of possible source markers in marine dissolved organic matter using ultrahigh resolution mass spectrometry. *Geochimica et Cosmochimica Acta* **73**, 4384–4399.

Kunenkov, E. V, Kononikhin, A.S., Perminova, I. V, Hertkorn, N., Gaspar, A., Schmitt-Kopplin, P., Popov, I. A., Garmash, A. V, & Nikolaev, E.N. 2009a. Total mass difference statistics algorithm: a new approach to identification of high-mass building blocks in electrospray ionization Fourier transform ion cyclotron mass spectrometry data of natural organic matter. *Analytical Chemistry* **81**, 10106–10115.

Kunenkov, E. V, Lock, R., Desor, M., Perminova, I., & Schmitt-kopplin, P. 2009b. Combined utilization of ion mobility and ultra-high-resolution mass spectrometry to identify multiply charged constituents in natural organic matter. *Rapid Communications in Mass Spectrometry* **23**, 683–688.

L

Landgraf, D., Leinweber, P., & Makeschin, F. 2006. Cold and hot water–extractable organic matter as indicators of litter decomposition in forest soils. *Journal of Plant Nutrition and Soil Science* **169**, 76–82.

Lauber, C.L., Hamady, M., Knight, R., & Fierer, N. 2009. Pyrosequencing-based assessment of soil pH as a predictor of soil bacterial community structure at the continental scale. *Applied and Environmental Microbiology* **75**, 5111–5120.

Lauber, C.L., Strickland, M.S., Bradford, M.A., & Fierer, N. 2008. The influence of soil properties on the structure of bacterial and fungal communities across land-use types. *Soil Biology & Biochemistry* **40**, 2407–2415.

Lechtenfeld, O.J., Kattner, G., Flerus, R., McCallister, S.L., Schmitt-Kopplin, P., & Koch, B.P. 2014. Molecular transformation and degradation of refractory dissolved organic matter in the Atlantic and Southern Ocean. *Geochimica et Cosmochimica Acta* **126**, 321–337.

Lejon, D.P.H., Chaussod, R., Ranger, J., & Ranjard, L. 2005. Microbial community structure and density under different tree species in an acid forest soil (Morvan, France). *Microbial Ecology* **50**, 614–25.

Lejon, D.P.H., Sebastia, J., Lamy, I., Chaussod, R., & Ranjard, L. 2007. Relationships between soil organic status and microbial community density and genetic structure in two agricultural soils submitted to various types of organic management. *Microbial Ecology* **53**, 650–663.

Lerch, T.Z., Nunan, N., Dignac, M.-F., Chenu, C., & Mariotti, A. 2010. Variations in microbial isotopic fractionation during soil organic matter decomposition. *Biogeochemistry* **106**, 5–21.

Li, L., Wang, D., Liu, X., Zhang, B., Liu, Y., Xie, T., Du, Y., & Pan, G. 2014. Soil organic carbon fractions and microbial community and functions under changes in vegetation: a case of vegetation succession in karst forest. *Environmental Earth Sciences* **71**, 3727–3735.

Löhnis, F. 1926. Nitrogen availability of green manures. *Soil Science* **22**, 253–290.

Luciani, X., Mounier, S., Paraquetti, H.H.M., Redon, R., Lucas, Y., Bois, A., Lacerda, L.D., Raynaud, M., & Ripert, M. 2008. Tracing of dissolved organic matter from the Sepetiba Bay (Brazil) by PARAFAC analysis of total luminescence matrices. *Marine Environmental Research* **65**, 148–157.

Luciani, X., Mounier, S., Redon, R., & Bois, A. 2009. A simple correction method of inner filter effects affecting FEEM and its application to the PARAFAC decomposition. *Chemometrics and Intelligent Laboratory Systems* **96**, 227–238.

Lutzow, M. V., Kögel-Knabner, I., Ekschmitt, K., Matzner, E., Guggenberger, G., Marschner, B., & Flessa, H. 2006. Stabilization of organic matter in temperate soils: mechanisms and their relevance under different soil conditions - a review. *European Journal of Soil Science* **57**, 426–445.

M

Malik, A., & Gleixner, G. 2013. Importance of microbial soil organic matter processing in dissolved organic carbon production. *FEMS Microbiology Ecology* **86**, 139–148.

Marhan, S., Kandeler, E., & Scheu, S. 2007. Phospholipid fatty acid profiles and xylanase activity in particle size fractions of forest soil and casts of Lumbricus terrestris L. (Oligochaeta, Lumbricidae). *Applied Soil Ecology* **35**, 412–422.

Maron, P.-A., Richaume, A., Potier, P., Lata, J.-C., & Lensi, R. 2004. Immunological method for direct assessment of the functionality of a denitrifying strain of Pseudomonas fluorescens in soil. *Journal of Microbiological Methods* **58**, 13–21.

Marschner, B., Brodowski, S., Dreves, A., Gleixner, G., Gude, A., Grootes, P.M., Hamer, U., Heim, A., Jandl, G., Ji, R., Kaiser, K., Kalbitz, K., Kramer, C., Leinweber, P., Rethemeyer, J., Schäffer, A., Schmidt, M.W.I., Schwark, L., & Wiesenberg, G.L.B. 2008. How relevant is recalcitrance for the stabilization of organic matter in soils? *Journal of Plant Nutrition and Soil Science* **171**, 91–110.

Marschner, B., & Kalbitz, K. 2003. Controls of bioavailability and biodegradability of dissolved organic matter in soils. *Geoderma* **113**, 211–235.

Marshall, A.G., Hendrickson, C.L., & Jackson, G.S. 1998. Fourier transform ion cyclotron resonance mass spectrometry: a primer. *Mass spectrometry reviews* **17**, 1–35.

Martin, M.P., Wattenbach, M., Smith, P., Meersmans, J., Jolivet, C., Boulonne, L., & Arrouays, D. 2011. Spatial distribution of soil organic carbon stocks in France. *Biogeosciences* **8**, 1053–1065.

McBratney, A.B., Mendonça Santos, M.L., & Minasny, B. 2003. On digital soil mapping. *Geoderma* **117**, 3–52.

McDowell, W.H., Zsolnay, Á., Aitkenhead-Peterson, J.A., Gregorich, E.G., Jones, D.L., Jödemann, D., Kalbitz, K., Marschner, B., & Schwesig, D. 2006. A comparison of methods to determine the biodegradable dissolved organic carbon from different terrestrial sources. *Soil Biology & Biochemistry* **38**, 1933–1942.

Mikutta, R., Mikutta, C., Kalbitz, K., Scheel, T., Kaiser, K., & Jahn, R. 2007. Biodegradation of forest floor organic matter bound to minerals via different binding mechanisms. *Geochimica et Cosmochimica Acta* **71**, 2569–2590.

Morvan, X., Saby, N.P.A., Arrouays, D., Le Bas, C., Jones, R.J.A., Verheijen, F.G.A., Bellamy, P.H., Stephens, M., & Kibblewhite, M.G. 2008. Soil monitoring in Europe: a review of existing systems and requirements for harmonisation. *Science of the Total Environment* **391**, 1–12.

Mosher, J.J., Klein, G.C., Marshall, A.G., & Findlay, R.H. 2010. Influence of bedrock geology on dissolved organic matter quality in stream water. *Organic Geochemistry* **41**, 1177–1188.

Müller, M., Alewell, C., & Hagedorn, F. 2009. Effective retention of litter-derived dissolved organic carbon in organic layers. *Soil Biology & Biochemistry* **41**, 1066–1074.

Murty, D., Kirschbaum, M.U.F., Mcmurtrie, R.E., & Mcgilvray, H. 2002. Does conversion of forest to agricultural land change soil carbon and nitrogen? a review of the literature. *Global Change Biology* **8**, 105–123.

N O

Nannipieri, P., Ascher, J., Ceccherini, M.T., Landi, L., Pietramellara, G., & Renella, G. 2003. Microbial diversity and soil functions. *European Journal of Soil Science* **54**, 655–670.

Nebbioso, A., Piccolo, A., Spiteller, M., Ii, F., & Animali, P. 2010. Limitations of electrospray ionization in the analysis of a heterogeneous mixture of naturally occurring hydrophilic and hydrophobic compounds. *Rapid Communications in Mass Spectrometry* **24**, 3163–3170.

Nkhili, E., Guyot, G., Vassal, N., & Richard, C. 2012. Extractability of water-soluble soil organic matter as monitored by spectroscopic and chromatographic analyses. *Environmental Science and Pollution Research International* **19**, 2400–2407.

Ohno, T., He, Z., Sleighter, R.L., Honeycutt, C.W., & Hatcher, P.G. 2010. Ultrahigh resolution mass spectrometry and indicator species analysis to identify marker components of soil- and plant biomass-derived organic matter fractions. *Environmental Science & Technology* **44**, 8594–8600.

Ohno, T., Parr, T.B., Gruselle, M.-C.I., Fernandez, I.J., Sleighter, R.L., & Hatcher, P.G. 2014. Molecular composition and biodegradability of soil organic matter: a case study comparing two new england forest types. *Environmental Science & Technology* **48**, 7229–7236.

P Q

Pascault, N., Ranjard, L., Kaisermann, A., Bachar, D., Christen, R., Terrat, S., Mathieu, O., Lévêque, J., Mougel, C., Henault, C., Lemanceau, P., Péan, M., Boiry, S., Fontaine, S., & Maron, P.-A. 2013. Stimulation of different functional groups of bacteria by various plant residues as a driver of soil priming effect. *Ecosystems* **16**, 810–822.

Paterson, E., Osler, G., Dawson, L.A., Gebbing, T., Sim, A., & Ord, B. 2008. Labile and recalcitrant plant fractions are utilised by distinct microbial communities in soil: Independent of the presence of roots and mycorrhizal fungi. *Soil Biology & Biochemistry* **40**, 1103–1113.

Perdrial, J.N., Perdrial, N., Harpold, A., Gao, X., Gabor, R., LaSharr, K., & Chorover, J. 2012. Impacts of Sampling Dissolved Organic Matter with Passive Capillary Wicks Versus Aqueous Soil Extraction. *Soil Science Society of America Journal* **76**, 2019–2030.

Perminova, I., Dubinenkov, I., Kononikhin, A., Konstantinov, A., Zherebker, A., Andzhushev, M., Lebedev, V., Bulygina, E., Holmes, R.M., Kostyukevich, Y., Popov, I., & Nikolaev, E. 2014. Molecular mapping of sorbent selectivities with respect to isolation of arctic dissolved organic matter as measured by fourier transform mass spectrometry. *Environmental Science & Technology* **48**, 7461–7468.

Peuravuori, J., Monteiro, A., Eglite, L., & Pihlaja, K. 2005. Comparative study for separation of aquatic humic-type organic constituents by DAX-8, PVP and DEAE sorbing solids and tangential ultrafiltration: elemental composition, size-exclusion chromatography, UV-vis and FT-IR. *Talanta* **65**, 408–422.

Piccolo, A. 2001. The supramolecular structure of humic substances. *Soil Science* **166**, 810–832.

Plante, A.F., Conant, R.T., Carlson, J., Greenwood, R., Shulman, J.M., Haddix, M.L., & Paul, E.A. 2010. Decomposition temperature sensitivity of isolated soil organic matter fractions. *Soil Biology & Biochemistry* **42**, 1991–1996.

Plassart, P., Akpa Vinceslas, M., Gangneux, C., Mercier, A., Barray, S., & Laval, K. 2008. Molecular and functional responses of soil microbial communities under grassland restoration. *Agriculture, Ecosystems & Environment* **127**, 286–293.

Qualls, R.G. 2005. Biodegradability of fractions of dissolved organic carbon leached from decomposing leaf litter. *Environmental Science & Technology* **39**, 1616–1622.

R

R Core Team. 2012. R: A Language and Environment for Statistical Computing. *Foundation for Statistical Computing, Vienna, Austria*.

Raich, J.W., & Tufekcioglu, A. 2000. Vegetation and soil respiration : Correlations and controls. *Biogeochemistry* **48**, 71–90.

Ranjard, L., Dequiedt, S., Chemidlin Prévost-Bouré, N., Thioulouse, J., Saby, N.P.A., Lelievre, M., Maron, P.-A., Morin, F.E.R., Bispo, A., Jolivet, C., Arrouays, D., & Lemanceau, P. 2013. Turnover of soil bacterial diversity driven by wide-scale environmental heterogeneity. *Nature communications* **4**, 1434.

Ranjard, L., Dequiedt, S., Jolivet, C., Saby, N.P.A., Thioulouse, J., Harmand, J., Loisel, P., Rapaport, A., Fall, S., Simonet, P., Joffre, R., Chemidlin Prévost-Bouré, N., Maron, P.-A., Mougel, C., Martin, M.P., Toutain, B., Arrouays, D., & Lemanceau, P. 2010. Biogeography of soil microbial communities: a review and a description of the ongoing french national initiative. *Agronomy for Sustainable Development* **30**, 359–365.

Ranjard, L., Lejon, D.P.H., Mougel, C., Schehrer, L., Merdinoglu, D., & Chaussod, R. 2003. Sampling strategy in molecular microbial ecology: influence of soil sample size on DNA fingerprinting analysis of fungal and bacterial communities. *Environmental Microbiology* **5**, 1111–1120.

Ranjard, L., Poly, F., Lata, J.-C., Mougel, C., Thioulouse, J., & Nazaret, S. 2001. Characterization of bacterial and fungal soil communities by automated ribosomal intergenic spacer analysis fingerprints : biological and methodological variability. *Applied and Environmental Microbiology* **67**, 4479–4487.

Reemtsma, T., & These, A. 2003. On-line coupling of size exclusion chromatography with electrospray ionization-tandem mass spectrometry for the analysis of aquatic fulvic and humic acids. *Analytical Chemistry* **75**, 1500–1507.

Rennert, T., Gockel, K.F., & Mansfeldt, T. 2007. Extraction of water-soluble organic matter from mineral horizons of forest soils. *Journal of Plant Nutrition and Soil Science* **170**, 514–521.

Rosenfeld, C.E., Mccormack, M.L., & Martínez, C.E. 2014. A novel approach to study composition of in situ produced root-derived dissolved organic matter. *Soil Biology & Biochemistry* **76**, 1–4.

Roth, V.-N., Dittmar, T., Gaupp, R., & Gleixner, G. 2013. Latitude and pH driven trends in the molecular composition of DOM across a north south transect along the Yenisei River. *Geochimica et Cosmochimica Acta* **123**, 93–105.

Roth, V.-N., Dittmar, T., Gaupp, R., & Gleixner, G. 2014. Ecosystem-Specific Composition of Dissolved Organic Matter. *Vadose Zone Journal* **13**, 1–10.

Rousk, J., & Jones, D.L. 2010. Loss of low molecular weight dissolved organic carbon (DOC) and nitrogen (DON) in H2O and 0.5M K_2SO_4 soil extracts. *Soil Biology & Biochemistry* **42**, 2331–2335.

Ruamps, L.S., Nunan, N., & Chenu, C. 2011. Microbial biogeography at the soil pore scale. *Soil Biology & Biochemistry* **43**, 280–286.

S

Saby, N.P.A., Thioulouse, J., Jolivet, C., Ratié, C., Boulonne, L., Bispo, A., & Arrouays, D. 2009. Multivariate analysis of the spatial patterns of 8 trace elements using the French soil monitoring network data. *Science of the Total Environment* **407**, 5644–5652.

Sainju, U.M., Whitehead, W.F., & Singh, B.P. 2005. Carbon accumulation in cotton, sorghum, and underlying soil as influenced by tillage, cover crops, and nitrogen fertilization. *Plant and Soil* **273**, 219–234.

Sanderman, J., & Amundson, R. 2008. A comparative study of dissolved organic carbon transport and stabilization in California forest and grassland soils. *Biogeochemistry* **92**, 41–59.

Scharlemann, J.P., Tanner, E.V., Hiederer, R., & Kapos, V. 2014. Global soil carbon: understanding and managing the largest terrestrial carbon pool. *Carbon Management* **5**, 81–91.

Schmidt, M.W.I., Torn, M.S., Abiven, S., Dittmar, T., Guggenberger, G., Janssens, I.A., Kleber, M., Kögel-Knabner, I., Lehmann, J., Manning, D.A.C., Nannipieri, P., Rasse, D.P., Weiner, S., & Trumbore, S.E. 2011. Persistence of soil organic matter as an ecosystem property. *Nature* **478**, 49–56.

Schmitt, A., Pausch, J., & Kuzyakov, Y. 2012. C and N allocation in soil under ryegrass and alfalfa estimated by ^{13}C and ^{15}N labelling. *Plant and Soil* **368**, 581–590.

Schmitt-Kopplin, P., Gabelica, Z., Gougeon, R.D., Fekete, A., Kanawati, B., Harir, M., Gebefuegi, I., Eckel, G., & Hertkorn, N. 2010a. High molecular diversity of extraterrestrial organic matter in Murchison meteorite revealed 40 years after its fall. *Proceedings of the National Academy of Sciences of the United States of America* **107**, 2763–2768.

Schmitt-Kopplin, P., Gelencsér, A., Dabek-Zlotorzynska, E., Kiss, G., Hertkorn, N., Harir, M., Hong, Y., & Gebefügi, I. 2010b. Analysis of the unresolved organic fraction in atmospheric aerosols with ultrahigh-resolution mass spectrometry and nuclear magnetic resonance spectroscopy: organosulfates as photochemical smog constituents. *Analytical Chemistry* **82**, 8017–8026.

Schmitt-Kopplin, P., Harir, M., Tziotis, D., Gabelica, Z., & Hertkorn, N. 2012. Ultrahigh resolution Fourier Transform ion cyclotron resonance mass spectrometry for the analysis of natural organic matter from various environmental systems. p. 443–459. *In* Comprehensive environmental mass spectrometry.

Schneider, M.P.W., Scheel, T., Miku, van Hees, P., Kaiser, K., & Kalbitz, K. 2010. Sorptive stabilization of organic matter by amorphous Al hydroxide. *Geochimica et Cosmochimica Acta* **74**, 1606–1619.

Schwesig, D., Göttlein, A., Haumaier, L., Blasek, R., & Ilgen, G. 1999. Soil organic matter extraction using water at high temperature and elevated pressure (ASE) as compared to conventional methods. *International Journal of Environmental Analytical Chemistry* **73**, 253–268.

Simpson, A.J., Kingery, W.L., Hayes, M.H., Spraul, M., Humpfer, E., Dvortsak, P., Kerssebaum, R., Godejohann, M., & Hofmann, M. 2002. Molecular structures and associations of humic substances in the terrestrial environment. *Naturwissenschaften* **89**, 84–88.

Sleighter, R.L., Liu, Z., Xue, J., & Hatcher, P.G. 2010. Multivariate statistical approaches for the characterization of dissolved organic matter analyzed by ultrahigh resolution mass spectrometry. *Environmental Science & Technology* **44**, 7576–7582.

Smith, C.R., Sleighter, R.L., Hatcher, P.G., & Lee, J.W. 2013. Molecular characterization of inhibiting biochar water-extractable substances using electrospray ionization Fourier transform ion cyclotron resonance mass spectrometry. *Environmental Science & Technology* **47**, 13294–13302.

Sollins, P., Homann, P., & Caldwell, B.A. 1996. Stabilization and destabilization of soil organic matter: mechanisms and controls. *Geoderma* **74**, 65–105.

Sparks, P., & Ehleringer, R. 1997. Leaf carbon isotope discrimination and nitrogen content for riparian trees along elevational transects. *Oecologia* **109**, 362–367.

Sparling, G., Vojvodic, M., & Schipper, L.A. 1998. Hot-water-soluble C as a simple measure of labile soil organic matter: the relationship with microbial biomass C. *Soil Biology & Biochemistry* **30**, 1469–1472.

Stedmon, C.A., & Bro, R. 2008. Characterizing dissolved organic matter fluorescence with parallel factor analysis : a tutorial. *Limnology and Oceanography: Methods* **6**, 572–579.

Stedmon, C.A., & Markager, S. 2005. Resolving the variability of dissolved organic matter fluorescence in a temperate estuary and its catchment using PARAFAC analysis. *Limnology and Oceanography* **50**, 686–697.

Strickland, T.C., & Fitzgerald, J.W. 1984. Formation and mineralization of organic sulfur in forest soils. *Biogeochemistry* **95**, 79–95.

Sutton, R., & Sposito, G. 2005. Molecular structure in soil humic substances : the new view. *Environmental Science & Technology* **39**, 9009–9015.

T U V

Toomet, O., & Henningsen, M.A. 2012. maxLik: Maximum Likelihood Estimation. *R package version 1.1-2*.

Treat, C.C., & Frolking, S. 2013. Carbon Storage: A permafrost carbon bomb? *Nature Climate Change* **3**, 865–867.

Tremblay, L.B. 2006. The ultrahigh resolution mass spectrometry of natural organic matter from different sources. Doctoral dissertation, Florida State University

de Troyer, I., Amery, F., van Moorleghem, C., Smolders, E., & Merckx, R. 2011. Tracing the source and fate of dissolved organic matter in soil after incorporation of a ^{13}C labelled residue: A batch incubation study. *Soil Biology & Biochemistry* **43**, 513–519.

Tseng, L.Y., Gonsior, M., Schmitt-Kopplin, P., Cooper, W.J., Pitt, P., & Rosso, D. 2013. Molecular characteristics and differences of effluent organic matter from parallel activated sludge and integrated fixed-film activated sludge (IFAS) processes. *Environmental Science & Technology* **47**, 10277–10284.

Uselman, S.M., Qualls, R.G., & Lilienfein, J. 2012. Quality of soluble organic C , N , and P produced by different types and species of litter : Root litter versus leaf litter. *Soil Biology & Biochemistry* **54**, 57–67.

Vogel, C., Mueller, C.W., Höschen, C., Buegger, F., Heister, K., Schulz, S., Schloter, M., & Kögel-Knabner, I. 2014. Submicron structures provide preferential spots for carbon and nitrogen sequestration in soils. *Nature communications* **5**, 2947.

W

Wagai, R., & Sollins, P. 2002. Biodegradation and regeneration of water-soluble carbon in a forest soil: leaching column study. *Biology and Fertility of Soils* **35**, 18–26.

Waldrop, M.P., & Firestone, M.K. 2004. Microbial community utilization of recalcitrant and simple carbon compounds: impact of oak-woodland plant communities. *Oecologia* **138**, 275–284.

Weishaar, J.L., Aiken, G.R., Bergamaschi, B.A., Fram, M.S., Fujii, R., & Mopper, K. 2003. Evaluation of specific ultraviolet absorbance as an indicator of the chemical composition and reactivity of dissolved organic carbon. *Environmental Science & Technology* **37**, 4702–4708.

Werth, M., & Kuzyakov, Y. 2010. ^{13}C fractionation at the root–microorganisms–soil interface: A review and outlook for partitioning studies. *Soil Biology & Biochemistry* **42**, 1372–1384.

Wertz, S., Degrange, V., Prosser, J.I., Poly, F., Commeaux, C., Freitag, T., Guillaumaud, N., & Roux, X. Le. 2006. Maintenance of soil functioning following erosion of microbial diversity. *Environmental Microbiology* **8**, 2162–2169.

Wertz, S., Degrange, V., Prosser, J.I., Poly, F., Commeaux, C., Guillaumaud, N., & Le Roux, X. 2007. Decline of soil microbial diversity does not influence the resistance and resilience of key soil microbial functional groups following a model disturbance. *Environmental Microbiology* **9**, 2211–2219.

van Wesemael, B., Paustian, K., Andrén, O., Cerri, C.E.P., Dodd, M., Etchevers, J., Goidts, E., Grace, P., Kätterer, T., McConkey, B.G., Ogle, S., Pan, G., & Siebner, C. 2011. How can soil monitoring networks be used to improve predictions of organic carbon pool dynamics and CO_2 fluxes in agricultural soils? *Plant and Soil* **338**, 247–259.

Wiesmeier, M., Hübner, R., Barthold, F., Spörlein, P., Geuß, U., Hangen, E., Reischl, A., Schilling, B., von Lützow, M., & Kögel-Knabner, I. 2013. Amount, distribution and driving factors of soil organic carbon and nitrogen in cropland and grassland soils of southeast Germany (Bavaria). *Agriculture, Ecosystems & Environment* **176**, 39–52.

Williams, M.A., Myrold, D.D., & Bottomley, P.J. 2006. Carbon flow from ^{13}C-labeled straw and root residues into the phospholipid fatty acids of a soil microbial community under field conditions. *Soil Biology & Biochemistry* **38**, 759–768.

Wu, Z., Rodgers, R.P., & Marshall, A.G. 2004. Two- and three-dimensional van Krevelen diagrams: a graphical analysis complementary to the Kendrick mass plot for sorting elemental compositions of complex organic mixtures based on ultrahigh-resolution broadband Fourier transform ion cyclotron resonance. *Analytical Chemistry* **76**, 2511–2516.

Y Z

Yassine, M.M., Harir, M., Dabek-Zlotorzynska, E., & Schmitt-Kopplin, P. 2014. Structural characterization of organic aerosol using Fourier transform ion cyclotron resonance mass spectrometry : Double bond index approach. *Analytical Chemistry. accepted for publication*

Yevdokimov, I., Ruser, R., Buegger, F., Marx, M., & Munch, J.C. 2006. Microbial immobilisation of ^{13}C rhizodeposits in rhizosphere and root-free soil under continuous ^{13}C labelling of oats. *Soil Biology & Biochemistry* **38**, 1202–1211.

Zaccone, C., D'Orazio, V., Shotyk, W., & Miano, T.M. 2009. Chemical and spectroscopic investigation of porewater and aqueous extracts of corresponding peat samples throughout a bog core (Jura Mountains, Switzerland). *Journal of Soils and Sediments* **9**, 443–456.

Zech, W., Senesi, N., Guggenberger, G., Kaiser, K., Lehmann, J., Miano, T.M., Miltner, A., & Schroth, G. 1997. Factors controlling humification and mineralization of soil organic matter in the tropics. *Geoderma* **79**, 117–161.

Zhao, Z., Chow, T.L., Rees, H.W., Yang, Q., Xing, Z., & Meng, F.-R. 2009. Predict soil texture distributions using an artificial neural network model. *Computers and Electronics in Agriculture* **65**, 36–48.

Zhao, M., Zhou, J., & Kalbitz, K. 2008. Carbon mineralization and properties of water-extractable organic carbon in soils of the south Loess Plateau in China. *European Journal of Soil Biology* **44**, 158–165.

Liste des Figures

Chapitre 2

Chapitre 3

Chapitre 4

Chapitre 5

Liste des Tables

Chapitre 2

Chapitre 4

Chapitre 5

Influence des facteurs biotiques et abiotiques sur la dynamique de la matière organique du sol à partir de la caractérisation biogéochimique des matières organiques solubles

Les sols sont le plus grand réservoir de carbone des écosystèmes terrestres, et la minéralisation des matières organiques par l'activité microbienne représente la majeure partie des flux de CO_2 émis à la surface des continents.

Dans ce travail, nous avons étudié les matières organiques extraites à l'eau (WEOM), qui correspondent à la fraction la plus réactive des matières organiques du sol (MOS). Nos objectifs étaient (i) d'identifier les liens de la dynamique du WEOM avec les communautés bactériennes, et avec les paramètres physico-chimiques du sol ; (ii) de réaliser une caractérisation chimique précise du WEOM.

Il existe un lien fort entre la solubilité des MOS et les structures des communautés bactériennes, et une baisse de leur diversité impacte la dynamique des MOS et du WEOM, et provoque une baisse de la minéralisation des matières organiques. Une étude à l'échelle régionale a également permis d'identifier que les taux de MOS et d'argile contrôlent les quantités de WEOM et leur aromaticité. La caractérisation au niveau moléculaire a montré la présence d'un grand nombre de molécules ubiquistes dans le WEOM. À partir de ces analyses, nous avons également pu décrire les effets du couvert végétal et des propriétés physico-chimiques des sols sur la composition chimique du WEOM.

Mots clés : biogéochimie des sols; matière organique extractible à l'eau; communautés bactériennes; caractérisation moléculaire; FTICR-MS; ^{13}C; fluorescence 3D

Influence of biotic and abiotic factors on soil organic matter dynamics assessed by the biogeochemical characterisation of soluble organic matter

Soils are the greatest reservoir of C on the continents, and organic matter mineralisation by microbial activity represents the major part of the CO_2 emitted by terrestrial ecosystems.

In this work, we studied water-extractable organic matter (WEOM), which corresponds to the more reactive fraction of soil organic matter (SOM). Our objectives were (i) to identify the relationships of WEOM dynamics with bacterial communities, and with soil physico-chemical parameters; (ii) to provide a precise chemical characterisation of WEOM.

There is a strong link between SOM solubility and the structure of bacterial communities, and an erosion of their diversity has an impact on SOM and WEOM dynamics, and leads to a decrease in organic matter mineralisation. A study at the regional scale then allowed us to identify that the SOM and clay contents control the quantities of WEOM and its aromaticity. The WEOM characterisation at the molecular level revealed the presence of a large number of ubiquitous molecules in the WEOM. Based on these analyses, we were also able to describe the effects of vegetation and soil physico-chemical properties on the chemical composition of WEOM.

Key-words: soil biogeochemistry; water-extractable organic matter; bacterial communities; molecular characterisation; FTICR-MS; ^{13}C; 3D-fluorescence